SëMA
BOLETÍN NÚMERO 38
Marzo 2007

sumario

Boletín de la Sociedad Española de Matemática Aplicada S$\vec{e}$MA

Página web de S$\vec{e}$MA
`http://www.sema.org.es/`

e-mail
`info@sema.org.es`

Dirección Editorial: Dpto. de Matemáticas. E.T.S.I. Industriales. Univ. de Castilla - La Mancha. Avda. de Camilo José Cela s/n. 13071. Ciudad Real. `omeva@uclm.es`

ISSN 1575-9822.
Depósito Legal: AS-1442-2002.

Imprime: Gráficas Lope. C/ Laguna Grande, parc. 79, Políg. El Montalvo II 37008. Salamanca.

Diseño de portada: Alfonso Bueno
Ilustración de portada: sucesivas aproximaciones del fractal de Mandelbrot

Estimados socios de la SEMA:

Recientemente hemos aceptado el encargo de asumir la edición de nuestro Boletín en el próximo periodo. No nos ha costado mucho decidirnos y creemos que varias han sido las razones que propiciaron esta decisión. Por un lado y ante todo, el atractivo que supone prestar este servicio a nuestra comunidad y tener la oportunidad de aportar nuestro granito de arena a esta labor que es de todos; por otro, el haber constatado "desde dentro" la tarea inmensa que han realizado nuestros compañeros de Salamanca, más recientemente, y el resto de grupos editores, hace más tiempo. Nos ha sorprendido gratamente que en realidad no hemos hecho sino recibir el relevo de algo que ya lleva muchos años funcionando muy bien. Este dato ha facilitado enormemente la decisión final.

Somos conscientes de que la dinámica de la Matemática Aplicada no nos permite instalarnos en el pasado y eludir así los retos que la Ciencia y la Sociedad nos presenta continuamente. En este sentido nuestro Boletín, como reflejo de nuestra Sociedad, no puede dejar de seguir buscando nuevos cauces para mejorar. Entendemos que esto supone un reto que, en lo referente a la edición y mejora de nuestro Boletín, hemos asumido. Y lo hemos hecho con entusiasmo, esperando poder ofrecer nueva savia que irá cristalizando a medida que vayamos conociendo mejor los entresijos y secretos de la edición de nuestro Boletín. No es necesario insistir en que cualquier sugerencia en este sentido será muy bien recibida y, ya desde ahora, pretendemos adoptar una actitud abierta hacia todos nuestros socios con el objetivo de mejorar esta herramienta de comunicación en nuestra Sociedad que es el Boletín de la SEMA.

A medida que se vayan produciendo cambios o mejoras os iremos haciendo partícipes de los mismos en la sección inicial que nos reservaremos, como es costumbre, en cada número; o vosotros mismo los iréis viendo cuando vayan apareciendo, aunque vayan acompañados de nuestros comentarios. En este primer número del que nos hemos encargado hemos implementado ya algunos cambios sencillos de forma que, creemos, pueden ayudar a mantener el atractivo visual del Boletín.

En este primer número os ofrecemos una entrevista con Ignacio Cirac, Premio Príncipe de Asturias de Investigación Científica y Técnica 2006. Confiamos en números sucesivos poder ofreceros algunas otras entrevistas con personas relevantes de la Ciencia o de la Matemática.

Esperamos no defraudar. Recibid un cordial saludo de los miembros del nuevo grupo editor: Ernesto Aranda, José Carlos Bellido, Alfonso Bueno, Alberto Donoso y Pablo Pedregal.

Juan Ignacio Cirac nació en Manresa en 1965 y en la actualidad desempeña su labor como director del Instituto de Óptica Cuántica Max Planck de Munich. Además de ser nuestro flamante premio Príncipe de Asturias, es Medalla de la Real Academia de Física Española, premio de Electrónica Cuántica de la Fundación Europea de la Ciencia y doctor Honoris Causa por la Universidad de Castilla la Mancha.

B.S.: *La primera pregunta es obligada: ¿Qué se siente al haber recibido un reconocimiento tan amplio a la labor científica propia?*

I.C.: Una satisfacción enorme. Siempre he dicho que soy un afortunado por poder hacer algo que me gusta y que me paguen por ello. Ahora, además, me lo reconocen de esta manera tan especial. Además, considero que este galardón premia también la tarea de mis colaboradores durante los últimos años.

B.S.: *Muchos de nuestros lectores desconocerán que Ignacio Cirac pasó algunos años como profesor titular en la UCLM, donde algunos miembros del grupo editor lo conocimos. ¿Qué recuerdos te trae la mente de aquellos años?*

I.C.: Sí, de hecho fue una época muy bonita de mi vida. En Ciudad Real pasé cinco años en los que hice muchos amigos y me inicié en el campo de investigación en el que trabajo actualmente. Recuerdo sobre todo el estar rodeado de mucha gente joven, como yo por aquel entonces, con muchas ganas de trabajar y de crear una buena universidad.

B.S.: *Teniendo en cuenta nuestra audiencia, ¿podrías explicarnos en pocas palabras en qué consiste la computación cuántica?*

I.C.: Se trata de utilizar las leyes de la Física Cuántica para construir ordenadores. De acuerdo con esa teoría, es posible tener estados de superposición, algo así como si un solo bit almacenase un cero y un uno a la vez, lo que se puede utilizar para construir nuevos algoritmos que resuelvan algunos problemas de manera mucho más eficiente que los ordenadores actuales.

B.S.: *¿Qué es lo que puede resultar más sorprendente de las posibles aplicaciones de este campo? ¿Podrías ponernos algún ejemplo sencillo?*

I.C.: En primer lugar, con un ordenador cuántico se podrían factorizar números de manera muy eficiente (el tiempo de cálculo escalaría polinómicamente con el número de dígitos del número que queremos factorizar). Esto nos permitiría, por ejemplo, descifrar

todos los mensajes secretos que actualmente se codifican utilizando métodos del tipo RSA. También sería posible hacer búsquedas en bases de datos desordenadas que tomarían un tiempo proporcional a la raíz cuadrada del número de entradas, en vez de ser proporcional al número de entradas, tal y como ocurre con los ordenadores ordinarios.

B.S.: *¿Hay alguna de tus contribuciones que te resulte especialmente querida?*

I.C.: La que más es en la que mostramos que es posible construir un ordenador cuántico, algo que por aquel entonces (hacia 1994) no estaba claro.

B.S.: *¿Qué percepción tienes de la Matemática Aplicada? ¿Qué importancia tiene la colaboración científica interdisciplinar?*

I.C.: Para mí es muy importante. En nuestro campo trabajamos con físicos, informáticos y matemáticos. Eso hace que surjan muchas ideas nuevas y que aprendamos también los unos de los otros.

B.S.: *¿Podrías enumerar algunos temas en que te parece que la interacción con la Matemática Aplicada, en un sentido amplio, podría ser interesante o relevante?*

I.C.: En varios sentidos. Para ser concreto, en estos momentos se está desarrollando la "teoría cuántica de la información", que es la extensión de la teoría de Shanon al caso cuántico. Ahí aparecen muchos problemas matemáticos complicados que necesitan de auténticos profesionales de este campo para poder atacarlos.

B.S.: *¿Qué impacto crees que podría tener la computación cuántica en la simulación numérica de grandes sistemas físicos, como por ejemplo las ecuaciones de la meteorología?*

I.C.: El mayor impacto se obtendría en la simulación de materiales (es decir, de ecuaciones de Schroedinger de muchas partículas) ya que ahí habría una ganancia en tiempo exponencial con el número de partículas. En otro tipo de ecuaciones, por el momento, la ganancia es más modesta.

B.S.: *¿Qué aspectos de la Matemática consideras imprescindibles en la formación de un físico, y más en concreto, en la formación de un físico cuántico?*

I.C.: La básica (cálculo, análisis, ecuaciones diferenciales, teoría de grupos, etc). Para un físico cuántico teórico, como es mi caso, también es muy importante el análisis funcional y el álgebra avanzada (teoría de conjuntos convexos, normas tensoriales, etc.).

B.S.: *El llevar ya varios años en Alemania seguro que te permite tener una visión más global de la Ciencia en España.*

¿Qué reflexiones te sugiere el tema? ¿Cómo se ve España en Ciencia desde lejos?

I.C.: Bastante bien. Tenemos el *handycap* de que nunca ha habido una tradición realmente científica en España, y de que la sociedad no la ha apreciado. Ahora, sin embargo, las cosas están cambiando y parece ser que los políticos de todos los signos, así como la sociedad, se van dando cuenta de la importancia, tanto de la ciencia básica, como de la aplicada. Pero aun nos queda un largo camino por recorrer...

B.S.: *Y con respecto al marco europeo de enseñanza superior, ¿qué puedes decir?*

I.C.: Desde el punto de vista práctico, me parece muy interesante. Ahora mismo existen problemas de convalidaciones que hacen imposible el realizar cierto tipo de estudios en otros países, algo que se puede arreglar en el futuro. Sin embargo, las tradiciones de distintos países son diferentes y, en algunos casos, no se si habrá un gran beneficio si todos optamos por alguno de los sistemas existentes.

B.S.: *Hoy día muchos jóvenes se enfrentan a decisiones nada fáciles en relación con una opción profesional de dedicación a la Ciencia frente a otras posibilidades. ¿Se te ocurre algún mensaje para este colectivo?*

I.C.: Ya lo he dicho antes, los científicos somos unos privilegiados pues podemos ganarnos la vida con algo que es como un *hobby*. Es cierto que hay que viajar mucho y pasar algunos años de incertidumbre hasta conseguir una plaza. Pero definitivamente merece la pena!

Bol. Soc. Esp. Mat. Apl.
n°38(2007), 11–37

ARTÍCULOS

FINITE ELEMENT METHODS FOR THE NUMERICAL SIMULATION OF INCOMPRESSIBLE VISCOUS FLUID FLOW MODELED BY THE NAVIER-STOKES EQUATIONS. PART III

ROLAND GLOWINSKI*, TSORNG-WHAY PAN*, L. HÉCTOR JUÁREZ V.† AND EDWARD DEAN*

*Department of Mathematics, University of Houston, Houston, Texas 77204-3008, USA

†Departamento de Matematicas, Universidad Autónoma Metropolitana-Iztapalapa, Iztaplapa, D.F. 09340, MEXICO

6 Numerical Experiments.

In this section we have considered two– and three–dimensional wall-driven cavity problems. The finite element spaces for the velocity field and pressure are P_1-*iso*-P_2 and P_1, respectively. The operator splitting scheme used in the simulation is the scheme à la Marchuk–Yanenko, i.e., the numerical results have been obtained via the algorithm (382)–(386). For the numerical results obtained via θ–scheme, some of them have been presented in Glowinski 1991 [82].

6.1 The wall-driven cavity problem

The first test problem that we consider is the celebrated wall-driven cavity flow problem. We consider this specific test problem since it is very well documented, a basic (if not *the* basic) reference being Ghia, Ghia, and Shin 1982 [104] (see also Schreiber and Keller 1983 [105]). We have then $\Omega = (0,1) \times (0,1)$ and $\mathbf{g}(\mathbf{x},t)$ defined by

$$\mathbf{g}(\mathbf{x},t) = \begin{cases} (f(x_1),0)^T \ on \ \{\mathbf{x} \mid \mathbf{x} = (x_1,1)^T, 0 < x_1 < 1\}, \\ \mathbf{0} \ elsewhere \ on \ \partial\Omega \end{cases} \tag{393}$$

where

$$f(x) = \begin{cases} \sin(x\pi/2a), & if \ \ 0 < x \leq a, \\ 1, & if \ \ a \leq x \leq 1-a, \\ \sin((1-x)\pi/2a), & if \ \ 1-a \leq x < 1. \end{cases} \tag{394}$$

The above Dirichlet data has been smoothed very locally in the two upper corners (the parameter a is 1/32 in all simulations reported in this section). In

Fecha de recepción: 21/10/2005

order to avoid possible difficulties associated to a genuine impulsive start we have multiplied $\mathbf{g}(\mathbf{x},t)$ in (393) by $\theta(t)$ defined by $\theta(t) = 1 - e^{-50t}$ if $t \in (0,.15)$ and $\theta(t) = 1$ for $t \geq .15$.

In Ghia, Ghia, and Shin 1982 [104] uniform grids were also chosen. Another reason we have chosen regular triangulations is that we wanted to use direct solvers like fast elliptic solvers based on cyclic reduction to solve elliptic problems from (383) and (386). When computing steady state solutions, we have taken $h_v = 1/128$ as mesh size for the velocity field for Reynolds numbers ($Re = 1/\nu$) up to 7500 and $h_v = 1/256$ for the range of Reynolds number from 5000 to 7500. Same mesh sizes were used in Ghia, Ghia, and Shin 1982 [104]. For the time discretization we have taken $\triangle t = 0.0005$ and $Q_1 = 5$ in (192)-(194).

In the simulation when the relative change, $\|\mathbf{u}^n - \mathbf{u}^{n-1}\|_2/\|\mathbf{u}^n\|_2$, is less than 10^{-7}, $\mathbf{u}^n$ is taken as steady state. With $h_v = 1/128$, we computed the $Re = 100$ case with $\mathbf{u}_0 = \mathbf{0}$ and then used the steady state of $Re = 100$ as the initial flow field condition for the $Re = 400$ case, and repeated this process up to the $Re = 8500$ case. We also used the steady state result at $Re = 5000$, obtained with $h_v = 1/128$, as the initial flow field condition for the case at $Re = 5000$ with $h_v = 1/256$, and repeated this process up to the $Re = 8500$ case.

On Figures 6.1–6.3, we have visualized the streamlines, the vorticity contours and the isobars of the steady state solutions computed at $Re = 100$, 400, 1000, 3200, 5000, and 7500 respectively. Those values used to draw the streamlines and the vorticity contours are taken from Table III in Ghia, Ghia, and Shin 1982 [104]. The values used to draw the isobars are from -0.1 to 0.1 with increment 0.01. In Figure 6.4, we have compared the computed u_1-velocity (resp., u_2-velocity) along the line $x_1 = 1/2$ (resp., $x_2 = 1/2$) with those results reported in Tables I and II in Ghia, Ghia, and Shin 1982 [104]. In Table 6.1, we have the minimum of the stream function and the location at which the minimum is attained at $Re = 100$, 400, 1000, 3200, 5000, and 7500 respectively from the numerical experiments and Ghia, Ghia, and Shin 1982 [104]. These results agree remarkably well with those obtained in Ghia, Ghia, and Shin 1982 [104] using the stream function-vorticity formulation of the steady Navier-Stokes equations.

At $Re = 8500$, we are beyond a Hopf bifurcation point. In order to ensure that the computed periodic solution is not a numerical artifact, we have run simulations with three sets of mesh size and time step, namely $(h_v, \triangle t) = (1/128, 0.0005)$, $(h_v, \triangle t) = (1/128, 0.00025)$ and $(h_v, \triangle t) = (1/256, 0.0005)$. For the local time step in (192)-(194), we still have taken $Q_1 = 5$. For the case where $(h_v, \triangle t) = (1/128, 0.0005)$, we started from a steady state solution at $Re = 7500$ with $h_v = 1/128$ and run it till $t = 1500$. It took about 0.18 second per time step on a DEC personal workstation 500au. For the second case where $(h_v, \triangle t) = (1/128, 0.00025)$, we started from a solution of the previous case and run it till $t = 1650$. It took about 0.146 second per time step. For the third case where $(h_v, \triangle t) = (1/256, 0.0005)$, we started from a steady state solution at $Re = 7500$ with $h_v = 1/256$ and run it till $t = 1500$. It took about 0.76 second per time step.

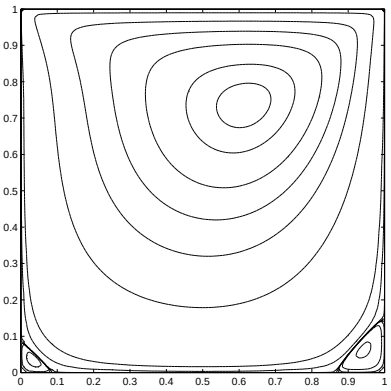

$Re = 100$, $h_v = 1/128$.

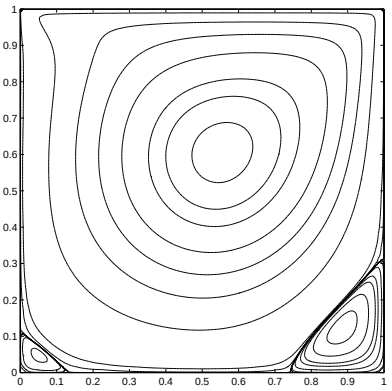

$Re = 400$, $h_v = 1/128$.

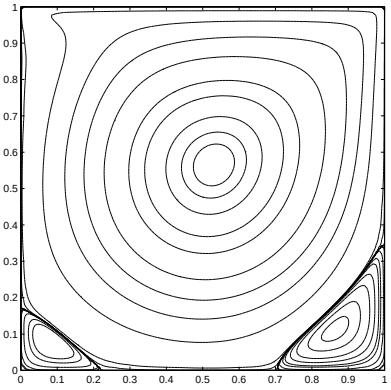

$Re = 1000$, $h_v = 1/128$.

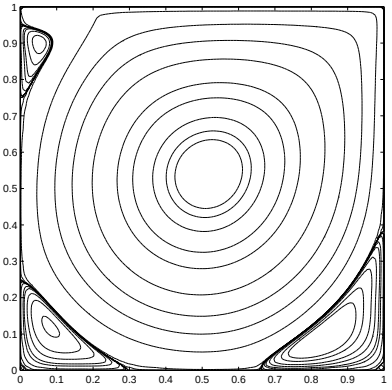

$Re = 3200$, $h_v = 1/128$.

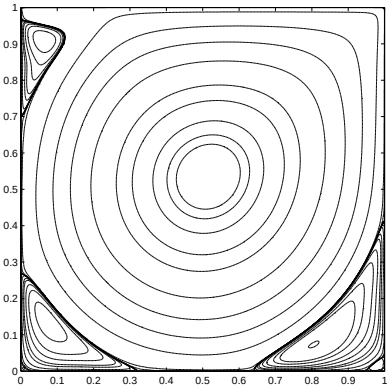

$Re = 5000$, $h_v = 1/256$.

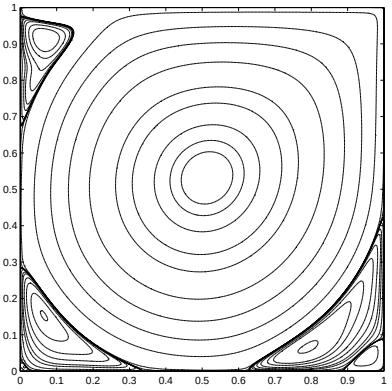

$Re = 7500$, $h_v = 1/256$.

Figure 6.1: Streamlines.

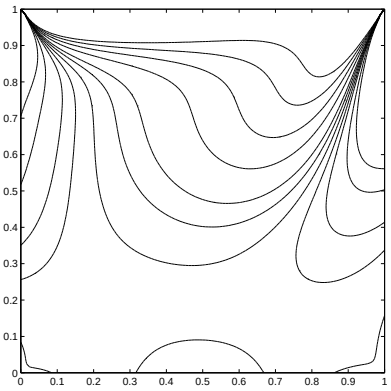

$Re = 100$, $h_v = 1/128$.

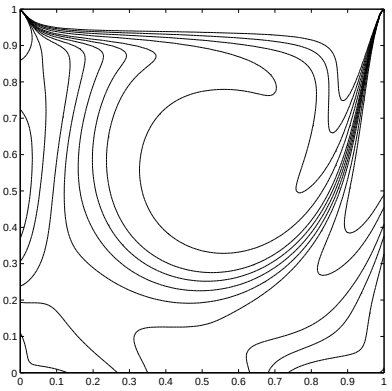

$Re = 400$, $h_v = 1/128$.

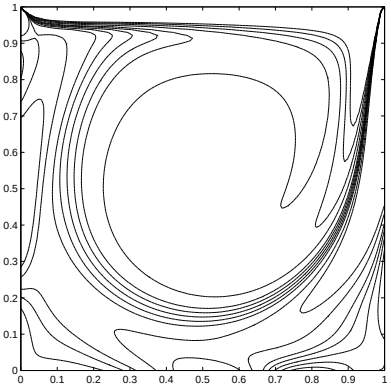

$Re = 1000$, $h_v = 1/128$.

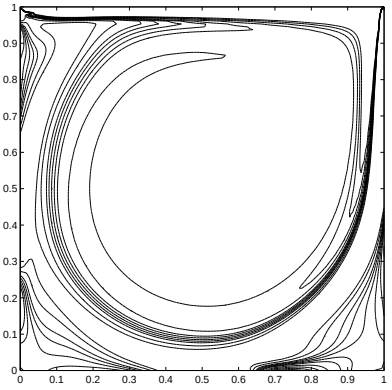

$Re = 3200$, $h_v = 1/128$.

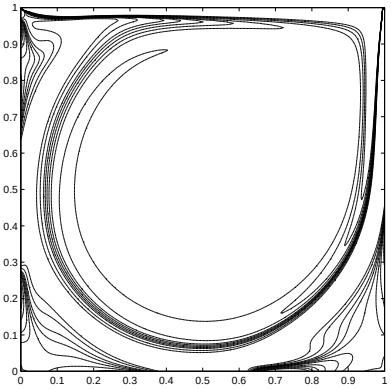

$Re = 5000$, $h_v = 1/256$.

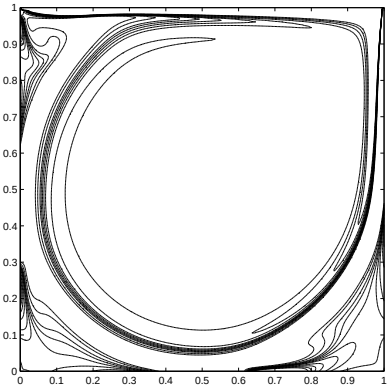

$Re = 7500$, $h_v = 1/256$.

Figure 6.2: Vorticity contours.

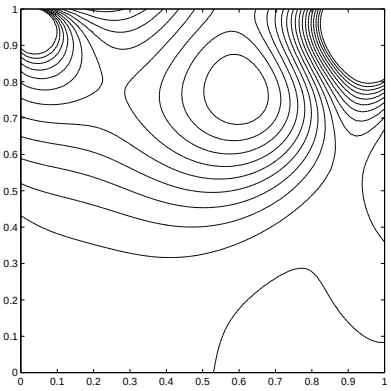

$Re = 100,\ h_v = 1/128.$

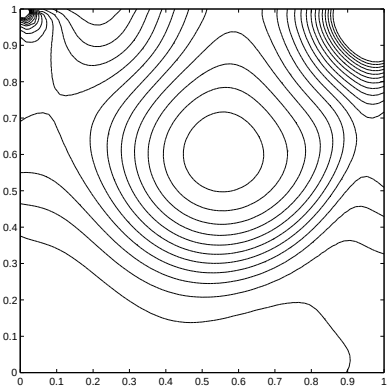

$Re = 400,\ h_v = 1/128.$

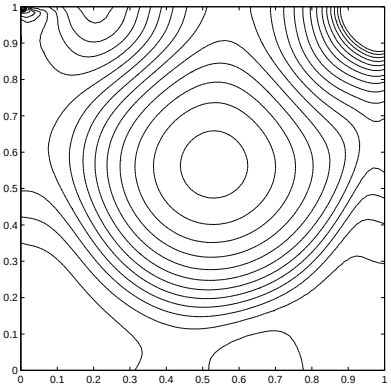

$Re = 1000,\ h_v = 1/128.$

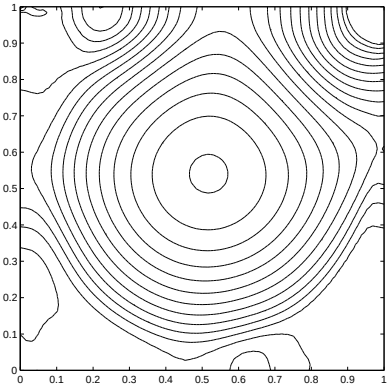

$Re = 3200,\ h_v = 1/128.$

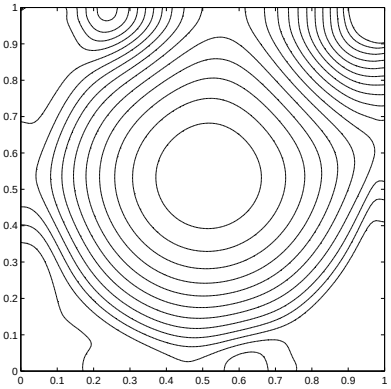

$Re = 5000,\ h_v = 1/256.$

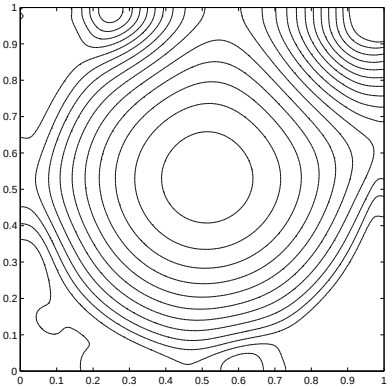

$Re = 7500,\ h_v = 1/256.$

Figure 6.3: Isobars.

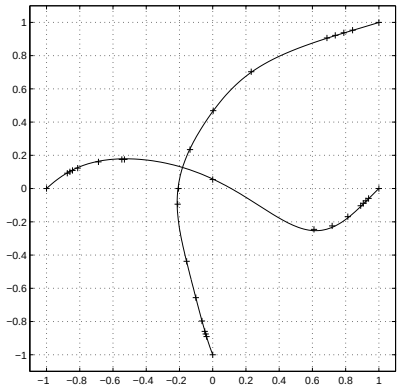

$Re = 100$, $h_v = 1/128$.

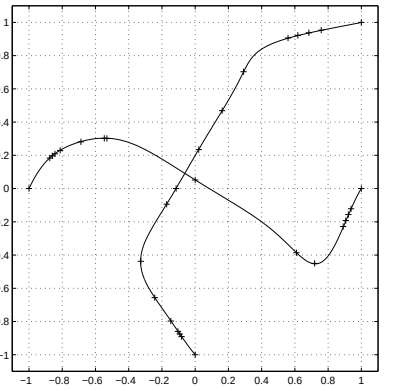

$Re = 400$, $h_v = 1/128$.

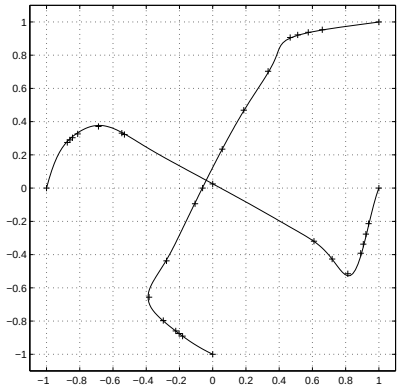

$Re = 1000$, $h_v = 1/128$.

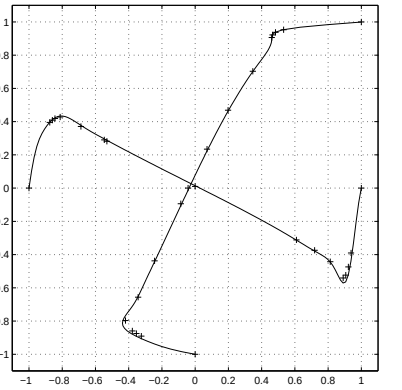

$Re = 3200$, $h_v = 1/128$.

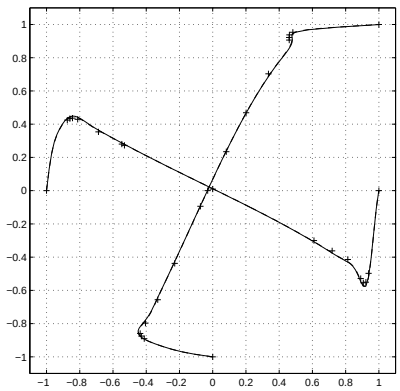

$Re = 5000$, $h_v = 1/256$.

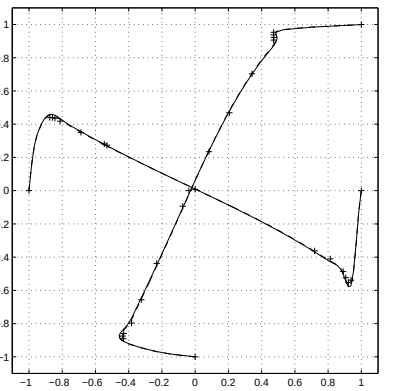

$Re = 7500$, $h_v = 1/256$.

Figure 6.4: Comparison between the computed u_1-velocity (resp., u_2-velocity) along the line $x_1 = 1/2$ (resp., $x_2 = 1/2$) (solid lines) and the results reported in Ghia, Ghia, and Shin 1982 [104] (denoted by "+").

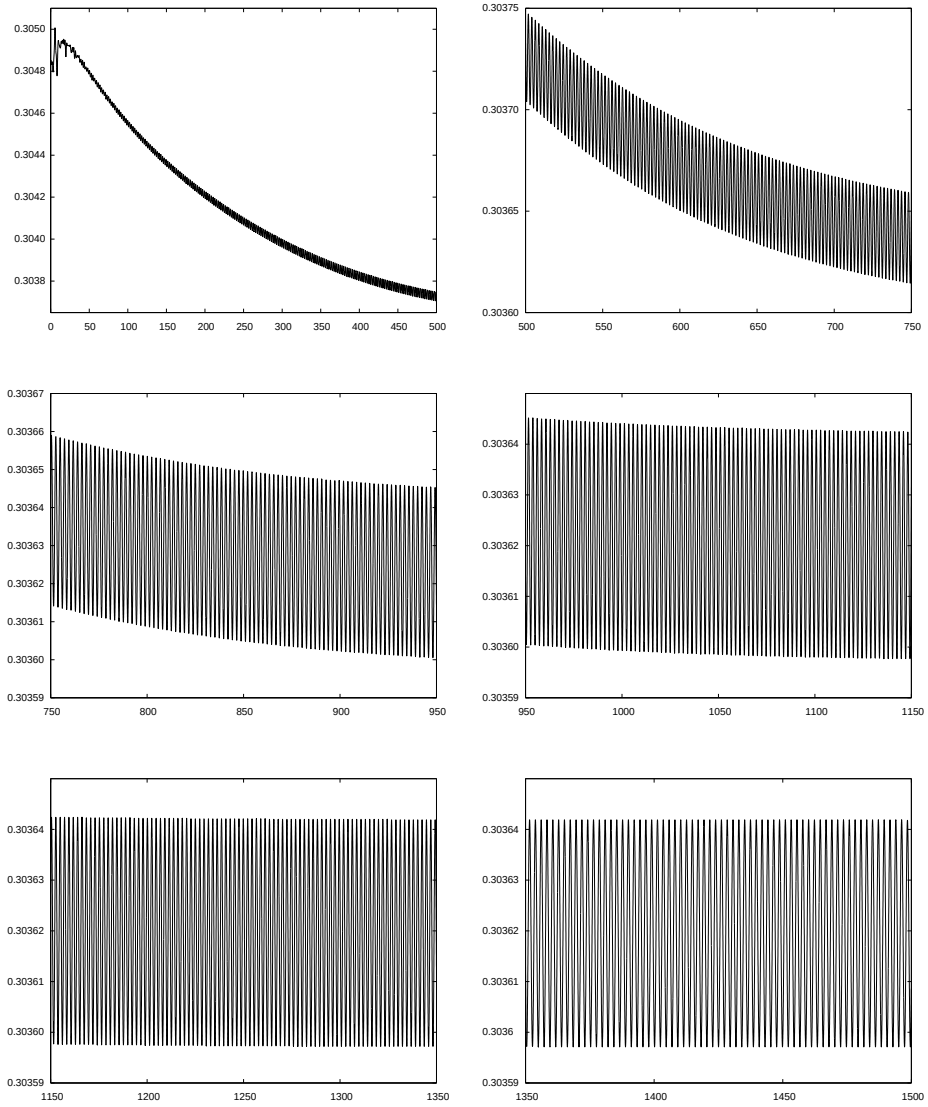

Figure 6.5: The history of $\|\mathbf{u}_h^n\|_2$ for the flow at $Re = 8500$ with $h_v = 1/256$ and $\triangle t = 0.0005$.

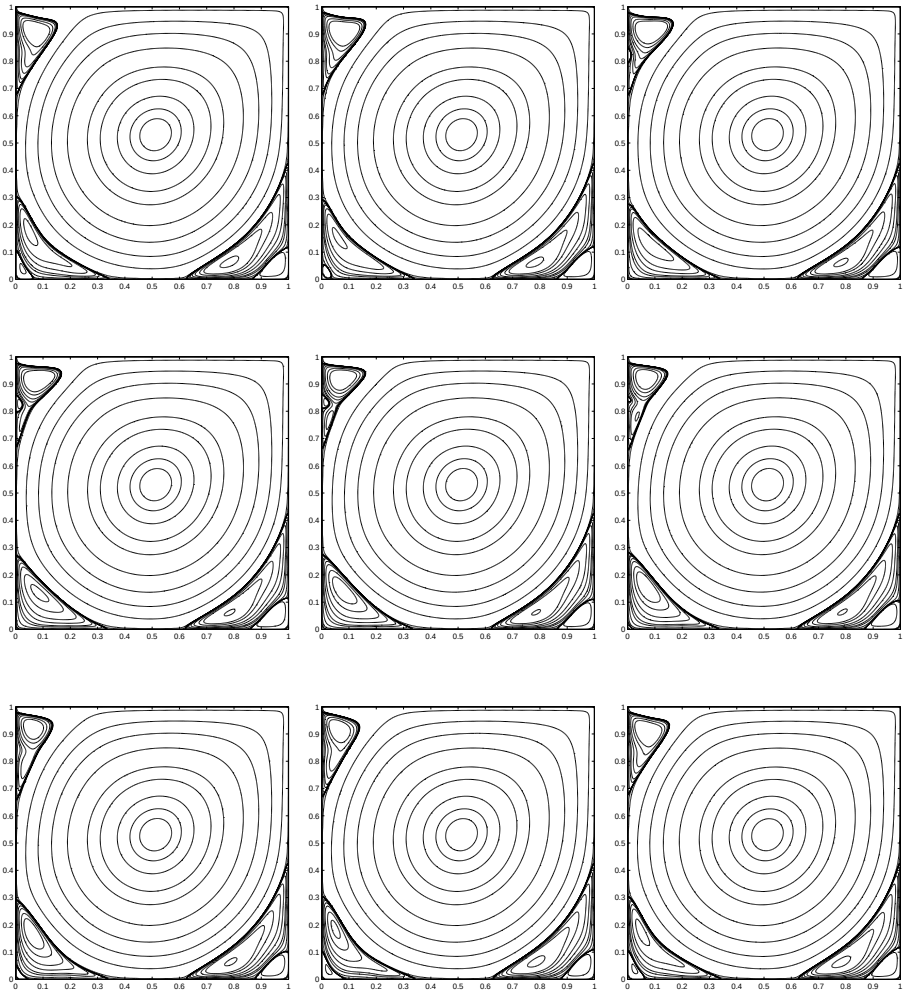

Figure 6.6: One complete cycle of streamline contours at time interval of 2.27 at $Re = 8500$ with $h_v = 1/256$ (from left to right and from top to bottom).

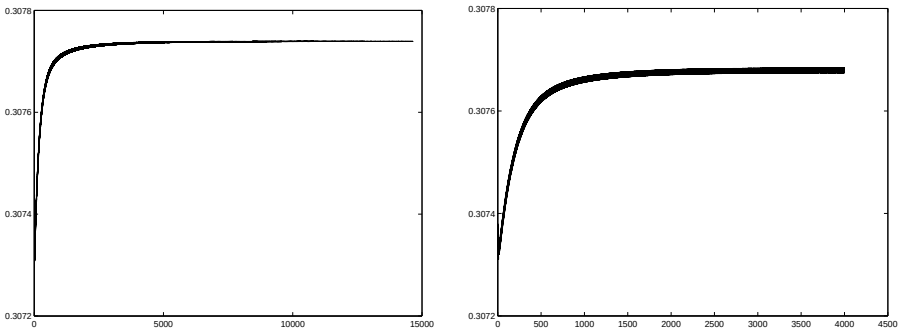

Figure 6.7: The history of $\|\mathbf{u}_h^n\|_2$ for the flow at $Re = 8343$ (left) $Re = 8375$ (right) with $h_v = 1/128$ and $\triangle t = 0.0005$.

The period of the Hopf bifurcated flow, at $Re = 8500$, is 2.24, 2.22, and 2.27 for the simulations done with $(h_v, \triangle t) = (1/128, 0.0005)$, $(h_v, \triangle t) = (1/128, 0.00025)$ and $(h_v, \triangle t) = (1/256, 0.0005)$, respectively. In Figure 6.5 the history of $\|\mathbf{u}_h^n\|_2$ for the flow at $Re = 8500$ with $(h_v, \triangle t) = (1/256, 0.0005)$ is presented. We can see, clearly, in Figure 6.5 that the solution reaches its asymptotic periodic state at $t = 1500$. In Figure 6.6, we have plotted a series of nine streamline contours for the flow at $Re = 8500$ with $(h_v, \triangle t) = (1/256, 0.0005)$ during a time interval of length 2.27 so that the nine plots make one complete period. We observe that there are persistent oscillations for all the secondary and tertiary vortices. The most significant changes during one period are the periodic appearance and disappearance of two tertiary vortices at the bottom left and at the top left. In Bruneau and Jouron 1988 [106], a transition to turbulence in the unit driven cavity flow was found for Reynolds number between 5000 and 10000 by solving the steady Navier-Stokes equations with a 512×512 grid. In Shen 1991 [107] due to the use of a regularized boundary condition $f(x) = 16x^2(1-x)^2$, the critical Reynolds number for Hopf bifurcation is in the $(10,000, 10,500]$ range which is higher than the one for the less smooth boundary conditions used in Bruneau and Jouron 1988 [106] and Goyon 1996 [108], and the one in this article. In Goyon 1996 [108] the critical Reynolds number for the Hopf bifurcation is in the $(7,500, 10,000]$ range. A periodic solution was found at $Re = 10,000$ with period 2.41. Our results indicate that the critical Reynolds number is between 7500 and 8500. We then did use the flow field at $Re = 8500$ with $(h_v, \triangle t) = (1/128, 0.0005)$ as initial condition to roughly locate the critical Reynolds number for the Hopf bifurcation. At $Re = 8343$, we have obtained steady state and the history of $\|\mathbf{u}_h^n\|_2$ is shown in Figure 6.7. At $Re = 8375$, we have obtained Hopf bifurcated flow and the period is 2.235, whose the history of $\|\mathbf{u}_h^n\|_2$ is shown in Figure 6.7. Thus the critical Reynolds number (when using $(h_v, \triangle t) = (1/128, 0.0005)$) is between 8343 and 8375.

Re	ψ_{min}	location	ψ^*_{min}	location*
100	–0.103435	(0.6172, 0.7344)	–0.103423	(0.6172, 0.7344)
400	–0.113909	(0.5547, 0.6094)	–0.113909	(0.5547, 0.6055)
1000	–0.119173	(0.5313, 0.5625)	–0.117929	(0.5313, 0.5625)
3200	–0.121768	(0.5156, 0.5391)	–0.120377	(0.5165, 0.5469)
5000	–0.121218	(0.5156, 0.5352)	–0.118966	(0.5117, 0.5325)
7500	–0.120816	(0.5156, 0.5313)	–0.119976	(0.5117, 0.5322)

Table 6.1: Location at which the minimum ψ_{min} of the stream function is attained and minimal value of the stream function (ψ^*_{min} and location* are values taken from Ghia, Ghia, and Shin 1982 [104]).

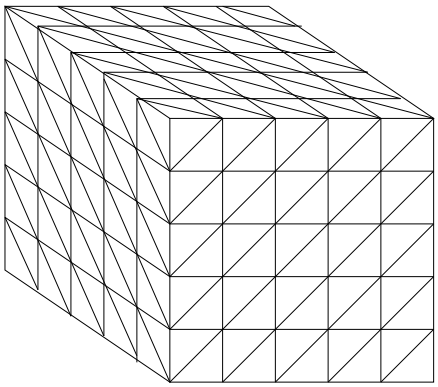

Figure 6.8: An example of a regular tetrahedrization $\mathcal{T}_h$ of Ω.

6.2 A three-dimensional wall-driven cavity problem

In this section we consider is a three-dimensional wall-driven cavity flow problem. We have $\Omega = (0,1) \times (0,1) \times (0,1)$ and $\mathbf{g}(\mathbf{x}, t)$ defined by

$$\mathbf{g}(\mathbf{x},t) = \begin{cases} (f(x_1)^2 f(x_2)^2 \theta(t), 0, 0)^T \ on \ \{\mathbf{x} \mid \mathbf{x} = (x_1, x_2, 1)^T, 0 < x_1, x_2 < 1\}, \\ \mathbf{0} \ elsewhere \ on \ \partial\Omega \end{cases} \tag{395}$$

where $f(x)$ and $\theta(t)$ are defined in the previous section but with $a = 1/20$.

The velocity $\mathbf{u}$ has been approximated by continuous piecewise affine vector-valued functions defined from a regular uniform "tetrahedrization" $\mathcal{T}_h$ with mesh size h_v (see Figure 6.8). The pressure p has been approximated by continuous piecewise affine functions, defined over a tetrahedrization $\mathcal{T}_{2h}$. Thus the mesh size for the pressure is $h_p = 2h_v$.

In the numerical experiments dedicated to steady flow computations, we have used two mesh sizes $h_v = 1/60$ and $1/80$ for $Re = 400$, 1000 and 1500. For

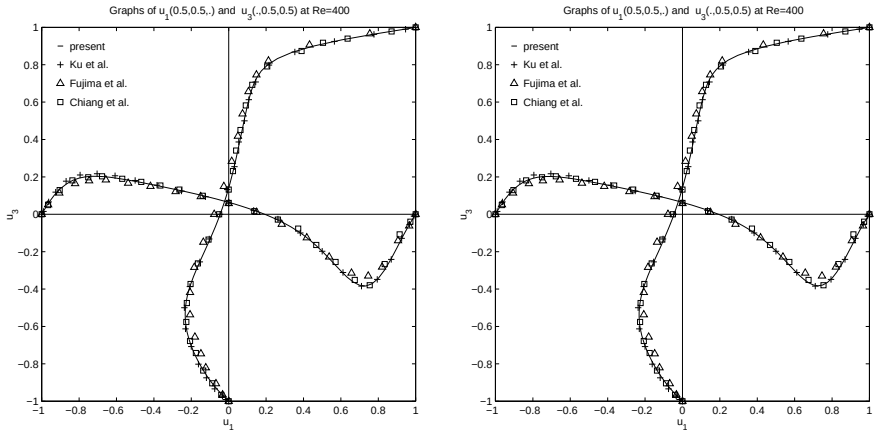

Figure 6.9: 3D cavity central plane velocity profiles for $Re = 400$ obtained using $\triangle t = 0.001$ and mesh size $h_v = 1/60$ (left) and $1/80$ (right).

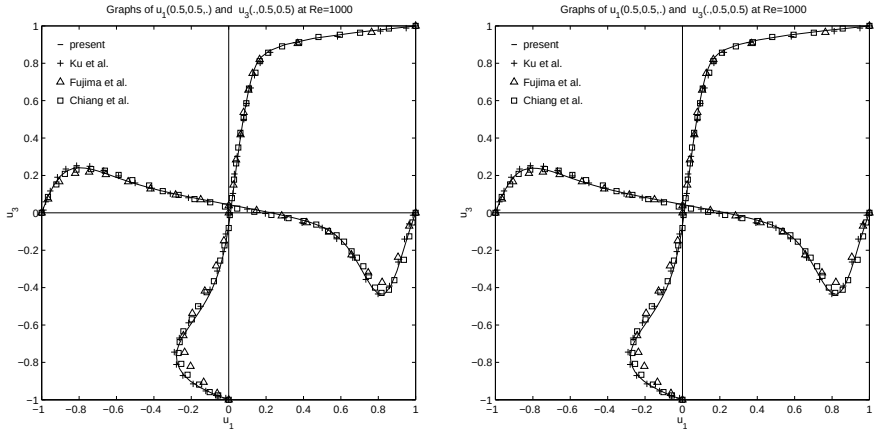

Figure 6.10: 3D cavity central plane velocity profiles for $Re = 1000$ obtained using $\triangle t = 0.001$ and mesh size $h_v = 1/60$ (left) and $1/80$ (right).

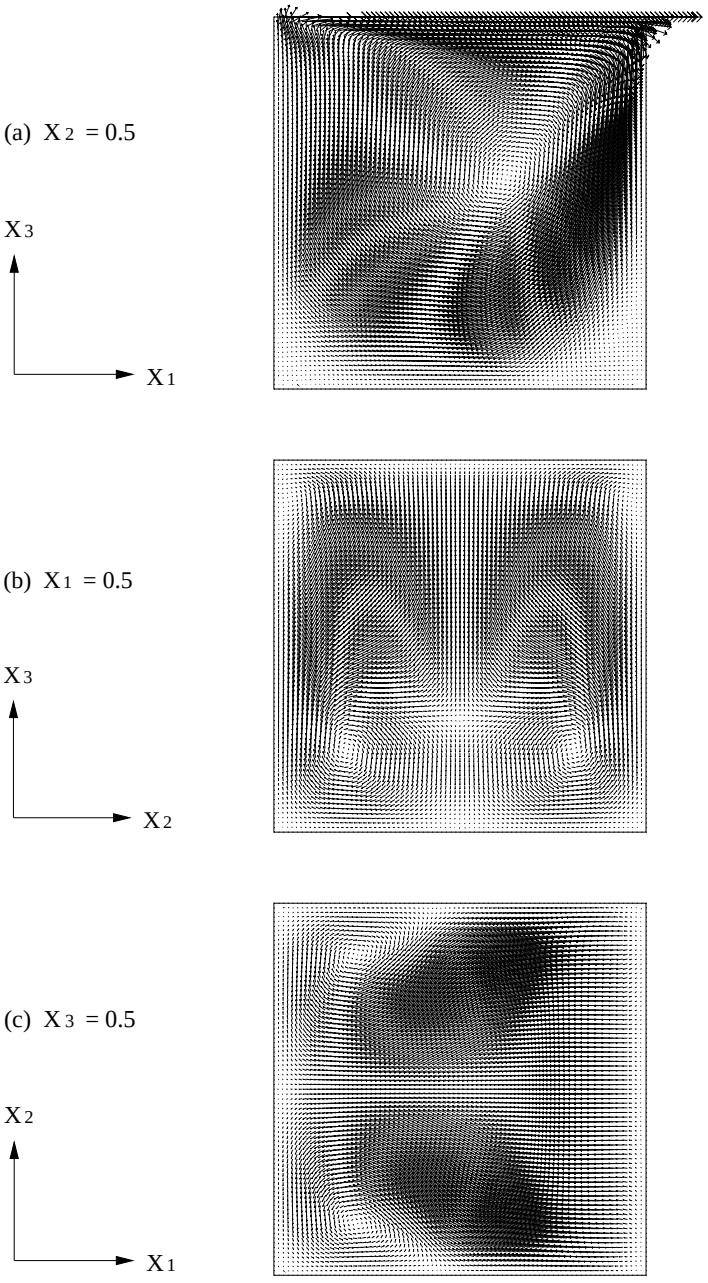

Figure 6.11: Velocity vector for Re =400 at $t = 20.352$ on the planes (a) $x_2 = 0.5$, (b) $x_1 = 0.5$, and (c) $x_3 = 0.5$ obtained with mesh size $h_v = 1/80$.

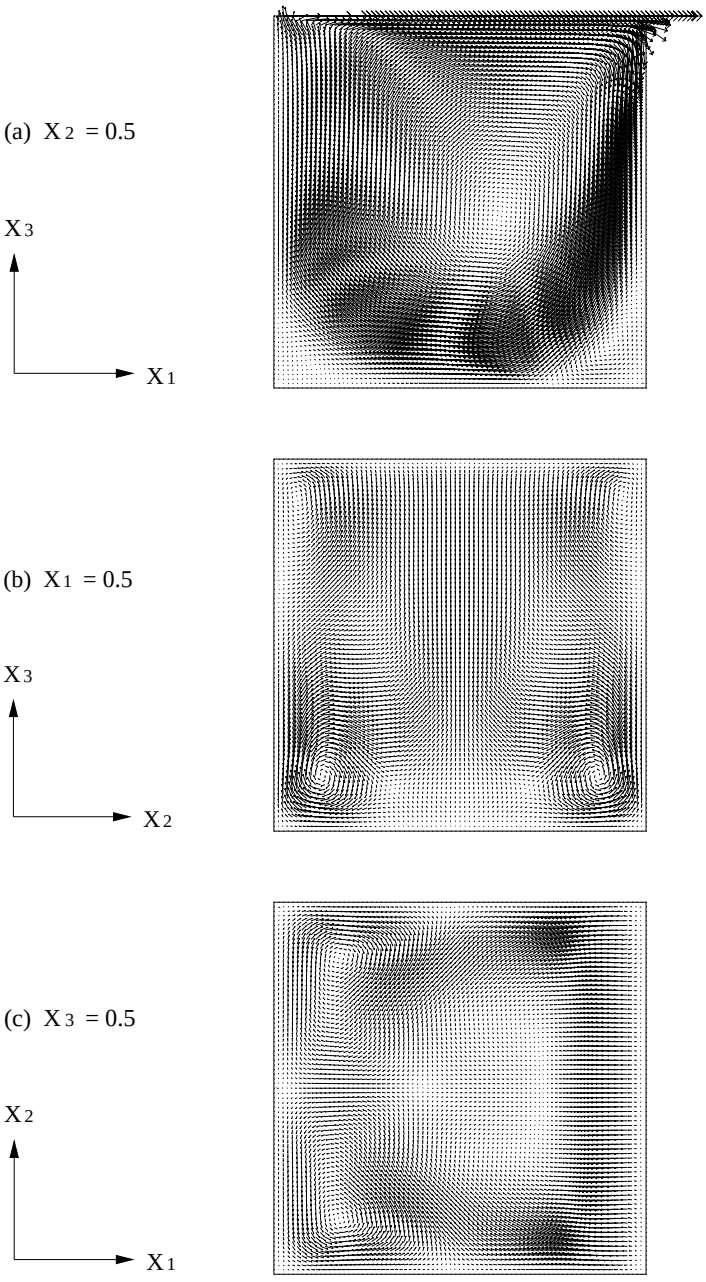

Figure 6.12: Velocity vector for Re =1000 at t = 35.409 on the planes (a) $x_2 = 0.5$, (b) $x_1 = 0.5$, and (c) $x_3 = 0.5$ obtained with mesh size $h_v = 1/80$.

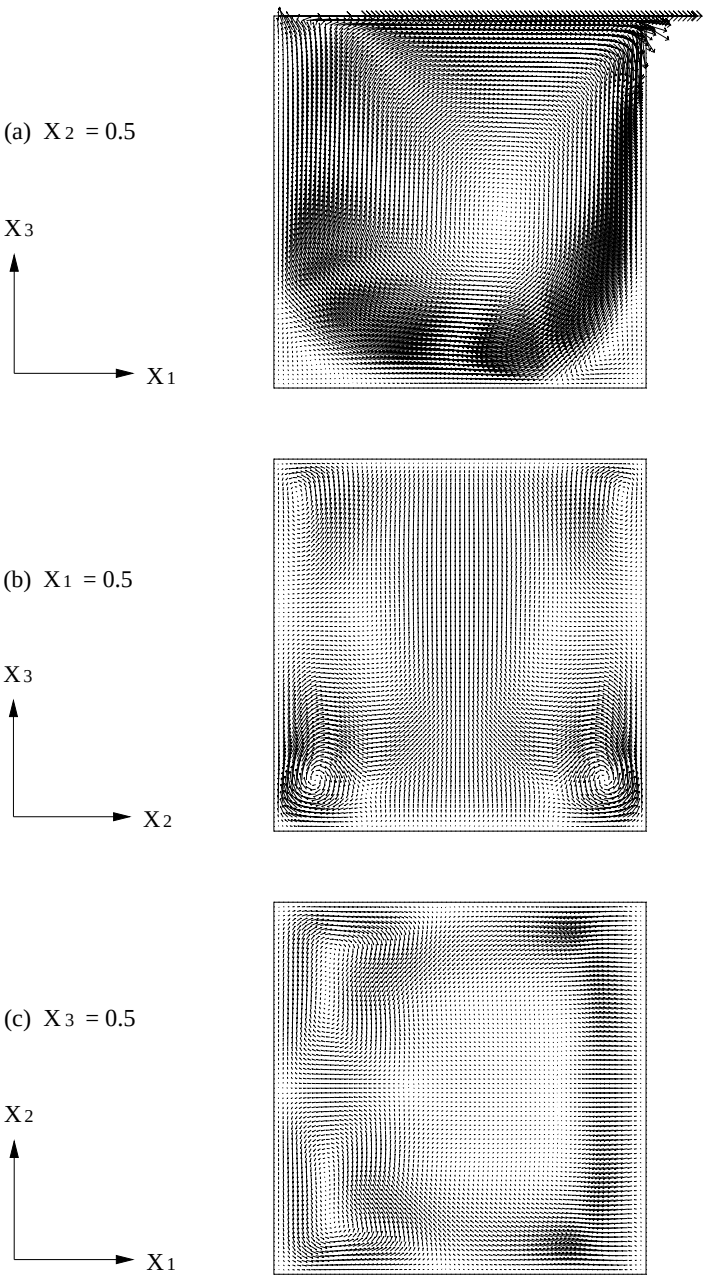

Figure 6.13: Velocity vector for Re =1500 at t = 64.511 on the planes (a) $x_2 = 0.5$, (b) $x_1 = 0.5$, and (c) $x_3 = 0.5$ obtained with mesh size $h_v = 1/80$.

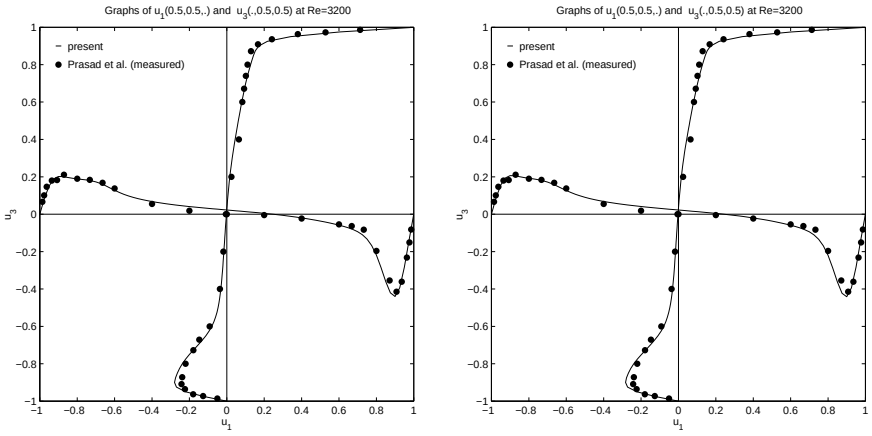

Figure 6.14: 3D cavity central plane velocity profiles for $Re = 3200$. The simulation results are averaged values obtained from $t = 220$ second to $t = 340$ second (left) and $t = 220$ second to $t = 400$ second (right).

the time discretization we have taken $\triangle t = 0.001$ and $Q_1 = 2$ in (192)-(194). Following the criterion used in Fujima, Tabata, Fukasawa 1994 [109], when the change in the simulation, $\|\mathbf{u}^n - \mathbf{u}^{n-1}\|_\infty / \triangle t$, is less than 10^{-4}, $\mathbf{u}^n$ is taken as steady state. The initial condition of fluid field for $Re = 400$ (resp, 1000 and 1500) is the steady-state solution of $\mathbf{u}^n$ obtained at $Re = 100$ (resp., 400 and 1000) using the same mesh size and time step.

Figures 6.9 and 6.10 show the comparison of the our computational results at $Re = 400$ and 1000 with results obtained by Fujima, Tabata, Fukasawa 1994 [109] and Ku, Hirsh, and Taylor 1987 [110], and Chiang, Sheu, Hwang [111]. All numerical results are in good agreement.

Velocity vectors of the steady flows obtained in the case of $Re = 400$, 1000, and 1500 are shown in Figures 6.11-6.13. Those vectors are projected orthogonally to the three planes, $x_2 = 0.5$, $x_1 = 0.5$, and $x_3 = 0.5$, and the length of the vectors has been doubled in the two later planes to observe the flow more clearly. We observe that the center of the primary vortex moves down as the Reynolds increases and secondary vortices appear in two lower corners, which is similar, in some sense, to what happens for the two-dimensional wall-driven cavity flow. At $x_1 = 0.5$, a pair of secondary vortices moves toward the lower corners when the Reynolds increases. Also another pair of vortices appears at the top corners at $Re = 1000$ and 1500.

At $Re = 3200$, the initial condition of fluid field is the steady-state solution of $\mathbf{u}^n$ obtained at $Re = 1500$ obtained with mesh size $h_v = 1/80$ and time step $\triangle t = 0.001$. In Figure 6.14 the two- and three-minute averaged values of the 3D cavity central plane velocity profiles are compared with the experimental

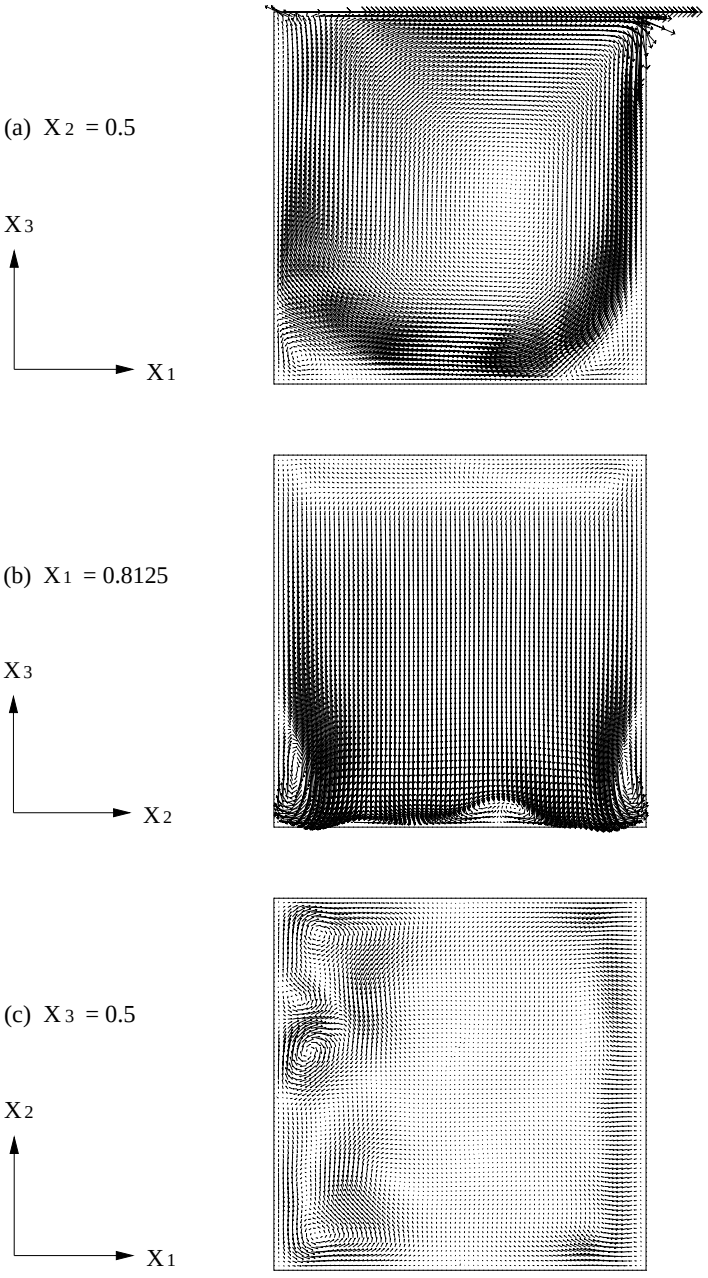

Figure 6.15: Velocity vector for Re =3200 at $t = 420$ on the planes (a) $x_2 = 0.5$, (b) $x_1 = 0.6125$, and (c) $x_3 = 0.5$ obtained with mesh size $h_v = 1/80$.

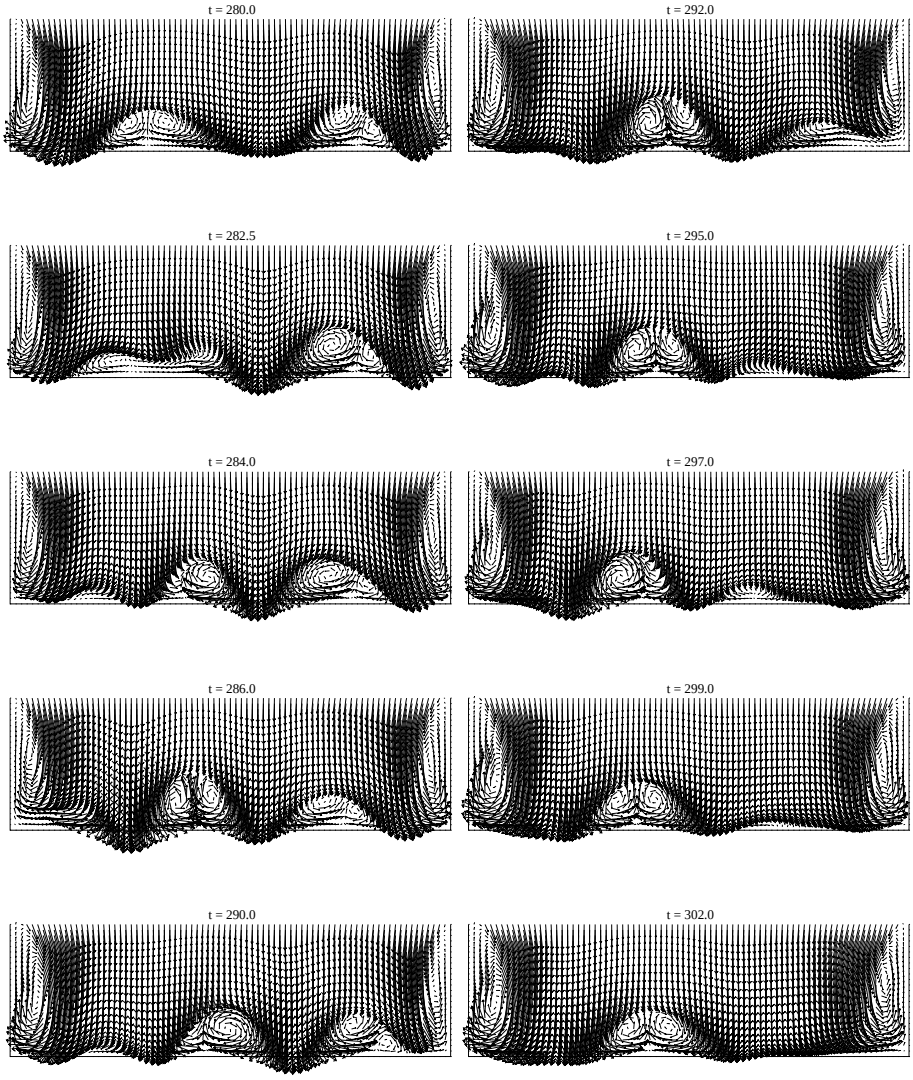

Figure 6.16: Flow filed projected to the plane $x_1 = 0.8125$ near the downstream sidewall at t =280, 282.5, 284, 286, 290 92, 295, 297, 299 and 302 second (from top to bottom and then from left to right) for $Re = 3200$.

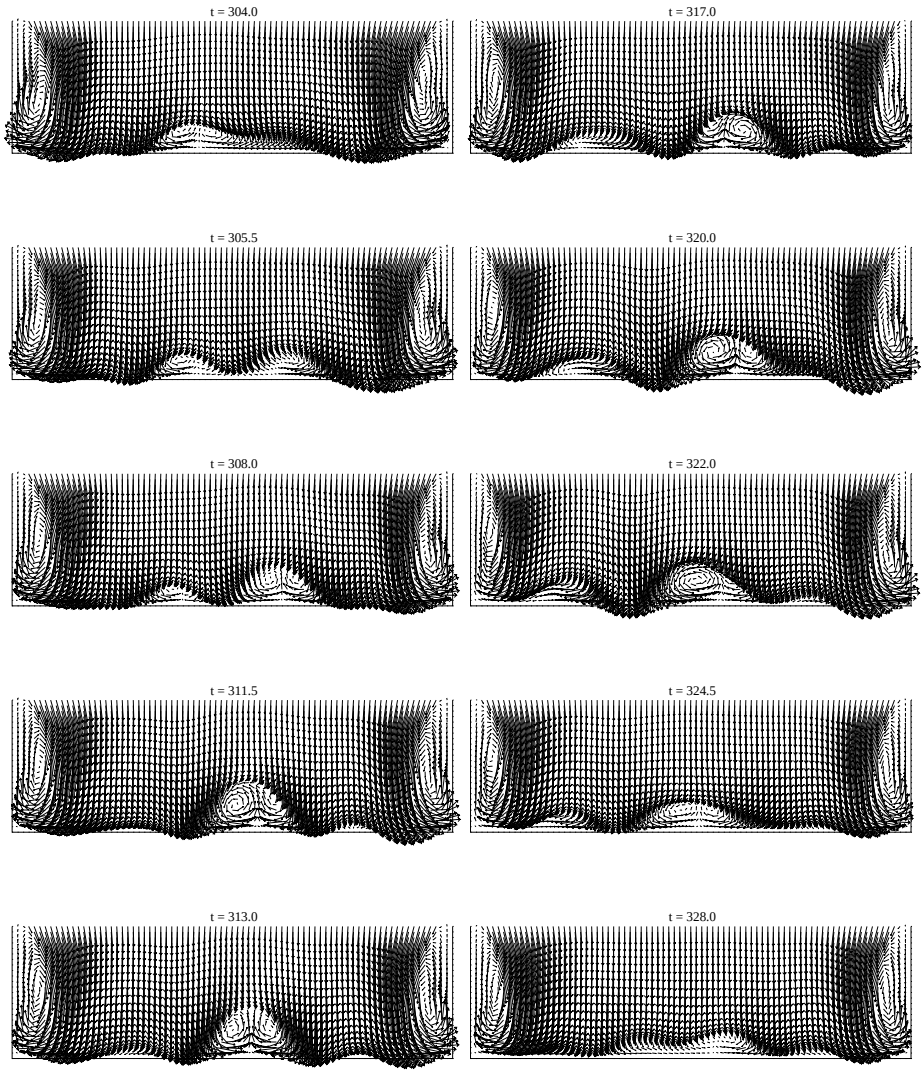

Figure 6.17: Flow filed projected to the plane $x_1 = 0.8125$ near the downstream sidewall at t =304, 305.5, 308, 311.5, 313 317, 320, 322, 324.5, and 328 second (from top to bottom and then from left to right) for $Re = 3200$.

values by Prasad and Koseff [112]. The agreement is good. The vectors of velocity field at $t = 420$ are projected orthogonally to the three planes, $x_2 = 0.5$, $x_1 = 0.8125$, and $x_3 = 0.5$, and the length of the vectors has been doubled in the two later planes to observe the flow more clearly. A well developed pair of Taylor–Göertler–like vortices can be first observed at $t = 12$ (at least $t = 9$ there is no sign of it at $x = 0.8125$). The meandering of Taylor–Görtler–like vortices and its interaction with corner vortices is shown in Figures 6.16-6.19.

Acknowledgement

We acknowledge the support of NSF (grants DMS–9973318, CCR–9902035, and DMS–0209066), Texas Board of Higher Education (ARP grant 003652–0383–1999), and DOE/LASCI (grant R71700K–292–000–99).

References

[1] C. Canuto, M.Y. Hussaini, A. Quarteroni, and T.A. Zang, *Spectral Methods in Fluid Dynamics*, Springer–Verlag, New York, 1988.

[2] M. Lesieur, *Turbulence in Fluids*, Kluwer, Dordrecht, 1990.

[3] E. Guyon, J.P. Hulin, and L. Petit, *Hydrodynamique Physique*, Intereditions/Editions du CNRS, Paris, 1991.

[4] R. Glowinski, Finite element methods for incompressible viscous flow, in *Handbook of Numerical Analysis*, **Vol. IX**, P.G. Ciarlet, J.-L. Lions (deceased) eds., North-Holland, Amsterdam, 2003.

[5] W. Prager, *Introduction to Mechanics of Continua*, Ginn and Company, Boston, MA, 1961.

[6] G.K. Batchelor, *An Introduction to Fluid Mechanics*, Cambridge University Press, Cambridge, U.K., 1967.

[7] A.J. Chorin and J.E. Marsden, *A Mathematical Introduction to Fluid Mechanics*, Springer–Verlag, New York, 1990.

[8] R. Glowinski, *Numerical Methods for Nonlinear Variational Problems*, Springer–Verlag, New York, 1984.

[9] M.O. Bristeau, R. Glowinski, B. Mantel, J. Periaux, P. Perrier, Numerical Methods for incompressible and compressible Navier-Stokes problems, in *Finite Element in Fluids*, **Vol. 6**, R.H. Gallagher, G. Carey, J.T. Oden, and O.C. Zienkiewicz eds., J. Wiley, Chicester, 1985, 1–40.

[10] O. Pironneau, *Finite Element Methods for Fluids*, J. Wiley, Chicester, 1989.

[11] J. Leray, Sur le mouvement d'un liquide visqueux emplissant l'espace, *Acta Mathematica*, **63**(1934), 193–248.

[12] J. Leray, Essai sur les mouvements d'un liquide visqueux que limitent des parois, *J. Math. Pures et Appl.*, **13**(1934), 331–418.

[13] E. Hopf, Uber die Anfangswertaufgabe fur die hydrodynamischen Grundgleichungen, *Math. Nachrichten*, **4**(1951), 213–231.

[14] J. Leray, Aspects de la mécanique théorique des fluides, *La Vie des Sciences*, Comptes Rendus de l'Académie des Sciences, Paris, Série Générale, **11**(1994), 287–290.

[15] J.L. Lions and G. Prodi, Un théorème d'existence et d'unicité dans les équations de Navier-Stokes en dimension2, *C.R. Acad. Sci., Paris* **248**, 3519–3521.

[16] J.L. Lions, *Equations Différentielles Opérationnelles et Problémes aux Limites*, Springer–Verlag, Berlin, 1961.

[17] J.L. Lions, *Quelques Méthodes de Résolution des Problémes aux Limites Non Linéaires*, Dunod, Paris, 1969.

[18] O. Ladysenskaya, *Theory and Numerical Analysis of the Navier-Stokes Equations*, Gordon and Breach, New York, NY, 1969.

[19] R. Temam, *The Mathematical Theory of Viscous Incompressible Flow*, North-Holland, Amsterdam, 1977.

[20] L. Tartar, *Topics in Nonlinear Analysis*, Publications Mathématiques d'Orsay, Université Paris-Sud, Départment de Mathématiques, Paris, 1978.

[21] H.O. Kreiss and J. Lorenz, *Initial-Boundary Value Problems and the Navier-Stokes Equations*, Academic Press, Boston, MA, 1989.

[22] P.L. Lions, *Mahtematical Topics in Fluid Mechanics, Vol I: Incompressible Models*, Oxford University, Oxford, UK, 1996.

[23] M. Marion and R. Temam, *Navier-Stokes Equations*, in *Handbook of Numerical Analysis*, **Vol. VI**, P.G. Ciarlet, J.-L. Lions (deceased) eds., North-Holland, Amsterdam, 1998, 503–689.

[24] P.G. Ciarlet, *The Finite Element Method for Elliptic Problems*, North-Holland, Amsterdam, 1978.

[25] F. Brezzi and M. Fortin, *Mixed and Hybrid Finite Element Methods*, Springer-Verlag, New York, NY, 1991.

[26] S.C. Brenner and L.R. Scott *The Mathematical Theory of Finite Element Methods*, Springer-Verlag, New York, NY, 1994.

[27] N.N. Yanenko, *The Method of Fractional Steps*, Springer-Verlag, Berlin, 1971.

[28] G.I. Marchuk, *Methods of Numerical Mathematics*, Springer-Verlag, New York, NY, 1975.

[29] G.I. Marchuk, Splitting and alternating direction methods. In Ciarlet, P.G., and Lions, J.L. (eds.) *Handbook of Numerical Analysis*, **Vol I**, North-Holland, Amsterdam, 1990, 197–462.

[30] M. Crouzeix and A. Mignot, *Analyse Numérique des Equations Différentielles Ordiuaires*, Masson, Paris, 1984.

[31] R. Glowinski and P. Le Tallec, *Augmented Lagrangians and Operator Splitting Methods in Nonlinear Mechanics*, SIAM, Philadelphia, PA, 1989.

[32] R. Glowinski, Viscous flow simulation by finite element methods and related numerical techniques. In Murman, E.M., and Abarbanel, S.S. (eds.) *Progress and Supercomputing in Computational Fluid Dynamics*, Birkhauser, Boston, MA, 1985, 173–210.

[33] R. Glowinski, Splitting methods for the numerical solution of the incompressible Navier-Stokes equations. In Balakrishnan, A.V., Dorodnitsyn, A.A., and Lions, J.L. (eds.) *Vistas in Applied Mathematics*, Optimization Software, New York, NY, 1986, 57–95.

[34] G. Strang, On the construction and comparison of difference schemes, *SIAM J. Num. Anal.*, **5**(1968), 506–517.

[35] J.T. Beale and A. Majda, Rates of convergence for viscous splitting of the Navier-Stokes equations, *Math. Comp.*, **37**(1981), 243–260.

[36] R. Leveque and J. Oliger, Numerical methods based on additive splitting for hyperbolic partial differential equations, *Math. Comp.*, **37** (1983), 243–260.

[37] P.A. Raviart and J.M. Thomas, *Introduction à l'Analyse Numérique des Equations aux Dérivées Partielles*, Masson, Paris, 1983.

[38] A.J. Chorin, A numerical method for solving incompressible viscous flow problems, *J. Comp. Phys.*, **2** (1967), 12–26.

[39] A.J. Chorin, Numerical solution of the Navier-Stokes equations, *Math. Comp.*, **23** (1968), 341–354.

[40] R. Temam, Sur l'approximation des équations de Navier-Stokes par la méthode des pas fractionnaires (I), *Arch. Rat. Mech. Anal.*, **32** (1969), 135–153.

[41] R. Temam, Sur l'approximation des équations de Navier-Stokes par la méthode des pas fractionnaires (II), *Arch. Rat. Mech. Anal.*, **33** (1969), 377–385.

[42] A. Quarteroni and A. Valli, *Numerical Approximation of Partial Differential Equations*, Springer-Verlag, Berlin, 1994.

[43] J. Daniel, *The Approximate Minimization of Functionals*, Prentice Hall, Englewood Cliffs, NJ, 1970.

[44] E. Polak, *Computational Methods in Optimization*, Academic Press, New York, NY, 1971.

[45] M.R. Hestenes and E.L. Stiefel, Methods of conjugate gradients for solving linear systems, *J. Res. Bureau National Standards*, Section B, **49** (1952), 409–436.

[46] R.W. Freund, G.H. Golub, and N.M. Nachtigal, Iterative solution of linear systems, *Acta Numerica 1992*, Cambridge University Press, 1992, 57–100.

[47] J. Nocedal, Theory of algorithms for unconstrained optimization, *Acta Numerica 1992*, Cambridge University Press, 1992, 199–242.

[48] C.T. Kelley, *Iterative Methods for Linear and Nonlinear Equations*, SIAM, Philadelphia, PA, 1995.

[49] Y. Saad, *Iterative Methods for Sparse Linear Systems*, PWS, Boston, MA, 1995.

[50] G.H. Golub and D.P. O'Leary, Some history of the conjugate gradient and Lanczos algorithms: 1948-1976, *SIAM Review*, **31** (1989), 50–102.

[51] E. Zeidler, *Nonlinear Functional Analysis and its Applications. Volume I: Fixed-Point Theorems*, Springer-Verlag, New York, NY, 1986.

[52] I. Ekeland and R. Teman, *Convex Analysis and Variational Problems*, North-Holland, Amsterdam, 1976.

[53] J.M. Ortega and W.C. Rheinboldt, *Iterative Solution of Nonlinear Equations in Several Variables*, Academic Press, New York, NY, 1970.

[54] J.M. Ortega, and W.C. Rheinboldt, Local and global convergence of generalized linear iterations. In Ortega, J.M., and Rheinboldt, W.C. (eds.) *Numerical Solution of Nonlinear Problems*, SIAM, Philadelphia, PA, 1970.

[55] J.M. Ortega and W.C. Rheinboldt, A general convergence result for unconstrained minimization methods, *SIAM J. Num. Anal.*, **9** (1972), 40–43.

[56] M. Avriel, *Nonlinear Programming: Analysis and Methods*, Prentice-Hall, Englewood Cliffs, NJ, 1976.

[57] M.J.D. Powell, Some convergence properties of the conjugate gradient method, *Math. Program.*, **11** (1976), 42–49.

[58] M.J.D. Powell, Restart procedures of the conjugate gradient method, *Math. Program.*, **12** (1977), 148–162.

[59] V. Girault and P.A. Raviart, *Finite Element Methods for Navier-Stokes Equations: Theory and Algorithms*, Springer-Verlag, Berlin, 1986.

[60] J.B. Hiriart-Urruty and C. Lemarechal, *Convex Analysis and Minimization Algorithms*, Springer-Verlag, Berlin, 1993.

[61] M. Crouzeix, Etude d'une méthode de linéarisation. Résolution numérique des équations de Stokes stationaires. In *Approximations et Méthodes Itératives de Résolution d'Inéquations Variationelles et de Problèmes Non Linéaires,* Cahiers de l'IRIA, **12** (1974), 139-244.

[62] M. Crouzeix, On an operator related to the convergence of Uzawa's algorithm for the Stokes equation. In Bristeau, M.O., Etgen, G., Fitzgibbon, W., Lions, J.L., Périaux, J., and Wheeler, M.F. (eds.) *Computational Science for the 21st Century,* Wiley, Chichester, 1997, 242–259.

[63] J. Cahouet and J.P. Chabard, Some fast 3-D solvers for the generalized Stokes problem, *Int. J. Numer. Meth. in Fluids*, **8** (1988), 269–295.

[64] J.E. Dennis and R.B. Schnabel, A view of unconstrained optimization. In Newhauser, G.L., Rinnooy Kan, A.H.G., and Todd, M.J. (eds.) *Handbook in Operations Research and Management Science,* **Vol. 1***: Optimization,* North-Holland, Amsterdam, 1989, 1–66.

[65] F. Thomasset, *Implementation of Finite Element Methods for Navier-Stokes Equations*, Springer-Verlag, New York, NY, 1981.

[66] R. Peyret and T.D. Taylor, *Computational Methods for Fluid Flow*, Springer-Verlag, New York, NY, 1982.

[67] C. Cuvelier, A. Segal, and A. Van Steenhoven, *Finite Element Methods and Navier-Stokes Equations*, Reidel, Dordrecht, 1986.

[68] M. Fortin, Finite element solution of the Navier-Stokes equations, *Acta Numerica 1993*, Cambridge University Press, 1993, 239–284.

[69] M.D. Gunzburger, *Finite Element Methods for Viscous Incompressible Flows*, Academic Press, Boston, MA, 1989.

[70] C.A.J. Fletcher, *Computational Techniques for Fluid Dynamics, Volume 1: Fundamental and General Techniques*, Springer-Verlag, Berlin, 1991.

[71] C.A.J. Fletcher, *Computational Techniques for Fluid Dynamics, Volume 2: Specific Techniques for Different Flow Categories*, Springer-Verlag, Berlin, 1991.

[72] M.D. Gunzburger and R.A. Nicolaides (eds.), *Incompressible Computational Fluid Dynamics,* Cambridge University Press, New York, NY, 1993.

[73] L. Quartapelle, *Numerical Solution of the Incompressible Navier-Stokes Equations*, Birkhauser, Basel, 1993.

[74] F.K. Hebeker, R. Rannacher, and G. Wittum (eds.), *Numerical Methods for the Navier-Stokes Equations*, Vieweg, Braunschweig/Wiesbaden, 1994.

[75] P.M. Gresho and R.L. SANI, *Incompressible Flow and the Finite Element Method: Advection-Diffusion and Isothermal Laminar Flow,* J. Wiley, Chichester, 1998.

[76] E. Fernandez-Cara and M.M. Beltran, The convergence of two numerical schemes for the Navier-Stokes equations, *Numerische Mathematik*, **55** (1989), 33–60.

[77] P. Kloucek and F.S. Rys, On the stability of the fractional step-θ-scheme for the Navier-Stokes equations, *SIAM J. Num. Anal.*, **31** (1994), 1312–1335.

[78] P. Hood and C. Taylor, A numerical solution of the Navier-Stokes equations using the finite element technique, *Computers and Fluids*, **1** (1973), 73–100.

[79] M. Bercovier and O. Pironneau, Error estimates for finite element method solution of the Stokes problem in the primitive variables, *Numer. Math.*, **33** (1979), 211–224.

[80] G. Strang and G. Fix, *An Analysis of the Finite Element Method*, Prentice Hall, Englewood Cliffs, NJ, 1973.

[81] P.G. Ciarlet, Basic error estimates for elliptic problems. In Ciarlet, P.G., and Lions, J.L. (eds.) *Handbook of Numerical Analysis*, **Vol. II**, North-Holland, Amsterdam, 1991, 17–351.

[82] R. Glowinski, Finite element methods for the numerical simulation of incompressible viscous flow. Introduction to the control of the Navier-Stokes equations. In Anderson, C.R., and Greengard, C. (eds.) *Vortex Dynamics and Vortex Methods*, Lecture in Applied Mathematics, Vol. 28, American Mathematical Society, Providence, RI, 1991, 219–301.

[83] M.O. Bristeau, R. Glowinski, and J. Periaux, Numerical methods for the Navier-Stokes equations. Applications to the simulation of compressible and incompressible viscous flow, *Computer Physics Reports*, **6** (1987), 73–187.

[84] E.J. Dean, R. Glowinski, and C.H. Li, Supercomputer solution of partial differential equation problems in Computational Fluid Dynamics and in Control, *Computer Physics Communications*, **53** (1989), 401–439.

[85] R. Glowinski and O. Pironneau, Finite element methods for Navier-Stokes equations, *Annual Review of Fluid Mechanics*, **24** (1992), 167–204.

[86] T.J.R. Hughes, L.P. Franca, and M. Balestra, A new finite element formulation for Computational Fluid Dynamics: V. Circumventing the Babaska-Brezzi Condition; A stable Petrov-Galerkin formulation of the Stokes problem accomodating equal-order interpolation, *Comp. Meth. Appl. Mech. Eng.*, **59** (1986), 85–100.

[87] J. Douglas and J. Wang, An absolutely stabilized finite element method for the Stokes problem, *Math. Comp.*, **52** (1989), 495–508.

[88] Z. Cai and J. Douglas, An analytic basis for multigrid methods for stabilized finite element methods for the Stokes problem. In Bristeau, M.O., Etgen, G., Fitzgibbon, W., Lions, J.L., Periaux, J., and Wheeler, M.F. (eds.) *Computational Science for the 21st Century*, Wiley, Chichester, 1997, 113–118.

[89] R. Glowinski and C.H. Li, On the numerical implementation of the Hilbert Uniqueness Method for the exact boundary controllability of the wave equation, *C.R. Acad. Sc., Paris*, t. 311 (1990), Série I, 135-142.

[90] Glowinski, R., C.H. Li, and J.L. Lions, A numerical approach to the exact boundary controllability of the wave equation (I) Dirichlet controls: Description of the numerical methods, *Japan J. Applied Math.*, **7** (1990), 1–76.

[91] R. Glowinski and J.L. Lions, Exact and approximate controllability for distributed parameter systems, Part II, *Acta Numerica 1995*, Cambridge University Press, 1995, 159–333.

[92] M. Crouzeix and P.A. Raviart, Conforming and nonconforming finite element methods for solving the stationary Stokes equations, *Revue Française d'Automatique, Informatique et Recherche Opérationnelle*, **R3** (1973), 33–76.

[93] J.E. Roberts and J.M. Thomas, Mixed and hybrid methods. In Ciarlet, P.G., and Lions, J.L. (eds.) *Handbook of Numerical Analysis*, **Vol. II**, North-Holland, Amsterdam, 1991, 523–639.

[94] R. Verfurth, Error estimates for a mixed finite element approximation of the Stokes problem, *Revue Française d'Automatique, Informatique et Recherche Opérationelle, Anal. Numer.*, **18** (1984), 175–182.

[95] R. Glowinski, T.W. Pan, T.I. Hesla, and D.D. Joseph, A distributed Lagrange multiplier/fictitious domain method for particulate flow, *Int. J. Multiphase Flow*, **25** (1999), 755–794.

[96] R. Glowinski, T.W. Pan, T.I. Hesla, D.D. Joseph, and J. Periaux , A distributed Lagrange multiplier/fictitious domain method for flows around moving rigid bodies: Application to particulate flow, *Int. J. Numer. Meth. in Fluids,* **30** (1999), 1043–1066.

[97] R. Glowinski, T.W. Pan, T.I. Hesla, D.D. Joseph, and J. Periaux, A distributed Lagrange multiplier/fictitious domain method for the simulation of flow around moving rigid bodies: Application to particulate flow, *Comp. Meth. Appl. Mech. Eng.,* **184** (2000), 241–267.

[98] R. Glowinski, T.W. Pan, T.I. Hesla, D.D. Joseph, and J. Periaux, A fictitious domain approach to the direct numerical simulation of incompressible viscous fluid flow past moving rigid bodies: Application to particulate flow, *J. Comp. Phys.,* **169** (2001), 363–426.

[99] S. Turek, A comparative study of time-stepping techniques for the incompressible Navier-Stokes equations: from fully implicit non-linear schemes to semi-implicit projection methods, *Int. J. Num. Math. in Fluids*, **22**(1996), 987-1011.

[100] E.J. Dean, R. Glowinski. A wave equation approach to the numerical solution of the Navier-Stokes equations for incompressible viscous flow, *C.R. Acad. Sci. Paris*, t. 325, Série I, (1997), 783–791.

[101] E. Dean, R. Glowinski, T.-W. Pan. A wave equation approach to the numerical simulation of incompressible viscous fluid flow modeled by the Navier-Stokes equations, in *Mathematical and numerical aspects of wave propagation*, J. De Santo ed., SIAM, Philadelphia, 1998, 65–74.

[102] R. Glowinski, O. Pironneau, Finite Element Methods for Navier-Stokes Equations, *Annu. Rev. Fluid Mech.*, **24**(1992), 167–204.

[103] C. Johnson, Streamline diffusion methods for problems in fluid mechanics, in *Finite Element in Fluids 6*, R. Gallagher ed., Wiley, 1986.

[104] U. Ghia, K.N. Ghia, and C.T. Shin, High-Reynolds solutions for incompressible flow using Navier-Stokes equations and a multigrid method, *J. Comp. Phys.*, **48**(1982), 387–411.

[105] R. Schreiber, H.B. Keller, Driven cavity flow by efficient numerical techniques, *J. Comp. Phys.*, **40**(1983), 310–333.

[106] C.H. Bruneau and C. Jouron, Un nouveau schéma décentré pour le probléme de la cavité entraînée, *C.R. Acad. Sci. Paris*, t. 307, Série I (1988), 359–362.

[107] J. Shen, Hopf bifurcation of the unsteady regularized driven cavity flow, *J. Comp. Phys.*, **95**(1991), 228–245.

[108] O. Goyon, High-Reynolds number solutions of Navier-Stokes equations using incremental unknowns, *Comput. Methods Appl. Mech. Engrg.*, **130** (1996), 319–335.

[109] S. Fujima, M. Tabata, Y. Fukasawa, Extension to three-dimensional problems of the upwind finite element scheme based on the choice up- and downwind points, Comp. Meth. Appl. Mech. Eng., **112**(1994), 109–131.

[110] H.C. Ku, R.S. Hirsh, T.D. Taylor, A pseudospectral method for solution of the three-dimensional incompressible Navier-Stokes equations, *J. Comp. Phys.*, **70**(1987), 439–462.

[111] T.P. Chiang, W.H. Sheu, R.R. Hwang, Effect of Reynolds number on the eddy structure in a lid–driven cavity, *Int. J. Numer. Meth. in Fluids,* **26**(1998), 557–579.

[112] A.K. Prasad and J.R. Koseff, Renolds number and end-wall efftects on a lid-driven cavity flow, *Phys. Fluids*, **A 1** (1989), 208–218.

Bol. Soc. Esp. Mat. Apl.
n°38(2007), 39–67

AN INTRODUCTION TO THE FINITE VOLUME METHOD FOR THE EQUATIONS OF GAS DYNAMICS

RICHARD SANDERS

Department of Mathematics, University of Houston
Houston, TX 77204-3476

sanders@math.uh.edu

1 Introduction

These notes are designed to give the student a brief introduction to many of the techniques used to solve the equations of high speed gas dynamics by the finite volume method. We give a somewhat classical presentation; most topics discussed here first appeared in the literature well over twenty years ago. Our goal is to give enough information and with sufficient detail so that the student can develop his or her own computer code to solve these interesting and challenging partial differential equations.

Section numbers and titles contained here are: (2) The Equations Governing Compressible Gas Dynamics, (3) Eigenvalues and Eigenvectors for the Euler Flux Jacobian, (4) Mathematical Preliminaries for the Hyperbolic Conservation Law, (5) Riemann Problems and Riemann Solvers, (6) High Order Godunov Schemes in One Space Dimension, and (7) Multidimensional Problems and the Finite Volume Method.

2 The Equations Governing Compressible Gas Dynamics

An observable volume of gas is composed of a huge number of discrete particles (e.g. air at room conditions has 2×10^{19} molecules/cm^3). What distinguishes a gas from a liquid is the average distance between fluid particles – gas molecules are typically separated by distances much much larger than the range of their inter-molecular collisional forces. Macroscopic flow variables such as density, velocity and temperature, quantities which are often regarded as characterizing a fluid continuum, are in reality observable manifestations of averaged microscopic quantities. We most often compute a flow in terms of these macroscopic variables. However, the microscopic picture can play an interesting role when modeling the thermodynamic and viscous properties of a gas observed at macroscopic scales.

Fecha de recepción: 21/10/2005

For the moment, suppose the positions of a continuum of fluid particles evolve according to the the differential equation

$$\frac{d}{dt}\,\mathbf{x} = \mathbf{v}(\mathbf{x}, t), \tag{1}$$

where we let $\mathbf{x}(\mathbf{y}; t)$ denote the position of a (macroscopic) particle at time t satisfying the initial condition $\mathbf{x}(\mathbf{y}; 0) = \mathbf{y}$. The following fact concerning the map from $\mathbf{R}^3 \to \mathbf{R}^3$ induced by $\mathbf{x}(\,\cdot\,; t)$ is easy to deduce from the product rule for determinants.

FACT. *If the velocity field* $\mathbf{v}$ *is differentiable, we have for any sufficiently small* $t > 0$

$$\frac{d}{dt}\det\left(\frac{\partial \mathbf{x}}{\partial \mathbf{y}}\right) = (\nabla \cdot \mathbf{v})\det\left(\frac{\partial \mathbf{x}}{\partial \mathbf{y}}\right).$$

This simple fact allows us to derive an important relationship for quantities which evolve along a fluid flow.

Theorem 1 (The Transport Theorem.) *Let* $\Omega(t)$ *denote a volume of fluid fixed to the flow of (1). That is,* $\Omega(t) = \{\ \mathbf{x}(\mathbf{y}; t) : \mathbf{y} \in \Omega(0)\ \}$. *Then as long as* $\Omega(t)$ *remains bounded, we have*

$$\frac{d}{dt}\int_{\Omega(t)} f(\mathbf{x}, t)\, d\mathbf{x} = \int_{\Omega(t)} \left(\frac{\partial}{\partial t} f + \nabla \cdot (\mathbf{v} f)\right) d\mathbf{x},$$

where $f(\mathbf{x}, t)$ *is any smooth scalar function of* $\mathbf{x}$ *and* t.

To see this result is true, change variables to write

$$\int_{\Omega(t)} f(\mathbf{x}, t)\, d\mathbf{x} = \int_{\Omega(0)} f(\mathbf{x}(\mathbf{y}; t), t)\det\left(\frac{\partial \mathbf{x}}{\partial \mathbf{y}}\right) d\mathbf{y},$$

differentiate this and use the earlier stated fact to find

$$\begin{aligned}
\frac{d}{dt}\int_{\Omega(t)} f(\mathbf{x}, t)\, d\mathbf{x} &= \int_{\Omega(0)} \frac{d}{dt}\left(f(\mathbf{x}(\mathbf{y}; t), t)\det\left(\frac{\partial \mathbf{x}}{\partial \mathbf{y}}\right)\right) d\mathbf{y} \\
&= \int_{\Omega(0)} \left(\left(\frac{\partial}{\partial t} f + \nabla f \cdot \frac{d\mathbf{x}}{dt}\right)\det\left(\frac{\partial \mathbf{x}}{\partial \mathbf{y}}\right) + f\frac{d}{dt}\det\left(\frac{\partial \mathbf{x}}{\partial \mathbf{y}}\right)\right) d\mathbf{y} \\
&= \int_{\Omega(0)} \left(\frac{\partial}{\partial t} f + \nabla f \cdot \mathbf{v} + f\,\nabla \cdot \mathbf{v}\right)\det\left(\frac{\partial \mathbf{x}}{\partial \mathbf{y}}\right) d\mathbf{y}.
\end{aligned}$$

Finally, use $\nabla f \cdot \mathbf{v} + f\,\nabla \cdot \mathbf{v} = \nabla \cdot (\mathbf{v} f)$ and pull variables back to $\Omega(t)$ to obtain the desired identity.

Actually, the transport theorem is physically obvious. The time rate of change of $\int_{\Omega(t)} f(\mathbf{x}, t)\, d\mathbf{x}$ must be equal to the sum of the time rate of change of f over $\Omega(t)$ plus the flux of f across the boundary of $\Omega(t)$ due to the flow. This latter component is given by $\int_{\partial\Omega(t)} (f\,\mathbf{v} \cdot \mathbf{n})\, ds$ and the former by

$\int_{\Omega(t)} (df/dt)\, d\mathbf{x} = \int_{\Omega(t)} (f_t + \nabla f \cdot \mathbf{v})\, d\mathbf{x}$. Applying the divergence theorem to the boundary integral shows that this physical interpretation is indeed completely justified.

The partial differential equations which govern the time evolution of a compressible gas can be derived by considering various physical balances applied to an arbitrary volume, say $\Omega(t)$, fixed to the flowing fluid. The total mass of $\Omega(t)$ is given by

$$\text{Mass}(\Omega(t)) = \int_{\Omega(t)} \rho(\mathbf{x}, t)\, d\mathbf{x},$$

where $\rho(\mathbf{x}, t)$ is the mass density of the fluid at position $\mathbf{x}$ and time t. The momentum carried by $\Omega(t)$ is given by

$$\text{Momentum}(\Omega(t)) = \int_{\Omega(t)} \rho(\mathbf{x}, t)\mathbf{v}(\mathbf{x}, t)\, d\mathbf{x},$$

where $\mathbf{v}$ is the fluid's velocity. The total energy contained in $\Omega(t)$ is

$$\text{Energy}(\Omega(t)) = \int_{\Omega(t)} \rho(\mathbf{x}, t)\, e(\mathbf{x}, t)\, d\mathbf{x},$$

where here e denotes the total energy density per unit mass given by the sum of kinetic and internal energy per unit mass $e = 1/2|\mathbf{v}|^2 + \epsilon$. Now, since mass is neither created or destroyed, we have from the transport theorem

$$\frac{d}{dt}\,\text{Mass}(\Omega(t)) = 0 \quad \Longrightarrow \quad \int_{\Omega(t)} (\rho_t + \nabla \cdot (\rho\, \mathbf{v}))\, d\mathbf{x} = 0.$$

Since $\Omega(t)$ is arbitrary, this yields the pointwise conservation of mass equation

$$\text{(mass)} \qquad \frac{\partial \rho}{\partial t} + \nabla \cdot (\rho\, \mathbf{v}) = 0.$$

Newton's second law states that the time rate of change of the momentum of a body is equal to the forces acting on it. That is

$$\frac{d}{dt}\,\text{Momentum}(\Omega(t)) = \text{Force}(\Omega(t)) \quad \Longrightarrow$$
$$\int_{\Omega(t)} \left(\frac{\partial}{\partial t} \rho\, \mathbf{v} + \nabla \cdot (\rho\, \mathbf{v} \otimes \mathbf{v}) \right) d\mathbf{x} = \text{Force}(\Omega(t)).$$

The forces acting on the volume $\Omega(t)$ are decomposed into body forces, that is forces which act on all fluid particles within a volume, and surface stresses, or forces which act only on the surface of a volume. A convenient way to write the surface stress term is the following: The force exerted on a surface element ds is given by $\Sigma(\mathbf{x}, t)\mathbf{n}\, ds$ where $\mathbf{x} \in \partial\Omega(t)$, $\mathbf{n}$ is the outward normal to $\Omega(t)$ at $\mathbf{x}$, and $\Sigma(\mathbf{x}, t)$ is a 3×3 stress tensor. Letting $\mathbf{f}_b$ denote the body force, write and then apply the divergence theorem to find

$$\text{Force}(\Omega(t)) = \int_{\partial\Omega(t)} (\Sigma\ \mathbf{n}) ds + \int_{\Omega(t)} (\mathbf{f}_b) d\mathbf{x} = \int_{\Omega(t)} (\nabla \cdot \Sigma + \mathbf{f}_b)\, d\mathbf{x},$$

which yields the pointwise conservation of momentum equation

$$\text{(momentum)} \qquad \frac{\partial}{\partial t}\rho\mathbf{v} + \nabla\cdot(\rho\mathbf{v}\otimes\mathbf{v}) = \nabla\cdot\Sigma + \mathbf{f}_b.$$

Neglecting internal heat generation, the first law of thermodynamics states that the time rate of change of the total energy contained in $\Omega(t)$,

$$\frac{d}{dt}\,\text{Energy}(\Omega(t)),$$

is equal to the rate of heat gained or lost by conduction across its boundary plus the rate of work done by the forces acting on it. The rate due to heat flux across the boundary of $\Omega(t)$ can be written in the form $\int_{\partial\Omega(t)}(\mathbf{q}\cdot\mathbf{n})\,ds$, and the work rate induced by the shear and body forces, whose form is given above, is $\int_{\partial\Omega(t)}(\mathbf{v}\cdot\Sigma\mathbf{n})\,ds + \int_{\Omega(t)}(\mathbf{v}\cdot\mathbf{f}_b)\,d\mathbf{x}$. Applying the divergence theorem to the boundary terms, we find that

$$\frac{d}{dt}\,\text{Energy}(\Omega(t)) = \int_{\Omega(t)}(\nabla\cdot\mathbf{q} + \nabla\cdot(\mathbf{v}\cdot\Sigma) + \mathbf{v}\cdot\mathbf{f}_b)\,d\mathbf{x}.$$

Therefore, the transport theorem can be again applied to deduce the pointwise conservation of energy equation

$$\text{(energy)} \qquad \frac{\partial}{\partial t}\rho e + \nabla\cdot(\rho e\mathbf{v} - (\mathbf{v}\cdot\Sigma)) = \nabla\cdot\mathbf{q} + \mathbf{v}\cdot\mathbf{f}_b.$$

It is convenient to decompose the stress tensor Σ into the sum of a scalar pressure times the identity plus what is called the viscous stress tensor. That is,

$$\Sigma = -pI + \Sigma^{\mathcal{V}}.$$

With this, we can rewrite the conservation equations above as

$$\begin{aligned}
&\text{(mass)} && \frac{\partial}{\partial t}\rho + \nabla\cdot(\rho\mathbf{v}) = 0,\\
&\text{(momentum)} && \frac{\partial}{\partial t}\rho\mathbf{v} + \nabla\cdot(\rho\mathbf{v}\otimes\mathbf{v}) + \nabla p = \nabla\cdot\Sigma^{\mathcal{V}} + \mathbf{f}_b, \qquad (2)\\
&\text{(energy)} && \frac{\partial}{\partial t}\rho e + \nabla\cdot((\rho e + p)\mathbf{v}) = \nabla\cdot\left(\mathbf{v}\cdot\Sigma^{\mathcal{V}}\right) + \nabla\cdot\mathbf{q} + \mathbf{v}\cdot\mathbf{f}_b
\end{aligned}$$

Physics is now required to close this system of equations. Specifically, the pressure p, the viscous stress $\Sigma^{\mathcal{V}}$ and the heat flux $\mathbf{q}$ must be related to the natural flow variables density ρ, velocity $\mathbf{v}$ and specific total energy e. In most compressible flow simulations, the body force $\mathbf{f}_b$ is either neglected or is assumed to be independently given. Interesting examples where this can not be assumed are self gravitating gases and/or plasmas.

The form of Σ can be closed in terms of measurable state quantities by modeling the fluid as a haze of discrete particles having macroscopic mean

velocity with microscopic random fluctuations superimposed. To determine a formula for Σ to first approximation, suppose that a particle's velocity is given by $\mathbf{v} + \mathbf{v}'$ where $\mathbf{v}'$ is a mean zero random variable. Think of $\mathbf{v}'$ as the thermal agitation of a molecule superimposed on the bulk fluid velocity $\mathbf{v}$. Let $f(\mathbf{x}, t; \mathbf{v}')$ denote the number of particles per unit volume at space-time coordinate $(\mathbf{x}, t)$ which have thermal velocity $\mathbf{v}'$. Letting m denote the molecular mass of the gas, write

$$\rho = \int_{\mathbf{R}^3} mf(\cdot; \mathbf{v}')\, d\mathbf{v}', \quad \mathbf{0} = \int_{\mathbf{R}^3} mf(\cdot; \mathbf{v}')\mathbf{v}'\, d\mathbf{v}',$$
$$\rho\epsilon^T = \int_{\mathbf{R}^3} 1/2mf(\cdot; \mathbf{v}')|\mathbf{v}'|^2\, d\mathbf{v}',$$

where ϵ^T denotes the *translational* internal energy of the fluid. (Every molecule has translational internal energy associated to its translational thermal motion. However, there may be other modes of internal energy which play no role in the bulk transport of momentum.) It is reasonable to assume that the distribution f is Gaussian. The Gaussian assumption together with the moments specified above uniquely determines f, yielding the well-known *Maxwellian distribution*:

$$f(\cdot; \mathbf{v}') = \frac{\rho}{m((4/3)\epsilon^T\pi)^{3/2}} \exp\left(-\frac{|\mathbf{v}'|^2}{(4/3)\epsilon^T}\right).$$

(From the *kinetic theory of gases*, this Gaussian assumption can be shown to be a valid first approximation. See [9] for example.) With these assumptions, we wish to measure the flux of momentum in unit time through a surface element of $\Omega(t)$ where the region $\Omega(t)$ is fixed to the mean fluid flow. Given a velocity $\mathbf{v}'$, the particles in a cylinder with volume $|\mathbf{v}' \cdot \mathbf{n}|\, ds$ flow into $\Omega(t)$ through a surface element $\mathbf{n}\, ds$ in unit time. Therefore, the momentum carried by all particles which flow into, and out of, $\Omega(t)$ in unit time through $\mathbf{n}\, ds$ is given by

$$\text{gained through } \mathbf{n}\, ds = \int_{v' \cdot n \le 0} mf(\cdot; \mathbf{v}')\, \mathbf{v}'\, (|\mathbf{v}' \cdot \mathbf{n}|\, ds)\, d\mathbf{v}'.$$

$$\text{lost through } \mathbf{n}\, ds = \int_{v' \cdot n \ge 0} mf(\cdot; \mathbf{v}')\, \mathbf{v}'\, (|\mathbf{v}' \cdot \mathbf{n}|\, ds)\; d\mathbf{v}'.$$

And so the net change of momentum through $\mathbf{n}\, ds$ in unit time is

$$(\Sigma\mathbf{n})\, ds = -2\left(\int_{v' \cdot n \ge 0} mf(\cdot; \mathbf{v}')\, \mathbf{v}'\, |\mathbf{v}' \cdot \mathbf{n}|\, d\mathbf{v}'\right) ds.$$

This integral can be explicitly calculated to yield

$$(\Sigma\mathbf{n}) = \left(-2/3\rho\epsilon^T\right)\mathbf{n}.$$
$$\Longrightarrow \qquad \Sigma = -p\, I \quad \text{with} \quad p = 2/3\rho\epsilon^T.$$

Internal energy ϵ can be calculated from total energy by $\rho e = 1/2\rho|\mathbf{v}|^2 + \rho\epsilon$. A monatomic molecule (a single atom) has only translational internal energy. Therefore, $\epsilon^T = \epsilon$. Diatomic molecules on the other hand, such as N_2 or O_2,

have both translational and *rotational* modes for internal energy; 3 degrees of freedom for translation and 2 for rotation. (Think of the diatomic molecule as a dumbbell.) Assuming the internal energy is distributed equally among the 5 total degrees, we would have $\epsilon^T = 3/5\epsilon$. From this discussion, we find a reasonable expression for pressure (sometimes called static or scalar pressure)

$$p = (\gamma - 1)\rho\epsilon, \quad \text{where} \quad \gamma = \begin{cases} 1 + \frac{2}{3} & \text{for a monatomic gas} \\ 1 + \frac{2}{5} & \text{for a diatomic gas (air).} \end{cases} \tag{3}$$

The above simple microscopic model allowed us to determine a closed form expression for the stress tensor $\Sigma = -p\, I$. However, we assumed fluid particles collide and reach equilibrium instantaneously. In reality, fluid particles travel a short but nonzero distance between collisions, (the average distance is called the gas' *mean free path*). It is possible to increase the level of approximation compared to what was done above by employing a more sophisticated microscopic model. A particularly systematic approach is found by using the Chapman-Enskog expansion to the Boltzmann equation; (again see most any text book treating the kinetic theory of gases). From these more detailed models of molecular collision, one can deduce that $\Sigma = -p\, I + \Sigma^v$, where the viscous stress tensor is given by

$$\Sigma^v = \mu_1(T)\left((\nabla \mathbf{v}) + (\nabla \mathbf{v})^t\right) + (\mu_2(T) - 2/3\mu_1(T))\,\mathrm{div}(\mathbf{v})\, I. \tag{4}$$

$\mu_1(T)$ and $\mu_2(T)$ are positive functions of the fluid's temperature T. (Kinetic theory is somewhat weak in predicting the actual values of μ_1 and μ_2. Often μ_2 is taken to be zero based on force balance considerations, and the value of μ_1 is assigned by an empirical law.) Newton was able to deduce the explicit functional form for Σ^v given above by essentially experimental reasoning. Fluids which have viscous stress tensors of this form are called Newtonian. Most gases can be regarded as Newtonian.

Fourier's name is attached to a form for the heat flux vector; namely $\mathbf{q} = k\nabla T$. The temperature T is proportional to internal energy $c_p T = \epsilon$ where c_p is a constant. This formula for $\mathbf{q}$ is called Fourier's law.

When the viscous stress tensor Σ^v and heat conduction $\mathbf{q}$ are neglected, we are led to a closed system of partial differential equations called the *compressible Euler equations*

$$\begin{aligned} &\frac{\partial}{\partial t}\rho + \nabla \cdot (\rho \mathbf{v}) = 0 \\ &\frac{\partial}{\partial t}\rho\mathbf{v} + \nabla \cdot (\rho \mathbf{v} \otimes \mathbf{v}) + \nabla p = 0 \qquad p = p(\rho, \epsilon) \\ &\frac{\partial}{\partial t}\rho e + \nabla \cdot ((\rho e + p)\mathbf{v}) = 0. \end{aligned} \tag{5}$$

This system is completed with appropriate boundary and initial conditions. The compressible Euler system is often used as a base set of equations in aerospace applications. Solving these around a proposed flight vehicle is often sufficient

to decide the vehicle's gross flight characteristics – for velocities ranging from subsonic to fairly large Mach numbers.

3 Eigenvalues and Eigenvectors for the Euler Flux Jacobian

In this section we compute the eigenvalues and eigenvectors to the Jacobian matrices of Euler equations fluxes. We encourage the reader to skip this section on first reading. However, knowing the explicit form of these matrices is necessary in order to employ the numerical techniques we present later.

We write ()5) in flux form:

$$\frac{\partial}{\partial t}\mathbf{V} + \frac{\partial}{\partial x_1}\mathbf{F}_1 + \frac{\partial}{\partial x_2}\mathbf{F}_2 + \frac{\partial}{\partial x_3}\mathbf{F}_3 = \mathbf{0},$$

where

$$\mathbf{V} = \begin{pmatrix} \rho \\ \rho\mathbf{v} \\ \rho e \end{pmatrix} \quad \text{and for } j = 1,2,3 \quad \mathbf{F}_j(\mathbf{V}) = \begin{pmatrix} \rho v_j \\ \rho\mathbf{v}v_j + p\,\mathbf{b}_j \\ (\rho e + p)v_j \end{pmatrix}. \tag{6}$$

The pressure p is assumed to be a function of ρ and specific internal energy $\epsilon = e - 1/2|\mathbf{v}|^2$. Each vector $\mathbf{b}_j$ is a unit vector pointing in the x_j direction.

We first calculate the eigenvalues and eigenvectors of the Jacobian matrix $D\mathbf{F}_1/D\mathbf{V}$

$$\left(\frac{D\mathbf{F}_1}{D\mathbf{V}}\right)_{i,j} = \frac{\partial}{\partial V_j}(\mathbf{F}_1(\mathbf{V}))_i.$$

Our work will be made considerably easier if we change to so-called *primitive variables*

$$\mathbf{W} = \begin{pmatrix} \rho \\ \mathbf{v} \\ \epsilon \end{pmatrix}.$$

Observe that by the chain rule

$$\frac{D\mathbf{F}_1}{D\mathbf{V}} = \frac{D\mathbf{F}_1}{D\mathbf{W}}\frac{D\mathbf{W}}{D\mathbf{V}},$$

and so we find by an explicit calculation

$$\frac{D\mathbf{V}}{D\mathbf{W}} = \begin{pmatrix} 1 & 0 & 0 \\ \mathbf{v} & \rho I_3 & 0 \\ \kappa + \epsilon & \rho\mathbf{v}^t & \rho \end{pmatrix},$$

$$\frac{D\mathbf{W}}{D\mathbf{V}} = \left(\frac{D\mathbf{V}}{D\mathbf{W}}\right)^{-1} = \frac{1}{\rho}\begin{pmatrix} \rho & 0 & 0 \\ -\mathbf{v} & I_d & 0 \\ \kappa - \epsilon & -\mathbf{v}^t & 1 \end{pmatrix},$$

where κ represents the specific kinetic energy $1/2|\mathbf{v}|^2$, and I_3 represents the 3×3 identity matrix. Now, a fairly lengthy calculation will reveal

$$\left[\frac{D\mathbf{W}}{D\mathbf{V}}\ \frac{D\mathbf{F}_1}{D\mathbf{W}}\right] = \begin{pmatrix} v_1 & \rho & 0 & 0 \\ p_\rho/\rho & v_1 & 0 & p_\epsilon/\rho \\ 0 & 0 & v_1 I_2 & 0 \\ 0 & p/\rho & 0 & v_1 \end{pmatrix}.$$

Above $p_\rho = \partial p(\rho, \epsilon)/\partial\rho$ and $p_\epsilon = \partial p(\rho, \epsilon)/\partial\epsilon$. Here I_2 denotes the 2×2 identity matrix. Determining the eigenvalue and eigenvectors to this matrix, which is similar to $(D\mathbf{F}_1/D\mathbf{V})$ since

$$\frac{D\mathbf{W}}{D\mathbf{V}}\ \frac{D\mathbf{F}_1}{D\mathbf{V}} = \left[\frac{D\mathbf{W}}{D\mathbf{V}}\ \frac{D\mathbf{F}_1}{D\mathbf{W}}\right] \frac{D\mathbf{W}}{D\mathbf{V}},$$

is now relatively straight forward. Clearly one easily sees that $\lambda = v_1$ is an eigenvalue to $[(D\mathbf{W}/D\mathbf{V})\,(D\mathbf{F}_1/D\mathbf{W})]$ with associated eigenvectors

$$\lambda = v_1 \qquad \overline{\mathbf{r}}_1 = \begin{pmatrix} p_\epsilon \\ 0 \\ 0 \\ 0 \\ -p_\rho \end{pmatrix} \qquad \overline{\mathbf{r}}_2 = \begin{pmatrix} 0 \\ 0 \\ 1 \\ 0 \\ 0 \end{pmatrix} \qquad \overline{\mathbf{r}}_3 = \begin{pmatrix} 0 \\ 0 \\ 0 \\ 1 \\ 0 \end{pmatrix}.$$

Using these and a change of basis allows us to determine the remaining two eigenvectors by reducing the 5×5 problem to a 2×2 eigenvalue problem. Doing this, we find the remaining two eigenvalues are $\lambda = v_1 - c$ and $\lambda = v_1 + c$, where the speed of sound c is given by

$$c^2 = p_\rho + p p_\epsilon/\rho^2,$$

and the associated eigenvectors are

$$\lambda = v_1 \mp c \qquad \overline{\mathbf{r}}_4 = \begin{pmatrix} \rho \\ -c \\ 0 \\ 0 \\ p/\rho \end{pmatrix} \qquad \overline{\mathbf{r}}_5 = \begin{pmatrix} \rho \\ +c \\ 0 \\ 0 \\ p/\rho \end{pmatrix}.$$

Later we will see that c is indeed the speed at which certain waves (i.e. sound waves) propagate relative to the fluid velocity. A *perfect gas* is one in which its pressure given by the formula $p = (\gamma - 1)\rho\epsilon$ with $\gamma > 1$ constant; see equation (3). Therefore, we compute that the speed of sound for a perfect gas is $c = \sqrt{\gamma(\gamma - 1)\epsilon}$.

The left eigenvectors (we'll need these later) are found by inverting the matrix of right eigenvectors. Using the same ordering as with the right eigenvectors, we find

$$
\begin{aligned}
\lambda = v_1 \qquad & \bar{\mathbf{l}}_1 = \big(1/p_\epsilon - p_\rho/(p_\epsilon c^2), \quad 0, \quad 0, \quad 0, \quad -1/c^2\big) \\
& \bar{\mathbf{l}}_2 = \big(0, \quad 0, \quad 1, \quad 0, \quad 0\big) \\
& \bar{\mathbf{l}}_3 = \big(0, \quad 0, \quad 0, \quad 1, \quad 0\big) \\
\lambda = v_1 - c \quad & \bar{\mathbf{l}}_4 = \frac{1}{2\rho c^2}\big(p_\rho, \quad -\rho c, \quad 0, \quad 0, \quad p_\epsilon\big) \\
\lambda = v_1 + c \quad & \bar{\mathbf{l}}_5 = \frac{1}{2\rho c^2}\big(p_\rho, \quad +\rho c, \quad 0, \quad 0, \quad p_\epsilon\big)\,.
\end{aligned}
$$

Finally, the right and left eigenvectors to the original Jacobian $D\mathbf{F}_1/D\mathbf{V}$, denoted below without the over-bars, can be found by matrix multiplication. That is, for each $k = 1, \ldots, 5$

$$\mathbf{r}_k = \frac{D\mathbf{V}}{D\mathbf{W}}\bar{\mathbf{r}}_k \qquad \mathbf{l}_k = \bar{\mathbf{l}}_k \frac{D\mathbf{W}}{D\mathbf{V}}.$$

Later in these notes, we will consider *upwind finite volume schemes* for solving the multi-dimensional Euler equations. In a finite volume calculation, fluxes of the form

$$\mathbf{F}(\mathbf{U}) \cdot \mathbf{n}$$

must be discretized, where $\mathbf{n}$ is the outward normal to a computational cell, and $\mathbf{F}$ is a spatial vector of fluxes. For upwind schemes, one must determine the eigenvalues and eigenvectors to the Jacobian of $\mathbf{F}(\mathbf{U}) \cdot \mathbf{n}$. We do this next for the single component Euler fluxes. Let the normal vector $\mathbf{n}$ have components $n_{x_1}, n_{x_2}, n_{x_3}$ and plug the Cartesian Euler fluxes into

$$\mathbf{F}(\mathbf{U}) \cdot \mathbf{n} = \mathbf{F}_1(\mathbf{U}) n_{x_1} + \mathbf{F}_2(\mathbf{U}) n_{x_2} + \mathbf{F}_3(\mathbf{U}) n_{x_3}$$

to find

$$\mathbf{F}(\mathbf{U}) \cdot \mathbf{n} = \begin{pmatrix} \rho(\mathbf{u} \cdot \mathbf{n}) \\ \rho\mathbf{u}(\mathbf{u} \cdot \mathbf{n}) + p\,\mathbf{n} \\ (\rho e + p)(\mathbf{u} \cdot \mathbf{n}) \end{pmatrix}.$$

Now, Let R denote a 3×3 rotation matrix composed of the following columns

$$R = \begin{pmatrix} \mathbf{n}_1 & \mathbf{n}_2 & \mathbf{n}_3 \end{pmatrix}$$

where $\mathbf{n}_1, \mathbf{n}_2, \mathbf{n}_3$ is an orthonormal basis with $\mathbf{n}_1$ here denoting the cell normal $\mathbf{n}$. Next, consider a 5×5 orthogonal matrix O given by

$$O = \begin{pmatrix} 1 & 0 & 0 \\ 0 & R & 0 \\ 0 & 0 & 1 \end{pmatrix}.$$

Define the change of variables $\mathbf{U} = O\mathbf{V}$ (or $\mathbf{V} = O^t\mathbf{U}$) to find

$$\mathbf{F}(\mathbf{U}) \cdot \mathbf{n} = \begin{pmatrix} \rho(\mathbf{u} \cdot \mathbf{n}) \\ \rho\mathbf{u}(\mathbf{u} \cdot \mathbf{n}) + p\,\mathbf{n} \\ (\rho e + p)(\mathbf{u} \cdot \mathbf{n}) \end{pmatrix} = \begin{pmatrix} 1 & 0 & 0 \\ 0 & R & 0 \\ 0 & 0 & 1 \end{pmatrix} \begin{pmatrix} \rho v_1 \\ \rho\mathbf{v}v_1 + p\,\mathbf{b}_1 \\ (\rho e + p)v_1 \end{pmatrix} = O\,\mathbf{F}_1(\mathbf{V}).$$

(Recall $\mathbf{b}_1$ is defined in (6).) So again by the chain rule

$$\frac{D}{D\mathbf{U}}(\mathbf{F}(\mathbf{U})\cdot\mathbf{n}) = \frac{D}{D\mathbf{V}}(\mathbf{F}(\mathbf{U})\cdot\mathbf{n})\,\frac{D\mathbf{V}}{D\mathbf{U}} = O\,\frac{D\mathbf{F}_1}{D\mathbf{V}}\,O^t.$$

Therefore, the Jacobian of $\mathbf{F}(\mathbf{U})\cdot\mathbf{n}$ with respect to the variable $\mathbf{U}$ is similar to the Jacobian of $\mathbf{F}_1(\mathbf{V})$ with respect to the rotated variable $\mathbf{V}$. This of course is a consequence of the rotation invariance of the Euler equations. We therefore can compute the right eigenvectors of $D(\mathbf{F}(\mathbf{U})\cdot\mathbf{n})/D\mathbf{U}$ by pre-multiplying the right eigenvectors already listed (i.e. $\bar{\mathbf{r}}_1,\ldots,\bar{\mathbf{r}}_5$) by the matrix

$$O\,\frac{D\mathbf{V}}{D\mathbf{W}} = \begin{pmatrix}1&0&0\\0&R&0\\0&0&1\end{pmatrix}\begin{pmatrix}1&0&0\\\mathbf{v}&\rho I_3&0\\\kappa+\epsilon&\rho\mathbf{v}^t&\rho\end{pmatrix} = \begin{pmatrix}1&0&0\\R\mathbf{v}&\rho R&0\\\kappa+\epsilon&\rho\mathbf{v}^t&\rho\end{pmatrix}$$

Doing so, we arrive at

- $\lambda = (\mathbf{u}\cdot\mathbf{n}_1)$

$$\mathbf{r}_1 = \begin{pmatrix}p_\epsilon\\p_\epsilon\mathbf{u}\\p_\epsilon(\kappa+\epsilon)-\rho p_\rho\end{pmatrix},\quad \mathbf{r}_2 = \rho\begin{pmatrix}0\\\mathbf{n}_2\\v_2\end{pmatrix},\quad \mathbf{r}_3 = \rho\begin{pmatrix}0\\\mathbf{n}_3\\v_3\end{pmatrix}.$$

(Note that above we have used $R\mathbf{v}=\mathbf{u}$, $R\,\mathbf{b}_k=\mathbf{n}_k$ and $v_k=(\mathbf{v}\cdot\mathbf{b}_k)=\mathbf{u}\cdot\mathbf{n}_k$.) The acoustic right eigenvectors are

- $\lambda = (\mathbf{u}\cdot\mathbf{n}_1)\mp c$

$$\mathbf{r}_4 = \rho\begin{pmatrix}1\\\mathbf{u}-c\,\mathbf{n}_1\\(\kappa+\epsilon)-cv_1+p/\rho\end{pmatrix},\qquad \mathbf{r}_5 = \rho\begin{pmatrix}1\\\mathbf{u}+c\,\mathbf{n}_1\\(\kappa+\epsilon)+cv_1+p/\rho\end{pmatrix}.$$

Similarly, we can compute the bi-orthonormal left eigenvectors of $D(\mathbf{F}(\mathbf{U})\cdot\mathbf{n})/D\mathbf{U}$ by post-multiplying the left eigenvectors already listed (i.e. $\bar{\mathbf{l}}_1,\ldots,\bar{\mathbf{l}}_5$) by the matrix

$$\frac{D\mathbf{W}}{D\mathbf{V}}\,O^t = \frac{1}{\rho}\begin{pmatrix}\rho&0&0\\-\mathbf{v}&I_3&0\\\kappa-\epsilon&-\mathbf{v}^t&1\end{pmatrix}\begin{pmatrix}1&0&0\\0&R^t&0\\0&0&1\end{pmatrix} = \frac{1}{\rho}\begin{pmatrix}\rho&0&0\\-\mathbf{v}&R^t&0\\\kappa-\epsilon&-\mathbf{v}^tR^t&1\end{pmatrix}.$$

Doing so, we arrive at

- $\lambda = (\mathbf{u}\cdot\mathbf{n}_1)$

$$\begin{aligned}\mathbf{l}_1 &= \frac{1}{\rho c^2}\left(p/\rho-(\kappa-\epsilon),\quad \mathbf{u}^t,\quad -1\right)\\ \mathbf{l}_2 &= \frac{1}{\rho}\left(-v_2,\quad \mathbf{n}_2^t,\quad 0\right)\\ \mathbf{l}_3 &= \frac{1}{\rho}\left(-v_3,\quad \mathbf{n}_3^t,\quad 0\right)\end{aligned}$$

and

- $\lambda = (\mathbf{u}\cdot\mathbf{n}_1)-c$

$$\mathbf{l}_4 = \frac{1}{2\rho c^2}\left(p_\rho+cv_1+(p_\epsilon/\rho)(\kappa-\epsilon),\quad -c\mathbf{n}_1^t-(p_\epsilon/\rho)\mathbf{u}^t,\quad (p_\epsilon/\rho)\right)$$

- $\lambda = (\mathbf{u}\cdot\mathbf{n}_1) + c$

$$\mathbf{l}_5 = \frac{1}{2\rho c^2}\left(p_\rho - cv_1 + (p_\epsilon/\rho)(\kappa-\epsilon), \quad +c\mathbf{n}_1^t - (p_\epsilon/\rho)\mathbf{u}^t, \quad (p_\epsilon/\rho)\right).$$

4 Mathematical Preliminaries for the Hyperbolic Conservation Law

First order Cauchy problems of the form

$$\frac{\partial}{\partial t}u + \sum_{i=1}^{d}\frac{\partial}{\partial x_i}f_i(u) = 0, \quad t>0 \quad \text{with} \;\; u(x,0) = u_0(x),$$

are often referred to as first order *conservation laws*. The system above is said to be a *hyperbolic* conservation law if the Jacobian matrix $\partial_u f(u)\cdot\mathbf{n}$, ($\mathbf{n}\in\mathbf{R}^d$ is an arbitrary unit vector), has real eigenvalues and a complete set of eigenvectors. It is known that only hyperbolic first order conservation laws are well-posed as initial value problems [10]. Moreover, it is well known that nonlinear hyperbolic conservation laws generally do not have globally defined classical solutions. After finite time, it should be expected that the solution to the nonlinear problem develops solution discontinuities even when its initial data are smooth [12]. For this reason, the notion of a *weak solution* to the hyperbolic conservation law was originally introduced.

A weak solution $u(x,t)$ to the hyperbolic conservation law is a bounded and measurable function which satisfies the integral relation

$$\int_0^\infty \int_{\mathbf{R}^d} u\phi_t + f(u)\cdot\nabla\phi \; dxdt + \int_{\mathbf{R}^d} u_0\phi(x,0)\; dx = 0,$$

for all smooth and compactly supported test functions $\phi(x,t)$. It is easily shown that at points where $u(x,t)$ is differentiable, $u(x,t)$ satisfies the pde in the classical sense. If $u(x,t)$ has a simple jump discontinuity along a smooth surface $\mathcal{S}$ with an outward time-space normal vector $(n_0,\mathbf{n})$, $\mathbf{n}=(n_1,\ldots,n_d)$, a weak solution must satisfy the Rankine-Hugoniot relation

$$[u]\,n_0 + [f(u)]\cdot\mathbf{n} = 0,$$

where $[\;\;]$ denotes the jump in a quantity across $\mathcal{S}$.

We consider the following Cauchy problem for the scalar Burgers' equation

$$\frac{\partial}{\partial t}u + \frac{\partial}{\partial x}(u^2/2) = 0, \quad \text{with} \quad u(x,0) = \begin{cases} -1 & \text{if } x<0 \\ +1 & \text{if } x\geq 0. \end{cases} \tag{7}$$

It is easily verified that

$$u(x,t) = \begin{cases} -1 & \text{if } x\leq -(1+\alpha)t \\ -(1+2\alpha) & \text{if } -(1+\alpha)t < x \leq 0 \\ +(1+2\alpha) & \text{if } 0\leq x < +(1+\alpha)t \\ +1 & \text{if } +(1+\alpha)t \leq x, \end{cases}$$

is a weak solution to Burgers' equation for any $\alpha \geq -1$. One need only check the Rankine-Hugoniot condition along the rays of discontinuity $x = -(1+\alpha)t$, $x = 0$ and $x = (1+\alpha)t$. This example demonstrates that a nonlinear conservation law can have an infinite number of weak solutions. This of course is physically absurd.

In aerodynamics, the first order conservation law serves merely as a model equation in which viscous effects are neglected. Across shock surfaces however, microscopic viscous effects have a considerable influence on the macroscopic flow. These effects can be characterized by the so-called *entropy condition*. We say that the nonlinear conservation law admits a convex entropy if there exists a convex function $V(u)$ and d associated entropy fluxes $F_i(u)$ satisfying $\nabla V(u)\partial_u(f_i(u)) = \nabla F_i(u)$. If the solution to the first order conservation law is the limit of its viscous approximation, and if the conservation law admits a convex entropy function, this limit must satisfy the integral inequality

$$\int_0^\infty \int_{\mathbf{R}^d} V(u)\phi_t + F(u)\cdot\nabla\phi \; dxdt + \int_{\mathbf{R}^d} V(u_0)\phi(x,0) \; dx \geq 0,$$

for all nonnegative test functions $\phi(x,t)$.

For the Burgers' equation example above, an admissible entropy pair is $V(u) = u^2$, $F(u) = \frac{2}{3}u^3$. None of the weak solutions stated above satisfy the entropy condition. Its unique entropy satisfying solution is given by

$$u(x,t) = \begin{cases} -1 & \text{if } x/t \leq -1 \\ x/t & \text{if } -1 < x/t < 1 \\ +1 & \text{if } x/t \geq +1, \end{cases}$$

This solution is called a *rarefaction wave*. Note that it is a continuous function of x when $t > 0$.

Existence and uniqueness of weak entropy satisfying solutions to the scalar Cauchy problem is well known; see [11]. There is a convex entropy for the compressible Euler equations. However, it has yet to be shown in a general setting that an entropy condition satisfying weak solution to the Euler equations is necessarily unique. The fundamental work of Oleinik [16] establishes the uniqueness of entropy condition satisfying weak solutions to the one dimensional hyperbolic system in the class of piecewise smooth solutions containing at most a finite number of simple jump discontinuities. See [12] or [21] for details concerning entropy conditions for hyperbolic systems.

5 Riemann Problems and Riemann Solvers

Most modern finite difference schemes for hyperbolic systems of conservation laws are based to some degree on the Riemann problem solution. The Riemann problem is a one dimensional problem with piecewise constant initial data:

$$\frac{\partial}{\partial t}u + \frac{\partial}{\partial x}f(u) = 0, \quad u(x,0) = \begin{cases} u_L & \text{if } x \leq 0 \\ u_R & \text{if } x > 0. \end{cases}$$

By a similarity argument, one can argue that the solution to the Riemann problem must be constant along rays $x/t = \zeta$. That is, the Riemann problem solution takes the form

$$u(x,t) = R(u_L, u_R; x/t),$$

for some to be determined function $R(u_L, u_R; \zeta)$. Moreover, there are numbers ζ_L and ζ_R (which depend on $f(u)$, u_L and u_R) such that $R(u_L, u_R; \zeta) = u_L$ for all $\zeta \leq \zeta_L$ and $R(u_L, u_R; \zeta) = u_R$ for all $\zeta \geq \zeta_R$. The existence of finite ζ_L and ζ_R follow by the finite speed of propagation principle obeyed by hyperbolic equations.

The Riemann problem for the γ-law compressible Euler equations is uniquely solvable provided the initial states are physical and the jump in the normal component of velocity is not too large; [21]. Its solution is composed of certain centered waves (shocks waves, contact and slip discontinuities and/or rarefaction waves) and can be found (almost) explicitly requiring only a single nonlinear inversion [21]. Unfortunately, this formula is quite complicated analytically and worse, is quite expensive computationally. Moreover, more general equations of state involving, say, real gas effects makes it essentially impossible to use the full Riemann problem solution in production applications.

An approximate Riemann problem solver is a function $R^A(u_L, u_R; \zeta)$ which satisfies the two simple conditions:

(i) $\quad R^A(u, u; \zeta) = u,$

(ii)
$$\int_{-\infty}^{0} \big(R^A(u_L, u_R; \zeta) - u_L\big) d\zeta + \int_{0}^{\infty} \big(R^A(u_L, u_R; \zeta) - u_R\big) d\zeta + f(u_R) - f(u_L) = 0.$$

A simple exercise using the divergence theorem will verify that the exact Riemann problem solution $R(u_L, u_R; \zeta)$ satisfies (ii). Therefore, (ii) actually requires nothing more of an approximate Riemann problem solver than

(ii')
$$\int_{-\infty}^{\infty} \big(R^A(u_L, u_R; \zeta) - R(u_L, u_R; \zeta)\big)\, d\zeta = 0.$$

This is, an approximate Riemann problem solution agrees with the exact Riemann solution in mean.

We now turn our attention to developing certain numerical flux functions for one space dimensional conservation laws. (These will be utilized to construct finite difference schemes in the next section.) A two point numerical flux function $h_f(u_L, u_R) \approx f(R(u_L, u_R; 0))$ is said to be consistent to $f(u)$ if

$$h_f(u, u) = f(u).$$

$h_f(u_L, u_R)$ is also required to be locally Lipschitz continuous. That is,

$$|h_f(u_1, v_1) - h_f(u_2, v_2)| \leq L\,(|u_1 - u_2| + |v_1 - v_2|)$$

for some finite positive constant L. One of the best known numerical flux functions was derived by Godunov [4]. It is given by

$$h_f(u_L, u_R) = f(R(u_L, u_R; 0)),$$

where $R(u_L, u_R; 0)$ is the associated Riemann problem solution evaluated along the ray $\zeta = 0$. However, since this numerical flux requires the analytical resolution of the associated Riemann problem, it is very difficult to derive for all but the simplest conservation laws.

Now, using the notion of approximate Riemann solvers, it is natural to build two point consistent numerical flux functions as follows. Consider

$$h_f(u_L, u_R) = \int_0^\infty \left(R^A(u_L, u_R; \zeta) - u_R\right) d\zeta + f(u_R),$$

or equivalently

$$h_f(u_L, u_R) = -\int_{-\infty}^0 \left(R^A(u_L, u_R; \zeta) - u_L\right) d\zeta + f(u_L),$$

and check that this formula defines a numerical flux which is consistent to $f(u)$. Moreover, when the exact Riemann problem solver is inserted into the formula above, the Godunov numerical flux function is recovered. It is interesting to note that the numerical flux generated by any approximate Riemann problem solver differs from the Godunov flux by

$$h_f(u_L, u_R) = f(R(u_L, u_R; 0)) + \int_0^\infty \left(R^A(u_L, u_R; \zeta) - R(u_L, u_R; \zeta)\right) d\zeta.$$

We conclude this section by deriving three approximate Riemann problem solvers and their associated numerical flux functions.

The Lax-Friedrichs numerical flux. The Lax-Friedrichs approximate Riemann solver is by far and away the simplest we present. One determines from the divergence theorem that

$$\frac{1}{2\Lambda}\int_{-\Lambda}^{\Lambda} R(u_L, u_R; \zeta)\, d\zeta = \frac{1}{2}(u_L + u_R) - \frac{1}{2\Lambda}\left(f(u_R) - f(u_L)\right) \equiv u_M,$$

where Λ is taken large enough so that the range of integration includes ζ_L and ζ_R. We may take as our approximate Riemann problem solution

$$R^A(u_L, u_R, \zeta) = \begin{cases} u_L & \text{if } \zeta < -\Lambda \\ u_M & \text{if } |\zeta| \le \Lambda \\ u_R & \text{if } \zeta > \Lambda \end{cases}$$

since by construction it agrees with the exact Riemann problem solution in mean. Finally, compute

$$\begin{aligned} h_f(u_L, u_R) &= \int_0^\Lambda (u_M - u_R) d\zeta + f(u_R) \\ &= \frac{1}{2}\left(-\Lambda(u_R - u_L) + f(u_L) + f(u_R)\right), \end{aligned}$$

which defines the well known Lax-Friedrichs numerical flux function.

A REFINED LAX-FRIEDRICHS NUMERICAL FLUX. We refine what was done above by assuming state dependent scalars $\lambda_L(u_L, u_R)$ and $\lambda_R(u_L, u_R)$, (which we denote simply by λ_L and λ_R), can be determined which satisfy $\lambda_L \leq \zeta_L \leq \zeta_R \leq \lambda_R$. Given these, we compute

$$\begin{aligned}&\frac{1}{\lambda_R - \lambda_L}\int_{\lambda_L}^{\lambda_R} R(u_L, u_R; \zeta)\, d\zeta \\ &= \frac{1}{\lambda_R - \lambda_L}\left(\lambda_R u_R - \lambda_L u_L\right) - \frac{1}{\lambda_R - \lambda_L}\left(f(u_R) - f(u_L)\right) \equiv u_M.\end{aligned}$$

Then use the approximate Riemann problem solution

$$R^A(u_L, u_R, \zeta) = \begin{cases} u_L & \text{if } \zeta < \lambda_L \\ u_M & \text{if } \lambda_L \leq \zeta \leq \lambda_R \\ u_R & \text{if } \zeta > \lambda_R \end{cases}$$

as done above to find

$$h_f(u_L, u_R) = \frac{1}{\lambda_R^+ - \lambda_L^-}\left(\lambda_L^- \lambda_R^+ (u_R - u_L) - \lambda_L^- f(u_R) + \lambda_R^+ f(u_L)\right),$$

where $\lambda^+ = \max(\lambda, 0)$ and $\lambda^- = \min(\lambda, 0)$. Formulae for λ_L and λ_R must be chosen carefully here so as to guarantee $h_f(u_L, u_R)$ is Lipschitz continuous. Observe that

$$h_f(u_L, u_R) = \begin{cases} f(u_L) & \text{if } \lambda_L \geq 0 \\ f(u_R) & \text{if } \lambda_R \leq 0. \end{cases}$$

Therefore, this approach yields a certain amount of upwinding.

THE ROE NUMERICAL FLUX. Instead of solving the full Riemann problem, Roe [19] suggested solving a much simpler linear problem and then using its Riemann problem solution to build a numerical flux function. Solving the linear and constant coefficient hyperbolic problem $u_t + Au_x = 0$ with Riemann data u_L, u_R and calling its solution $R^A(u_L, u_R; x)$ at $t = 1$, we find by again applying the divergence theorem

$$\int_{-\infty}^{\infty}\left(R^A(u_L, u_R; \zeta) - R(u_L, u_R; \zeta)\right) d\zeta = -(Au_R - Au_L) + (f(u_R) - f(u_L)).$$

Therefore, $R^A(u_L, u_R; \zeta)$ can be regarded as an approximate Riemann solver if and only if the matrix A satisfies

$$A(u_R - u_L) = f(u_R) - f(u_L).$$

This is the well known Roe condition. Suppose for the moment that such a matrix can be found (this matrix is referred to as a Roe matrix), and that it has real eigenvalues and a complete set of eigenvectors. Let R denote the

matrix whose columns are right eigenvectors to A and let L denote the inverse to R; (L is a matrix whose rows are left eigenvectors to A). Decoupling the system $u_t + Au_x = 0$ by multiplying on the left by L, we calculate that the Roe approximate Riemann problem solver is

$$R^A(u_L, u_R; \zeta) = \frac{1}{2}(u_L + u_R) - \frac{1}{2} R\ \Psi(\zeta) L(u_R - u_L),$$

where,

$$\Psi(\zeta) = \text{diag}(\text{sgn}(\lambda_k - \zeta)) \quad \lambda_k \text{ is the } k\text{th eigenvalue to } A.$$

To obtain its associated numerical flux, use divergence theorem to find

$$\begin{aligned}\int_0^\infty \left(R^A(u_L, u_R; \zeta) - u_R\right) d\zeta &= -\left(Au_R - AR^A(u_L, u_R; 0)\right) \\ &= -\left(\frac{1}{2}A(u_R - u_L) + \frac{1}{2} R\ \text{diag}(\lambda_k)\Psi(0)L(u_R - u_L)\right),\end{aligned}$$

and the Roe condition implies

$$= -\frac{1}{2}\left(f(u_R) - f(u_L) + |A|(u_R - u_L)\right).$$

($|A| = R\ \text{diag}(|\lambda_k|)L$.) This identity establishes

$$h_f(u_L, u_R) = \frac{1}{2}\left(-|A|(u_R - u_L) + f(u_L) + f(u_R)\right),$$

which is the Roe numerical flux.

For scalar problems, there is only one choice for the Roe (1×1) matrix and it is exactly the Rankine-Hugoniot shock speed. That is,

$$A(u_L, u_R) = s = \frac{f(u_R) - f(u_L)}{u_R - u_L}.$$

For systems, the Roe matrix need not be unique, and for arbitrary state values u_L and u_R, it may not generate a hyperbolic initial value problem. A recipe that always formally generates a Roe matrix is to define $u(\sigma) = (1-\sigma)u_L + \sigma u_R$ and with the fundamental theorem of calculus and chain rule calculate that

$$\begin{aligned}f(u_R) - f(u_L) &= \int_0^1 \frac{d}{d\sigma} f(u(\sigma))\ d\sigma \\ &= \int_0^1 \frac{\partial}{\partial u} f(u(\sigma)) \frac{d}{d\sigma} u(\sigma)\ d\sigma \\ &= \left(\int_0^1 \frac{\partial}{\partial u} f(u(\sigma))\ d\sigma\right)(u_R - u_L).\end{aligned}$$

A Roe matrix A can be identified above as the last integral. When $f(u)$ contains only quadratic terms in the conserved variables, this formulation gives a particular pleasing Roe matrix, A in this case is the Jacobian of f evaluated at $u_M = 1/2(u_L + u_R)$. Unfortunately, for the equations of gas dynamics, $f(u)$ is not quadratic in the conserved variables. However, for the γ-law gas, one can find a change of variables so that it is, and in this case one finds

$$A = \frac{D}{Du} f(u_M), \quad \text{where } u_M \text{ is computed from}$$
$$\rho_M = \frac{1}{4}\left(\sqrt{\rho_L} + \sqrt{\rho_R}\right)^2, \quad q_M = \frac{\sqrt{\rho_L} q_L + \sqrt{\rho_R} q_R}{\sqrt{\rho_L} + + \sqrt{\rho_R}},$$

with q above representing the components of velocity u, v, w and enthalpy $H = e + P/\rho$.

The Roe approximate Riemann problem solver reduces to the exact Riemann problem solution for linear constant coefficient problems. It can be shown however, that the Roe solver as stated above needs some modification in order to always yield entropy satisfying converged solutions to nonlinear conservation laws. Since the Roe solver can be regarded as a *shocks only* approximation it can be fooled. Rarefaction waves containing sonic points may be resolved numerically as a shock. Fortunately, fixes to this problem abound [6,17]. The Lax-Friedrichs numerical flux function, while very simple and easy to use, is extremely diffusive and yields less than satisfactory results when incorporated into a first order difference scheme. However, when incorporated into certain high order formulations, it is robust and may yield highly satisfactory results.

6 High Order Godunov Schemes in One Space Dimension

For the moment we will restrict our attention to first order in time forward Euler schemes applied to one dimensional hyperbolic systems. Higher temporal accuracy will be discussed later in this section. Multidimensional extensions will be treated in the next section.

Partition the real line into cells $\Omega_i = [x_{i-1/2}, x_{i+1/2}]$ where $\mathbf{R} = \bigcup_i \Omega_i$. An idea due to Godunov is the following. Suppose at time t^n, our approximate solution to the hyperbolic system is given by $u^n(x) = \sum_i u_i^n \chi_i(x)$ where χ_i is the indicator function to the interval Ω_i. That is, $u^n(x)$ is a piecewise constant function with value u_i^n in cell Ω_i. Now, solve the problem

$$\frac{\partial}{\partial t} u + \frac{\partial}{\partial x} f(u) = 0 \quad t > t^n, \quad u(x, t^n) = u^n(x),$$

and set

$$u^{n+1}(x) = \sum_i u_i^{n+1} \chi_i(x) \quad \text{where} \quad u_i^{n+1} = \frac{1}{|\Omega_i|} \int_{\Omega_i} u(x, t^{n+1}) dx.$$

By a simple application on the divergence theorem on $\Omega_i \times [t^n, t^{n+1}]$, Godunov

observed that the exact average of $u(x, t^{n+1})$ over cell Ω_i is given explicitly by

$$u_i^{n+1} = u_i^n - \frac{\Delta t^n}{|\Omega_i|} \left(f(u(x_{i+1/2}, t^n + 0)) - f(u(x_{i-1/2}, t^n + 0)) \right),$$

where $u(x_{j+1/2}, t^n + 0)$ denotes the exact solution to the Riemann problem with left and right states u_i^n and u_{i+1}^n. (We have assumed that Δt^n is small enough so that wave interactions between Riemann problems do not affect flux calculations.) Using the notation of the previous section, (i.e. $R(u_L, u_R; \zeta)$), we observe that

$$f(u(x_{i+1/2}, t^n + 0)) = f(R(u_i^n, u_{i+1}^n; 0)).$$

Therefore, a Godunov *type* finite difference scheme based on approximate Riemann problem solvers can be written as

$$u_i^{n+1} = u_i^n - \frac{\Delta t^n}{|\Omega_i|} \left(h_f(u_i^n, u_{i+1}^n) - h_f(u_{i-1}^n, u_i^n) \right), \tag{8}$$

where $h_f(u_L, u_R)$ denotes a two point numerical flux function consistent to f; (see the previous section).

The following theorem is due to Lax and Wendroff [13].

Theorem 2 *Suppose that u_i^n is given by*

$$u_i^{n+1} = u_i^n - \frac{\Delta t^n}{|\Omega_i|} \left(h_{i+1/2} - h_{i-1/2} \right),$$

where $h_{i+1/2}$ is a multipoint continuous numerical flux function consistent to f. Then, if the associated approximate solution converges boundedly almost everywhere to a function $u(x,t)$, $u(x,t)$ is a weak solution to the hyperbolic conservation law.

The key to above is the *conservation form* of the difference scheme. Unless a scheme is in conservation form, the result of this theorem can not possibly hold in all situations.

Incorporating any one of the approximate Riemann problem numerical fluxes from the previous section into the conservation form finite difference scheme above yields a first order accurate finite difference scheme. While only having first order accuracy, they all generate non-oscillatory approximations.

We now offer numerical results for two of the first order Godunov type schemes discussed above. Consider the one dimensional version of the Euler equations, see (6), using a γ-law equation of state with $\gamma = 1.4$. We take Riemann initial data

$$\mathbf{V}(x, 0) = \begin{cases} \mathbf{V}_L & \text{if } x < 0.5 \\ \mathbf{V}_R & \text{if } x \geq 0.5, \end{cases}$$

where $\mathbf{V}_L$ is obtained from the primitive variables $\rho = 0.445$, $u = 0.698$ and $p = 3.528$, and $\mathbf{V}_R$ is obtained from $\rho = 0.5$, $u = 0$ and $p = 0.571$. This data

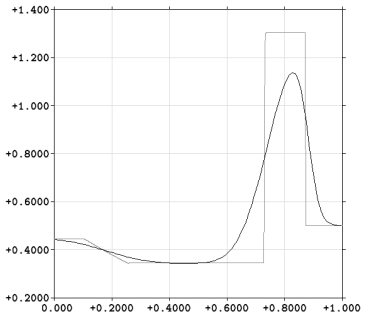

Fig. 1: The Lax problem using the Lax-Friedrichs flux.

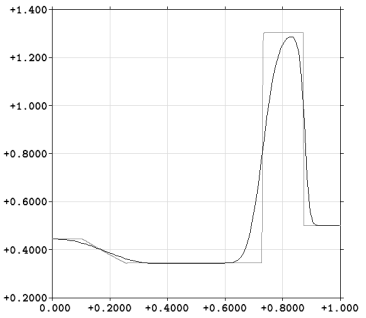

Fig. 2: The Lax problem using the Roe flux.

corresponds to what is known in the literature as the *Lax* shock-tube problem. Its exact solution is composed of a rarefaction wave, followed by a contact discontinuity, followed by a shock. So that adjoining approximate Riemann problem solutions do not interact, we fix Δt so that $\frac{\Delta t}{|\Omega|}|\lambda_{max}| \leq 0.5$. 100 equally spaced grid points are used with $0 \leq t \leq t_{max} = 0.15$. The computed density (dark line) is compared to the exact solution (gray line) in Fig. 1 using the Lax-Friedrichs numerical flux, and the results coming from the Roe numerical flux are depicted in Fig. 2.

It is a relatively simple matter to derive spatially high order accurate non-oscillatory Godunov type finite difference schemes. Suppose at every cell interface $i + 1/2$ we have values $u^-_{i+1/2}$ and $u^+_{i+1/2}$; (for the first order schemes above we have taken $u^-_{i+1/2} = u^n_i$ and $u^+_{i+1/2} = u^n_{i+1}$). We now consider more general (or extended) Godunov type schemes of the form

$$u^{n+1}_i = u^n_i - \frac{\Delta t^n}{|\Omega_i|}\left(h_f(u^-_{i+1/2}, u^+_{i+1/2}) - h_f(u^-_{i-1/2}, u^+_{i-1/2})\right). \tag{9}$$

The manner in which u^- and u^+ are chosen determines the accuracy (as described below) and stability (as discussed below) of the underlying method. Throughout, we assume that these *interface values* are given functionally by a finite number of cell averages,

$$\begin{aligned} u^-_{i+1/2} &= u^-(u_{i-p}, \ldots, u_{i+p+1}), \\ u^+_{i+1/2} &= u^+(u_{i-p}, \ldots, u_{i+p+1}), \end{aligned} \tag{10}$$

and that these functions are Lipschitz continuous and consistent to u.

We must stress the following at this point. It is generally a very bad idea to use spatially high order schemes in the first order forward Euler framework as indicated in (9). This is obvious from the perspective of accuracy. However, but speaking loosely, it is impossible to derive a linearly stable scheme of the

form (9) which is higher than second order in space. High order temporal discretization will be discussed later in this section.

A scheme of the above form is said to be order Δx^r accurate in space *in the sense of cell averages* if for any smooth function $u(x)$ we have at grid cell Ω_i

$$\frac{1}{|\Omega_i|}\left(f(u(x_{i+1/2})) - f(u(x_{i-1/2}))\right) = \frac{1}{|\Omega_i|}\left(h_f(\bar{u}^-_{i+1/2}, \bar{u}^+_{i+1/2}) - h_f(\bar{u}^-_{i-1/2}, \bar{u}^+_{i-1/2})\right) + O(\Delta x^r).$$

This notion of accuracy measure the difference between the numerical approximation u_i^n to the cell average of the exact solution $\frac{1}{|\Omega_i|}\int_{\Omega_i} u(x,t^n)dx$. It is not the same as the usual pointwise notion of spatial accuracy!

One can not take the interface values u^- and u^+ in (10) arbitrarily. For example, using

$$u^-_{i+1/2} = u^+_{i+1/2} \equiv \frac{1}{2}(u_i + u_{i+1})$$

would lead to a pure central difference scheme

$$u_i^{n+1} = u_i^n - \frac{\Delta t^n}{|\Omega_i|}\left(f(u^n_{i+1/2}) - f(u^n_{i-1/2})\right).$$

However, for the linear case $f(u) = u$, Fourier analysis will show this scheme amplifies every Fourier mode unconditionally!

There are formulae for u^- and u^+ which yield nonlinearly stable and spatially high order Godunov schemes and yet yield very poor numerical results. To see this, consider the minmod function, defined by

$$\text{minmod}(a,b) = \begin{cases} a & \text{if } ab > 0 \text{ and } |a| \le |b| \\ b & \text{if } ab > 0 \text{ and } |b| < |a| \\ 0 & \text{if } ab \le 0 \end{cases}, \tag{11}$$

and interface values given by

$$u^-_{i+1/2} = u_i + \frac{1}{2}\,\text{minmod}((u_{i+1} - u_i), \rho(u_i - u_{i-1}))$$
$$u^+_{i+1/2} = u_{i+1} - \frac{1}{2}\,\text{minmod}((u_{i+1} - u_i), \rho(u_{i+2} - u_{i+1})),$$

where ρ is a nonnegative finite constant. For any finite $\rho \ge 1$, one easily argues that these generate a second order Godunov type scheme, and in fact, one can show (but we do not here) the resulting approximations remain uniformly bounded (and are in fact non-oscillatory). Now, we pose a paradox: Study $u^\pm$ above to find if, say $\rho = 2$, we have away from local extrema $u^\pm_{i+1/2} = \frac{1}{2}(u_i + u_{i+1})$. Therefore, for the equation $u_t + u_x = 0$, all consistent Godunov type schemes must reduce to the central difference scheme away from extreme points in its solution. Now, suppose the solution that we are trying

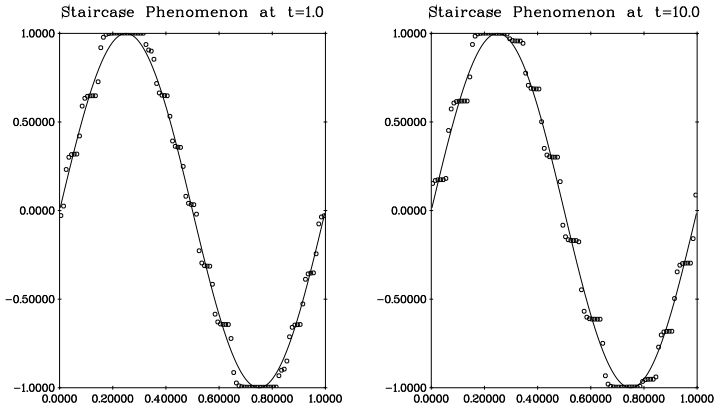

Figure 3: The staircase effect for a nonlinearly stable but linearly unstable second order scheme. Left at $t = 1.0$, right at $t = 10.0$.

to approximate by such a scheme has only a couple of extreme points; (e.g. $u(x,t) = \sin(x-t)$ on a periodic domain). One is therefore assured that a variation stable approximation (which can be shown to be the case for this scheme) will also have only a couple of extrema – implying that central space differencing is stable. But this is absurd as already noted! The solution to the paradox is that the variation stable approximation develops a *staircase* instability. In regions away from true extrema, the scheme goes unstable, it tries to oscillate but the nonlinear mechanism in $u^{\pm}$ *kicks in* and flattens the oscillations into plateaus. This is, therefore, an example of a formally second order and nonlinearly stable scheme that produces results far worse than its first order counterpart. See Fig. 3.

Two useful approaches to generate interface values are now given. The first is the classic minmod method:

$$\begin{aligned} u^{-}_{i+1/2} &= u_i + \frac{1}{2}\,\mathrm{minmod}((u_{i+1}-u_i),(u_i-u_{i-1})) \\ u^{+}_{i+1/2} & u_{i+1} - \frac{1}{2}\,\mathrm{minmod}((u_{i+1}-u_i),(u_{i+2}-u_{i+1})). \end{aligned} \tag{12}$$

This is identical to what was used to produce the staircase flaw above, except the parameter ρ is taken here to be identically 1. The second is due to van Leer [14]:

$$\begin{aligned} &\delta^L_i = \mathrm{minmod}((u_i-u_{i-1}),\rho(u_{i+1}-u_i)) \\ &\delta^R_i = \mathrm{minmod}((u_{i+1}-u_i),\rho(u_i-u_{i-1})) \\ &u^{-}_{i+1/2} = u_i + \frac{1}{6}\left(2\delta^R_i + \delta^L_i\right), \qquad u^{+}_{i+1/2} = u_{i+1} - \frac{1}{6}\left(\delta^R_{i+1} + 2\delta^L_{i+1}\right), \end{aligned} \tag{13}$$

where the parameter is required to satisfy $1 \leq \rho < 3$. These interface values generate a nonlinearly stable spatially third order accurate scheme.

The fatal flaw in the scheme depicted in Fig. 3 lies in the fact that we have tried to obtain high spatial accuracy using a forward Euler time marching scheme. We will now discuss an alternate approach to time discretization. A simple approach to gain second order temporal accuracy is given by Runge-Kutta time marching. We demonstrate this by considering the most primitive high order TVD Runge-Kutta method – the second order Heun's method. We wish to discretize in time the system of odes

$$\begin{aligned}\frac{d}{dt}u_i &= -\frac{1}{|\Omega_i|}\left(h_f(u^-_{i+1/2}, u^+_{i+1/2}) - h_f(u^-_{i-1/2}, u^+_{i-1/2})\right)\\ &\equiv -\mathcal{H}_i(u(t)).\end{aligned}$$

Now recall that Heun's method, or the trapezoidal rule, is given by

$$\begin{aligned}u^{n+1/2} &= u^n - \Delta t\mathcal{H}(u^n)\\ u^{n+1} &= u^n - \frac{\Delta t}{2}\left(\mathcal{H}(u^n) + \mathcal{H}(u^{n+1/2})\right),\end{aligned}$$

and since the first step is a first order in time prediction followed by a second order in time correction, the full integration scheme is second order in time. Moreover, if the first order in time forward Euler scheme is variation stable, so is this second order in time integration scheme. To see this, we write the correction step above as

$$u^{n+1} = \frac{1}{2}\left(u^n - \Delta t\mathcal{H}(u^{n+1/2})\right) + \frac{1}{2}\left(u^n - \Delta t\mathcal{H}(u^n)\right).$$

and with the prediction step

$$= \frac{1}{2}\left(u^{n+1/2} - \Delta t\mathcal{H}(u^{n+1/2})\right) + \frac{1}{2}u^n.$$

Now exploiting the two facts that the forward Euler scheme is variation nonexpansive and that the variation functional is convex, will immediately verify the final result. See Shu [20] for a broad description and analysis of Runge-Kutta time marching techniques for hyperbolic conservation laws.

The interface values coming from (12) and (13) are only defined for scalar equations. They are extended to systems as follows. The minmod slope limiting is performed in characteristic variables. That is, let R and L denote the matrices of right and left eigenvectors to the flux Jacobian evaluated at cell average u_i, and compute component-wise

$$\begin{aligned}\delta_i^L &= R \cdot \text{minmod}(L \cdot (u_i - u_{i-1}), \rho\, L \cdot (u_{i+1} - u_i)),\\ \delta_i^R &= R \cdot \text{minmod}(L \cdot (u_{i+1} - u_i), \rho\, L \cdot (u_i - u_{i-1})).\end{aligned}$$

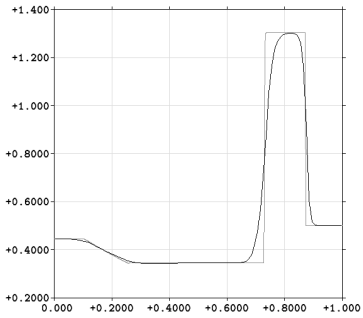

Fig. 4: The Lax problem using a spatially second order method.

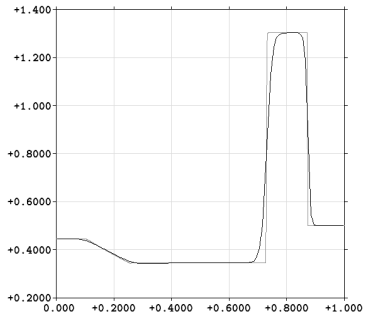

Fig. 5: The Lax problem using a spatially third order method.

This is the only way to guarantee no spurious oscillations appear when applied to a linear conservation law.

We end this section by again solving the Lax shock-tube problem. This time, we use the second order minmod interface values (12) with Heun's time marching and the spatially third order method from (13) also using the second order Heun's method. In both cases, we use the Roe Riemann solver. The results are depicted in Fig. 4 and Fig. 5.

7 Multidimensional Problems and the Finite Volume Method

To treat multidimensional problems, we follow the *finite volume* philosophy. Throughout, we assume $\mathbf{R}^d$, $d \geq 2$ is partitioned in a logically rectangular fashion. That is $\mathbf{R}^d = \bigcup_{\mathcal{I}} \Omega_{\mathcal{I}}$ where $\mathcal{I}$ denotes a multi-index $\mathcal{I} = i_1, \ldots, i_d$, and where $\Omega_{\mathcal{I}}$ is diffeomorphic to a d dimensional cube. This grid is referred to as a *structured grid*. Integrate the exact solution to the conservation law

$$\frac{\partial}{\partial t} u + \sum_{i=1}^{d} \frac{\partial}{\partial x_i} f_i(u) = 0$$

over $\Omega_{\mathcal{I}} \times [t^n, t^{n+1}]$ to find that the exact cell average $u_{\mathcal{I}}^n$ of the solution $u(x,t)$ solves

$$u_{\mathcal{I}}^{n+1} = u_{\mathcal{I}}^n - \frac{1}{|\Omega_{\mathcal{I}}|} \int_{t^n}^{t^{n+1}} \int_{\partial\Omega_{\mathcal{I}}} (\mathbf{f} \cdot \mathbf{n})(u(x,t))\, dS_x dt,$$

where $\mathbf{n}$ denotes the outward unit normal to $\Omega_{\mathcal{I}}$, and where $\partial\Omega_{\mathcal{I}}$ denotes its surface. Unlike the one dimensional case, we can not assume the time independence of the integrand above even in the case when the data at t^n are piecewise constant. Nevertheless, we apply this forward Euler approximation and let $u_{\mathcal{I}}^n$ denote an approximation to $\frac{1}{|\Omega_{\mathcal{I}}|} \int_{\Omega_{\mathcal{I}}} u(x,t^n) dx$ evolving according to

$$u_{\mathcal{I}}^{n+1} = u_{\mathcal{I}}^n - \frac{\Delta t^n}{|\Omega_{\mathcal{I}}|} \int_{\partial\Omega_{\mathcal{I}}} h_{(\mathbf{f}\cdot\mathbf{n})}(u^-(x), u^+(x))\, dS_x,$$

where $h_{(\mathbf{f}\cdot\mathbf{n})}$ denotes a two point numerical flux, consistent to $(\mathbf{f}\cdot\mathbf{n})$, and $u^-(x)$ and $u^+(x)$ denote inner and outer interface values defined on the boundary of $\Omega_{\mathcal{I}}$. We moreover assume that the interface values are given functionally by continuous functions of nearby cell averages. With this, we should remark that the conclusion of the Lax-Wendroff theorem in Section 6 remains valid for approximations coming from finite volume schemes of the form above. That is, if the approximation converges, its limit is a weak solution to the conservation law.

The notion of accuracy in the sense of cell averages introduced in the previous section carries over naturally to the finite volume framework. We say that the finite volume scheme is of spatial order r if for all smooth functions $u(x)$ we have that

$$\begin{aligned}\frac{1}{|\Omega_{\mathcal{I}}|}\int_{\partial\Omega_{\mathcal{I}}}(\mathbf{f}\cdot\mathbf{n})(u(x))\;dS_x\\ =\frac{1}{|\Omega_{\mathcal{I}}|}\int_{\partial\Omega_{\mathcal{I}}}h_{(\mathbf{f}\cdot\mathbf{n})}(u^-(x),u^+(x))\;dS_x+O(\Delta x^r),\end{aligned}$$

where Δx is some characteristic length associated to $\Omega_{\mathcal{I}}$ and where $u^{\pm}(x)$ is constructed using the nearby cell averages of $u(x)$. Most applications of the finite volume method are done in a quasi one dimensional fashion. That is, first, if we let S_l denote a single face to the cube $\Omega_{\mathcal{I}}$ in the lth grid direction, only cell averages in this one dimensional direction are used to form the interface values along S_l, and second, $u^{\pm}(x)$ along S_l are taken as constant. This approach is certainly economical but has the following price. When the differential equations being approximated contains nonlinear fluxes $f(u)$, the maximum order possible from a quasi one dimensional finite volume scheme is two. The one space dimensional accuracy is retained for linear problems, but not nonlinear ones. This follows from the fact that

$$\frac{1}{|S|}\int_S f(u)\,dS=f\left(\frac{1}{|S|}\int_S u\,dS\right)$$

is true only for affine functions. For most applications however, a quasi one dimensional approach with, say, a third order one dimensional scheme, will produce slightly better results compared to results coming from a second order scheme.

We conclude these notes by applying the variety of techniques discussed in the last several sections to a steady two dimensional supersonic flow down an expanding nozzle. The modeling equations are the steady compressible Euler equations

$$\frac{\partial}{\partial x}f(u)+\frac{\partial}{\partial y}g(u)=0,$$

where

$$u=\begin{pmatrix}\rho\\ \rho u\\ \rho v\\ \rho e\end{pmatrix}\quad f(u)=\begin{pmatrix}\rho u\\ \rho u^2+p\\ \rho uv\\ (\rho e+p)u\end{pmatrix}\quad g(u)=\begin{pmatrix}\rho v\\ \rho uv\\ \rho v^2+p\\ (\rho e+p)v\end{pmatrix}.$$

(Refer back to Sections 2 and 3.) In these equations ρ is the fluid's density, (u, v) its (x, y) velocity and e its total energy per unit mass. p represents the fluid's pressure and is given by the perfect gas equation of state $p = (\gamma - 1)\rho(e - \frac{1}{2}(u^2 + v^2))$ where we take $\gamma = 1.4$.

Theses equations are ideally suited to the finite volume formulation. We will use its quasi one dimensional version exclusively. The finite volume numerical fluxes are evaluated as follows: Let $\Omega_{i,j}$ denote a typical quadrilateral grid cell with sides $S^i_{i\pm1/2,j}$ (sitting on the left and right of $\Omega_{i,j}$) and $S^j_{i,j\pm1/2}$ (sitting on the bottom and top of $\Omega_{i,j}$). Also let $\mathbf{n}^i_{i\pm1/2,j}$ respectively $\mathbf{n}^j_{i,j\pm1/2}$ denote a unit normal vector to the sides $S^i_{i\pm1/2,j}$ resp. $S^j_{i,j\pm1/2}$ oriented in the direction of increasing i resp. j. The scheme we wish to solve then takes the explicit flux difference form

$$\frac{1}{|\Omega_{i,j}|}\left(h_{i+1/2,j} - h_{i-1/2,j} + h_{i,j+1/2} - h_{i,j-1/2}\right) = 0,$$

where,

$$h_{i+1/2,j} = |S^i_{i+1/2,j}| h_{(f,g)\cdot\mathbf{n}^i_{i+1/2,j}}(u^-_{i+1/2,j}, u^+_{i+1/2,j})$$
$$h_{i,j+1/2} = |S^j_{i,j+1/2}| h_{(f,g)\cdot\mathbf{n}^j_{i,j+1/2}}(u^-_{i,j+1/2}, u^+_{i,j+1/2}),$$

and where $u^\pm_{i+1/2,j}$ are computed solely from cell averages $u_{i-p,j}, \ldots, u_{i+p+1,j}$ and $u^\pm_{i,j+1/2}$ from $u_{i,j-p}, \ldots, u_{i,j+p+1}$. (Note we have tacitly assumed that $h_{-f}(u_2, u_1) = -h_f(u_1, u_2)$.)

Now, owing to the the rotational invariance of the Euler equations (or most other physical problems for that matter) $(f(u), g(u)) \cdot (n_x, n_y)$ can be written as

$$\begin{pmatrix} 1 & 0 & 0 & 0 \\ 0 & n_x & -n_y & 0 \\ 0 & n_y & n_x & 0 \\ 0 & 0 & 0 & 1 \end{pmatrix} \begin{pmatrix} \rho u_n \\ \rho u_n^2 + p \\ \rho u_n u_t \\ (\rho e + p) u_n \end{pmatrix},$$

where (n_x, n_y) is an arbitrary unit vector and $u_n = (u, v) \cdot (n_x, n_y)$ is the flow velocity in the direction of (n_x, n_y) and $u_t = (u, v) \cdot (-n_y, n_x)$ is the flow velocity perpendicular. All numerical flux evaluations are performed as if the problem is one dimensional (see Section 6) across opposite sides of a cell. To point limit $u^+_{i-1/2,j}, u^-_{i+1/2,j}$ we use the eigenmatrices associated to the Jacobian matrix of the flux projected into the "cell centered" normal vector parallel to $\mathbf{n}^i_{i-1/2,j} + \mathbf{n}^i_{i+1/2,j}$. These eigenmatrices are derived in Section 3.

The nozzle's geometry runs from $-0.10 \le x \le 2.80$ with the upper boundary given by the function

$$y = \frac{1}{4}\begin{cases} 3 & \text{if } x \le 0 \\ -(x+1)^2(x-1)^2 + 4 & \text{if } 0 < x < 1 \\ 4 & \text{if } x \ge 1 \end{cases},$$

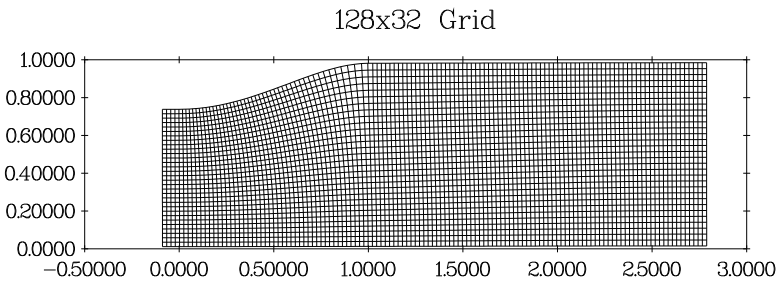

Figure 6: The 128×32 cell grid for the nozzle experiments.

and the lower boundary is a $y = 0$. The lower boundary is treated as a line of symmetry. The upper boundary is treated as a hard wall and is simulated by reflection. At the inflow throat ($x = -0.10$) the flow is at Mach 1.0 corresponding to a stagnation pressure, temperature of 10000.0 Pascal, 5000.0° Kelvin. The outflow ($x = 2.80$) Mach number is set at 1.69545. The specific primitive variables left and right boundary conditions are

$$\begin{pmatrix} \rho_l \\ u_l \\ v_l \\ p_l \end{pmatrix} = \begin{pmatrix} 4.41769\ 10^{-3} \\ 1293.90 \\ 0.0 \\ 5282.82 \end{pmatrix} \quad \begin{pmatrix} \rho_r \\ u_r \\ v_r \\ p_r \end{pmatrix} = \begin{pmatrix} 2.23876\ 10^{-3} \\ 1914.90 \\ 0.0 \\ 2039.88 \end{pmatrix},$$

and the maximum Mach number of this flow is around 2.172. The computational grid size is 128 grid cells to span the length of the nozzle and 32 grid cells to span its width; see Fig. 6 In all cases below, the flow is driven to steady state (when steady state can be achieved) by artificial time relaxation.

Fig. 7 depicts local Mach number contours ($|\mathbf{v}|/c$) coming from the first order Roe scheme. A numerical boundary layer resulting from a Roe flux *entropy fix* we incorporated into our solver is evident at the lower (subsonic) portion of the outflow boundary. Clearly, the main features of this flow are not well resolved; see Figs. 8 and 10 below. However, the characteristic diamond shock patten can be seen as is a weak slip line emanating from the region of strong compression behind the leading shock parallel to the nozzle's upper wall.

The popular minmod scheme was used to produce the results given in Fig. 8, again using the Roe numerical flux. The interface values are given by linear interpolation of cell averages across cell interfaces and are point limited via the minmod function with compression factor $\rho = 1$; see equation (12). Note the sharpening of the shocks as compared to the first order result. Note too how the resolution of the slip line is improved.

Fig. 9 depicts result coming from a scheme base on these same minmod interface values as above, but this time using the highly diffusive Lax-Friedichs numerical flux. Almost all second order detail is lost here. In particular note that the slip line seen in the Roe calculations is almost entirely lost. Also note the exceptionally strong numerical boundary layer at the outflow boundary.

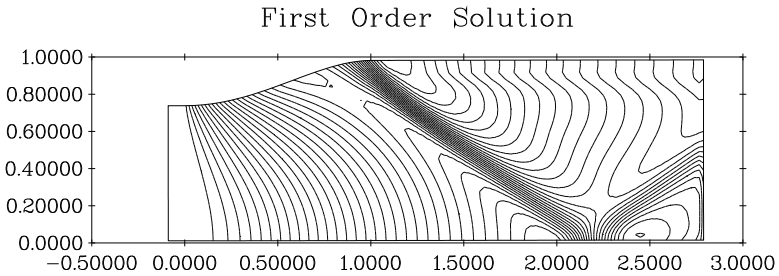

Figure 7: The first order Roe solver.

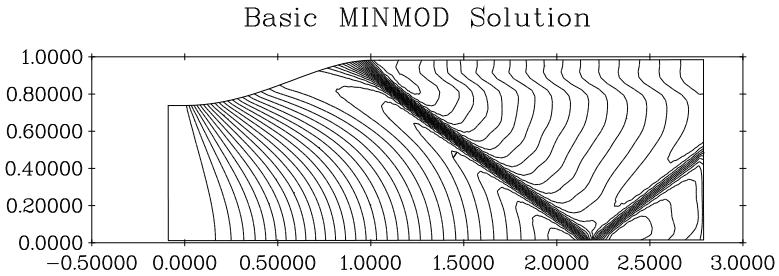

Figure 8: Second order minmod using the Roe solver.

Fig. 10 depicts the local Mach numbers coming from van Leer's interface values, see equation (13), with compression factor ρ set to 2. The Roe numerical flux is used again. Note that the diamond shock patten is now very well resolved. Also, the boundary layer at the subsonic portion of the outflow boundary is now only one grid zone wide.

While all except the first numerical experiments presented here are formally second order accurate, and all are so-called TVD schemes, they vary greatly in quality. One can easily argue that the Roe flux schemes give superior results compared to the results offered by the Lax-Friedrichs numerical flux. However, the Roe flux requires rather ad-hoc modifications in order to reliably capture sonic rarefaction waves. Moreover, it requires a great deal of human effort to derive for fluid equations with very complicated equations of state. There are always tradeoffs unfortunately.

References

[1] P. Colella and P. Woodward, "The piecewise-parabolic method (PPM) for gas dynamical simulations", *J. Comp. Phys.*, 54 (1984), pp. 104-117.

[2] B. Engquist and S. Osher, "Stable and entropy satisfying approximations for transonic flow calculations", *Math. Comp.*, 34 (1980), pp. 45-75.

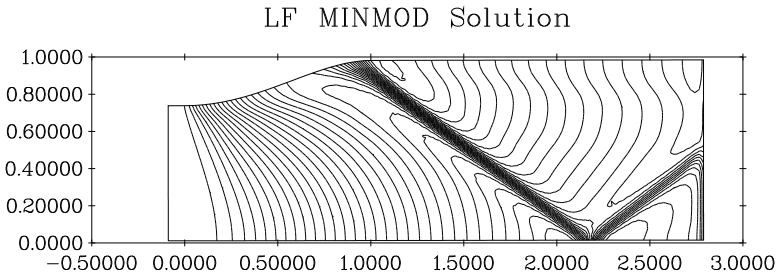

Figure 9: Second order minmod using the Lax-Friedrichs solver.

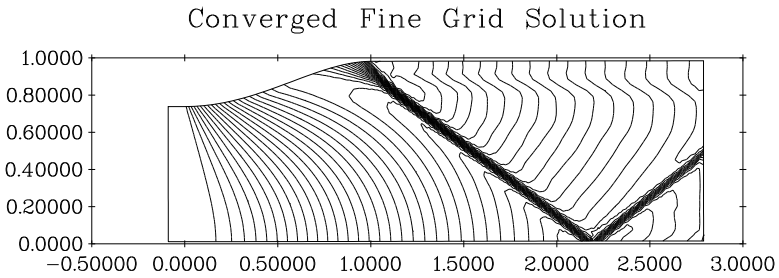

Figure 10: Mach numbers coming from van Leer's interface values using a Roe solver.

[3] J. Glimm, "Solutions in the large for nonlinear hyperbolic systems of equations", *Comm. Pure Appl. Math.*, 18 (1965), pp. 95-105.

[4] S.K. Godunov, "A finite difference method for the numerical computation of discontinuous solutions of the equations of fluid dynamics", *Mat. Sb.*, 47 (1959), pp. 271-290.

[5] J.B. Goodman and R.J. LeVeque, "On the accuracy of stable schemes for 2d scalar conservation laws", *Math. Comp.*, 45 (1985), pp. 15-21.

[6] A. Harten, "High resolution schemes for hyperbolic conservation laws", *J. Comp. Phys.* 49 (1983), pp. 357-393.

[7] A. Harten, "On high order interpolation for non-oscillatory shock capturing schemes", MRC Technical Report 2829, 1985, University of Wisconsin.

[8] A. Harten and S. Osher, "Uniformly high order accurate nonoscillatory schemes, I", *SIAM J. Num. Anal.*, 24 (1987), pp. 279-309.

[9] J.O. Hirschfelder, C.F. Curtis and R.B. Bird, Molecular Theory of Gases and Liquids, Wiley, New York (1954).

[10] H-O Kreiss and J. Lorenz, Initial-Boundary Value Problems and the Navier-Stokes Equations, Academic Press, San Diego, (1989).

[11] S.N. Kruzcov, " First order quasi-linear equations in several space variables", *Math. USSR Sb.*, 10 (1970), pp. 217-243.

[12] P.D. Lax, "Hyperbolic systems of conservation laws and the mathematical theory of shock waves", *SIAM Reg. Conf. Series in Appl. Math.*, 11, (1972).

[13] P.D. Lax and B. Wendroff, "Systems of conservation laws", *Comm. Pure Appl. Math.*, 13 (1960), pp. 217-237.

[14] B. van Leer, "Towards the ultimate conservative difference scheme, V: A second order sequel to Godunov's method", *J. Comp. Phys.*, 32 (1979), pp. 101-136.

[15] B. van Leer, "Upwind-difference methods for aerodynamic problems governed by the Euler equations", in Lectures in Applied Mathematics, v.22-2, Amer. Math. Soc, Providence, (1985).

[16] O.A. Oleinik, "On the uniqueness of the generalized solution of the Cauchy problem for a nonlinear system of equations occurring in mechanics", *Ibid.*, 12 (1957), pp. 169-176.

[17] S. Osher, "Riemann solvers, the entropy condition, and difference approximations", *SIAM J. Numer. Anal.*, 21 (1984), pp. 217-235.

[18] S. Osher and F. Solomon, "Upwind schemes for hyperbolic systems of conservation laws", *Math. Comp.*, 38 (1982), pp. 339-377.

[19] P.L. Roe, "Approximate Riemann solvers, parameter vectors, and difference schemes", *J. Comp. Phys.*, 43 (1981), pp. 357-372.

[20] C.W, Shu, "Total variation diminishing time discretizations", *SIAM J. Sci. Stat. Comp.*, 9 (1988), pp. 1073-1084.

[21] J. Smoller, Shock Waves and Reaction-Diffusion Equations, Springer-Verlag, New York, (1983).

Bol. Soc. Esp. Mat. Apl.
nº 38(2007), 69–91

DINÁMICA DE FRENTES DE LA ECUACIÓN 2D QUASI-GEOSTRÓFICA

DIEGO CÓRDOBA GAZOLAZ

Consejo Superior de Investigaciones Científicas
C/ Serrano 123, 28006 Madrid

dcg@imaff.cfmac.csic.es

Resumen

En estas notas describimos algunos resultados recientes que nos ayudan a entender la posible formación y evolución de singularidades para la ecuación 2D quasi-geostrófica.

Palabras clave: *Ecuación quasi-geostrófica, singularidades, ecuaciones de Euler.*

Clasificación por materias AMS: *86A10 35Q35 76U05 42A24*

1 Introducción

En lo que sigue, C designará distintas constantes positivas que permitirán expresar estimaciones uniformes adecuadas. Llamaremos Π^N al toro unidad de $\mathbf{R}^{N+1}$ y pondremos $Q = \mathbf{R}^2 \times \mathbf{R}_+$ o $Q = \Pi^2 \times \mathbf{R}_+$.

La ecuación quasi-geostrófica bidimensional, que en lo sucesivo, representaremos por las siglas QG, se deduce dentro de un contexto geofísico y tiene la siguiente forma:

$$\begin{cases} (\partial_t + u \cdot \nabla)\,\theta = 0, \\ u = \nabla^\perp \psi = (\partial_2 \psi, -\partial_1 \psi), \quad \psi = -(-\triangle)^{-1/2}\theta. \end{cases} \tag{1}$$

Aquí, $\theta = \theta(x,t)$, con $(x,t) \in Q$, es el escalar de temperatura, $u = u(x,t)$ es la velocidad y $\psi = \psi(x,t)$ es la función de corriente. El operador no local $\Lambda^\gamma = (-\triangle)^{\gamma/2}$ está definido mediante la transformada de Fourier por $\widehat{\Lambda^\gamma f}(\xi) = |\xi|^\gamma \hat{f}(\xi)$, donde $\hat{f}$ es la transformada de Fourier de f y el espacio de Sobolev H^s es por definición el formado por todas las funciones f tales que la norma $\|f\|_{H^s} = \|\Lambda^s f\|_{L^2}$ está acotada. La ecuación QG debe ser satisfecha en Q y ha de ser complementada con condiciones iniciales para θ, condiciones "en el infinito" cuando $Q = \mathbf{R}^2 \times \mathbf{R}_+$ y condiciones de periodicidad en espacio cuando $Q = \Pi^2 \times \mathbf{R}_+$.

Fecha de recepción: 2/11/2005, Revisión 31/05/2006

Esta ecuación, que tiene aplicaciones en Meteorología y Oceonografía, es un caso especial de la ecuación general quasi-geostrófica (tridimensional) que modela fluidos atmosféricos y oceánicos para constantes de Rossby y Eckman pequeñas (véase [30], [38] y [41]).

Debido a la incompresibilidad del fluido, las normas L^p de θ se conservan para todo tiempo. En particular, se conserva la norma L^2 de θ y esto implica que la energía

$$E(t) = \frac{1}{2}\|u(\cdot,t)\|_{L^2}^2$$

también se conserva, debido a que la velocidad se puede escribir como

$$u = (-\partial_2\Lambda^{-1}\theta,\, \partial_1\Lambda^{-1}\theta) = (-R_2\theta,\, R_1\theta),$$

donde los operadores R_j son las transformadas de Riesz:

$$(R_j\theta)(x,t) = \partial_j(\Lambda^{-1}\theta)(x,t) = \frac{1}{2\pi}\,\text{V.P.}\int \frac{y_j\cdot\theta(x+y,t)}{|y|^3}\,dy.$$

En los últimos años ha habido un intenso interés científico por entender el comportamiento de las ecuaciones quasi-geostróficas, por ser un posible modelo para explicar la formación de frentes de masas de aire caliente y frío. Por otra parte, Constantin, Majda y Tabak [16] mostraron que la ecuación QG es un análogo bidimensional de la ecuación de Euler en tres dimensiones y que los resultados que se verifican para cada una de ellas se dan también en el caso de la otra, aunque la existencia de singularidades para cualquiera de las dos ecuaciones es un problema que sigue abierto.

Para comprender mejor esta similitud, consideremos el sistema incompresible de Euler en dimension tres

$$\begin{cases} \dfrac{\partial u_i}{\partial t} + \displaystyle\sum_{1\le j\le n} u_j\frac{\partial u_i}{\partial x_j} = -\frac{\partial P}{\partial x_i}, \quad 1\le i\le 3, \\ \nabla\cdot u := \displaystyle\sum_{1\le i\le 3}\partial_i u_i = 0, \end{cases} \tag{2}$$

donde $u=(u_1,u_2,u_3)$ es un campo de velocidades y la presión viene dada por la función escalar P.

La vorticidad se define por $\omega = \nabla\times u$. Las ecuaciones (2) pueden escribirse en términos de ω como sigue:

$$\begin{cases} (\partial_t + u\cdot\nabla)\omega = (\nabla u)\omega, \\ \nabla\cdot u = 0. \end{cases} \tag{3}$$

Usando la ley de Biot-Savart, la velocidad puede ser recuperada a partir de ω por la igualdad

$$u(x,t) = \frac{1}{4\pi}\int_{\mathbf{R}^3}\frac{y\times\omega(x+y,t)}{|y|^3}\,dy.$$

De forma análoga, la ecuación QG (1) se puede escribir como sigue:

$$\begin{cases} (\partial_t + u \cdot \nabla)\nabla^\perp \theta = (\nabla u) \cdot \nabla^\perp \theta, \\ \nabla \cdot u = 0. \end{cases} \tag{4}$$

La función de corriente ψ se obtiene de θ mediante la identidad

$$\psi(x,t) = -\int_{\mathbf{R}^2} \frac{\theta(x+y,t)}{|y|}\, dy.$$

Por tanto,

$$u(x,t) = -\int_{\mathbf{R}^2} \frac{\nabla^\perp \theta(x+y,t)}{|y|}\, dy.$$

Los dos sistemas (3) y (4) son similares: el vector $\nabla^\perp \theta = (\partial_2 \theta, -\partial_1 \theta)$ desempeña el papel de $\omega = \nabla \times u$ en (3). Además, en el caso de la ecuación QG, ∇u es una integral singular en dimensión dos con respecto a $\nabla^\perp \theta$. Mientras que, para (3), ∇u es una integral singular con respecto a la vorticidad; véase [43] y [44].

La similitud también es geométrica, puesto que los vectores ω y $\nabla^\perp \theta$ son tangentes a las líneas de vorticidad y a las curvas de nivel de θ, respectivamente. Las líneas de vorticidad y las curvas de nivel de θ satisfacen la propiedad de moverse con el fluido. En la monografía [3] se describen con más detalle las propiedades de QG y sus similitudes con la ecuación de Euler.

Los primeros resultados de regularidad para (1) se obtuvieron en [16] (resultados equivalentes para Euler en [14],[1], [6] y [34]):

• Si $\theta_0 \in H^k$ con $k \geq 3$, es condición necesaria y suficiente que sea

$$\int_0^T \|\nabla^\perp \theta\|_\infty \, dt = +\infty \tag{5}$$

para tener una singularidad en el tiempo T. Usando técnicas del análisis microlocal, se puede mejorar el criterio sustituyendo la norma L^∞ por normas en los espacios BMO y Triebel-Lizorkin [7].

• Si el vector dirección

$$\xi = \frac{\nabla^\perp \theta}{|\nabla^\perp \theta|} \tag{6}$$

es regular en las regiones donde $|\nabla^\perp \theta|$ es grande, entonces no se puede producir una singularidad.

La ecuación QG tiene una propiedad adicional: todas las normas L^p $(1 < p < \infty)$ de la velocidad se mantienen acotadas por la norma L^p del dato inicial. Pero esto no conduce a una mejora en los resultados de regularidad respecto de los que son conocidos para las ecuaciones de Euler.

2 Singularidades

En [16] se considera la ecuación QG junto con el dato inicial

$$\theta_0(x) = \operatorname{sen} x_1 \operatorname{sen} x_2 + \cos x_2$$

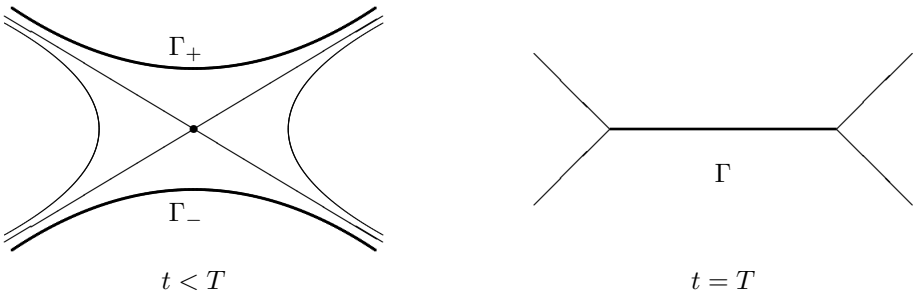

Figura 1: Curvas de nivel de θ.

como posible candidato a desarrollar una singularidad en tiempo finito. Las simulaciones numéricas indican la formación de un frente cuando las curvas de nivel contienen un punto hiperbólico. Las curvas de nivel tienden a colapsar sobre una curva, pasándose de una configuración X a una configuración doble Y :

La función θ es constante sobre curvas del tipo

$$\Gamma_\pm = \{(x_1, x_2) \in \mathbf{R}^2 : x_2 = f_\pm(x_1, t), x_1 \in [a, b]\} \quad para \quad 0 \le t < T. \tag{7}$$

Tres años después, Ohkitani y Yamada [37], con una resolución numérica mucho más precisa, sugirieron que, en vez de una singularidad racional, el crecimiento de las derivadas conduce a una singularidad (al menos) comparable al de una doble exponencial con respecto al tiempo. Constantin, Nie y Schorghofer [17] confirmaron los resultados de [37]. Un resumen de los resultados obtenidos es por tanto el siguiente:

$$\begin{aligned}
&1994: \quad \sup_x |\nabla_x \theta(x,t)| \gtrsim \frac{1}{(8{,}25 - t)^{1{,}66}}, \text{ véase [16]};\\
&1997: \quad \sup_x |\nabla_x \theta(x,t)| \gtrsim e^{e^{[b(t-t_0)]}}, \text{ véase [37]};\\
&1998: \quad \sup_x |\nabla_x \theta(x,t)| \gtrsim e^{e^{[0{,}038(t-4{,}1)]}}, \text{ véase [17]}.
\end{aligned}$$

Estos escenarios resultan de la colisión de las trayectorias de las partículas del fluido sobre la curva Γ. Cada trayectoria $X = X(q,t)$ se obtiene al resolver el problema de Cauchy

$$\frac{dX(q,t)}{dt} = u(X(q,t),t), \quad X(q,0) = q.$$

Para que se produzca la colisión en el tiempo T de las trayectorias $X(p,\cdot)$ y $X(q,\cdot)$ que en el instante inicial están respectivamente ubicadas en $p \in \Gamma_+(0)$

y $q \in \Gamma_-(0)$, se necesita la condición siguiente:

$$\int_0^T \|\nabla u\|_{L^\infty}\, ds = +\infty. \tag{8}$$

Este criterio se obtiene al aplicar el teorema del valor medio a la diferencia de las velocidades de cada trayectoria:

$$|X_t(q,t) - X_t(p,t)| = |u(X(q,t),t) - u(X(p,t),t)| \le |X(q,t) - X(p,t)| \|\nabla u\|_{L^\infty}.$$

Integrando respecto de t se obtiene la estimación

$$|X(q,t) - X(p,t)| \ge |X(q,0) - X(p,0)| e^{-\int_0^t \|\nabla u\|_{L^\infty} ds},$$

de la que se deduce la condición (8).

El criterio clásico para la formación de singularidades en la evolución de un fluido está dado por el teorema de Beale, Kato y Majda [1] (el equivalente para QG es (5)). Este criterio sirve para cualquier tipo de ellas y es una mejora de la estimación (8). Desde el punto de vista de la geometría de las curvas de nivel, el resultado (6) implica que la dirección de ellas tiene que cambiar bruscamente en un entorno de la singularidad, que es exactamente lo que ocurre alrededor de un punto hiperbólico cuando el ángulo de las hipérbolas tiende a cero.

Para atacar el problema analíticamente, supongamos que las curvas de nivel en un entorno U del punto hiperbólico son hipérbolas "simples", definidas por las igualdades $\rho = \text{Const.}$ (supongamos que el punto hiperbólico está en el origen), con

$$\rho = (y_1\beta(t) + y_2)(y_1\delta(t) - y_2). \tag{9}$$

Aquí se ha realizado un cambio de coordenadas no lineal dependiente del tiempo

$$y_1 = F_1(x_1, x_2, t), \quad y_2 = F_2(x_1, x_2, t).$$

Suponemos que las funciones β, δ y F_i verifican

$$\begin{cases} \beta, \delta \in C^1([0,T_*)), \quad F_i \in C^2(\overline{U} \times [0,T_*)), \\ |\beta|, |\delta| \le C, \quad \beta + \delta \ge 0, \\ |\det \dfrac{\partial F_i}{\partial x_j}| \ge c > 0 \quad \forall x \in U, \quad \forall t \in [0,T_*). \end{cases} \tag{10}$$

Como las curvas de nivel se mueven con el fluido, es lógico suponer que para cada t la temperatura $\theta(\cdot,t)$ es constante a lo largo de ρ. Con estas hipótesis demostramos en el teorema siguiente que el ángulo $\alpha(t) = \beta(t) + \delta(t)$ no puede cerrarse más rápidamente que una doble exponencial en tiempo y que las derivadas de la temperatura están acotadas por una cuádruple exponencial también en el tiempo:

Teorema 1 *Sea $\theta = \theta(x,t)$ una solución de* (1)*. Supongamos que θ es constante a lo largo de las curvas $\rho = \text{Const.}$ definidas por* (9) − (10) *con $T_* = +\infty$. Para*

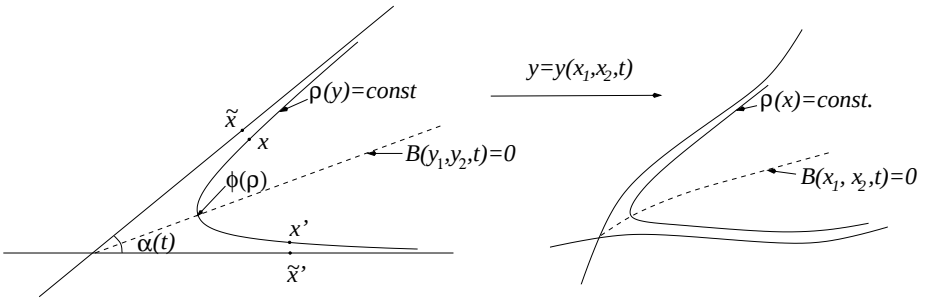

Figura 2: Cambio de coordenadas no lineal dependiente del tiempo.

cada t, supongamos además que θ no es constante en un entorno de U y que las C^2-seminormas de las F_i están acotadas. Entonces

$$|\log\log\frac{1}{\alpha(t)}| \leq Ct + C.$$

Idea de la demostración: La demostración se divide en dos partes. En la primera se obtiene una expresión de la función de corriente en las nuevas variables (ρ, σ). La variable ρ está asociada a las curvas de nivel y la variable σ satisface las siguientes ecuaciones

$$\frac{\partial x_1}{\partial \sigma} = -\frac{\partial \rho}{\partial x_2}, \quad \frac{\partial x_2}{\partial \sigma} = \frac{\partial \rho}{\partial x_1}.$$

Haciendo el cambio de variables en la ecuación original, bajo la hipótesis $\frac{\partial \theta}{\partial \rho} \neq 0$ en U y escribiendo que $\tilde{\theta}(\rho, t) := \theta(x_1, x_2, t)$, obtenemos:

$$u \cdot \nabla_x \theta = \frac{\partial \tilde{\theta}}{\partial \rho}(u \cdot \nabla_x \rho) = -\frac{\partial \tilde{\theta}}{\partial \rho}(\frac{\partial \psi}{\partial x_2}\frac{\partial x_2}{\partial \sigma} + \frac{\partial \psi}{\partial x_1}\frac{\partial x_1}{\partial \sigma}).$$

Por tanto,

$$\frac{\partial \tilde{\theta}}{\partial t} + \frac{\partial \tilde{\theta}}{\partial \rho}(\frac{\partial \rho}{\partial t} - \frac{\partial \psi}{\partial \sigma}) = 0,$$

donde la velocidad satisface $u = \nabla^{\perp}\psi$. Podemos escribir que

$$\frac{\partial \psi}{\partial \sigma} = \frac{\partial \rho}{\partial t} + E_1(\rho, t).$$

Integrando con respecto a σ, obtenemos la expresión deseada de la función de corriente en las nuevas variables:

$$\psi(\rho, \sigma, t) = E_1(\rho, t) \cdot \sigma + \int_0^{\sigma} \frac{\partial \rho}{\partial t}\, d\sigma + E_2(\rho, t), \tag{11}$$

donde E_1 y E_2 son funciones independientes de la variable σ.

En la segunda parte de la demostración elegimos dos puntos x y x' en la misma curva de nivel, pero situadas en distintas ramas de la hipérbola. Evaluamos la función de corriente en los dos puntos y restamos un valor del otro. Luego tomamos límites cuando $\rho \to 0$. De la igualdad (11) se obtiene que

$$\lim_{\rho\to 0}[\psi(x) - \psi(x')] = C\frac{d\alpha}{dt} + O(\alpha). \tag{12}$$

También se puede escribir la función de corriente en la forma

$$\psi(x,t) = -\int_{\mathbf{R}^2} \frac{\theta(x+y,t)}{|y|}\, dy,$$

expresión que proviene de la igualdad $\theta = -(-\triangle)^{\frac{1}{2}}\psi$. Por tanto, tomando límite cuando $\rho \to 0$, obtenemos que

$$\lim_{\rho\to 0} |\psi(x) - \psi(x')| \leq K|\log\alpha|\alpha|. \tag{13}$$

El teorema es una consecuencia de (12) y (13) e implica que

$$\alpha(t) \geq c_1 e^{-e^t},$$

que es una estimación local. Por otra parte, para obtener una cota superior de las derivadas de θ, es necesario tener en cuenta el comportamiento de la solución en el exterior de un entorno U.

Corolario 2 *Supongamos que θ es como en el teorema anterior y que, además, $\xi(x) = \frac{\nabla^\perp\theta}{|\nabla^\perp\theta|}$ satisface $|\nabla\xi| \leq \Phi(t)$ en $(\mathbf{R}^2 \setminus U) \times [0,\infty)$, donde Φ es una función integrable. Entonces*

$$|\nabla\theta| \leq \exp\left(\exp\left(c\int_0^t (e^{e^s} + \Phi(s))\, ds\right)\right)$$

en $\mathbf{R}^2 \times [0,\infty)$.

La posibilidad de tener una singularidad a lo largo de una curva de nivel ayudaría a entender el fenómeno denominado "frontogénesis". Modelar adecuadamente este fenómeno, la formación de frentes de aire frío y aire caliente, es uno de los principales objetivos de la Meteorología.

Los arcos $\Gamma_+(t), \Gamma_-(t)$, definidos anteriormente en (7), representan las curvas de nivel que se mueven con el fluido. Las funciones $f_\pm$ verifican

$$f_\pm \in C^1([a,b]\times[0,T)),$$

$$f_-(x_1,t) < f_+(x_1,t) \quad \forall x_1 \in [a,b], \quad \forall t \in [0,T).$$

La longitud del frente viene dado por la medida del intervalo $[a,b]$. Las curvas $\Gamma_\pm(t)$ están determinadas por las soluciones $f_\pm$ de la ecuación

$$u_2(x_1,x_2,t)=\frac{\partial f}{\partial x_1}(x_1,t)\cdot u_1(x_1,x_2,t)+\frac{\partial f}{\partial t}(x_1,t). \tag{14}$$

En particular, las curvas de nivel de la función escalar $g(x,t)$, que satisface la ecuación $(\partial_t+u\cdot\nabla_x)\,g=0$, también cumplen (14). El colapso de las curvas $\Gamma_\pm(t)$ en la curva Γ en el instante T quiere decir que

$$\lim_{t\to T^-}(f_+(x_1,t)-f_-(x_1,t))=0\quad\forall x_1\in[a,b] \tag{15}$$

y $f_+(x_1,t)-f_-(x_1,t)$ está acotada para $x_1\in[a,b]$, $t\in[0,T)$. Una vez formalizada la dinámica de un frente, se mejora en [23] el criterio de singularidades: no puede darse (15) si

$$\int_0^T \sup\{\,|u(x_1,x_2,t)|:x_1\in[a,b],f_-(x_1,t)\le x_2\le f_+(x_1,t)\,\}\,dt<+\infty. \tag{16}$$

Un frente es uniforme cuando tenemos dos curvas de nivel evolucionando de manera que la distancia (en una región) de los puntos de una de ellas a la otra es comparable. Esto quiere decir que, si definimos δ a partir de la relación

$$\delta(x_1,t)=|f_+(x_1,t)-f_-(x_1,t)|,$$

entonces existe una constante $C>0$ tal que

$$\text{mín}\,\delta(x_1,t)\ge C\,\text{máx}\,\delta(x_1,t).$$

En [24] se obtiene la siguiente estimación de un frente uniforme:

$$\sup_x|\nabla_x\theta(x,t)|\le e^{e^{At+B}},$$

donde A y B son constantes. Este resultado es independiente del crecimiento de la velocidad.

3 Soluciones viscosas

En esta sección consideramos el problema de Cauchy para la ecuación quasi-geostrófica con viscosidad, denotada QGV. Esta ecuación ha sido estudiada en [5], [12], [18], [13], [37], [39], [9], [19], [20], [42], [45], [46] y [47] y es la siguiente:

$$\begin{cases}(\partial_t+u\cdot\nabla)\,\theta=-\kappa(-\triangle)^\gamma\theta,\\ u=\nabla^\perp\psi,\quad \psi=-(-\triangle)^{-1/2}\theta\quad\text{en}\quad Q,\end{cases} \tag{17}$$

donde $\gamma\in(0,1]$.

En [37] también se realizaron simulaciones de la ecuación viscosa en el caso $\gamma=1$ y se observó un crecimiento sólo exponencial de las derivadas de θ en el entorno de un punto hiperbólico.

Con $\kappa > 0$, Constantin y Wu [18] demostraron la existencia de solución global para $1/2 < \gamma \leq 1$, y recientemente se ha resuelto el caso crítico en [33] y [4]. Es un problema abierto la existencia o no de singularidades cuando $\gamma < 1/2$. Hasta el momento, los resultados de existencia global que se conocen son válidos para datos iniciales cuya norma (en un espacio funcional adecuado) es más pequeña que la viscosidad.

En el siguiente cálculo mostramos que si el dato inicial $\sum_{l\in\mathbb{Z}^2} |\widehat{\theta}(l,0)|$ es pequeño comparado con la viscosidad, entonces

$$\sum_{l\in\mathbb{Z}^2} |\widehat{\theta}(l,t)| \leq \sum_{l\in\mathbb{Z}^2} |\widehat{\theta}(l,0)| \tag{18}$$

para todo tiempo.

En el dominio periodico Π^2, los coeficientes de Fourier de las soluciones de la ecuación QGV satisfacen:

$$\frac{d}{dt}\widehat{\theta}(l,t) + \kappa|l|^{2\gamma}\widehat{\theta}(l,t) = i \sum_{j+k=l} \frac{j^{\perp}\cdot k}{|j|}\widehat{\theta}(j,t)\widehat{\theta}(k,t).$$

Multiplicando la ecuación por $\widehat{\theta}(l,t)^*$, se obtiene

$$\frac{1}{2}\frac{d}{dt}|\widehat{\theta}(l,t)|^2 + \kappa|l|^{2\gamma}\,|\widehat{\theta}(l,t)|^2 = \mathrm{Re}\; i\;\widehat{\theta}(l,t)^* \sum_{j+k=l} \frac{j^{\perp}\cdot k}{|j|}\widehat{\theta}(j,t)\widehat{\theta}(k,t),$$

donde $\mathrm{Re}\, z$ denota la parte real de z. Entonces

$$\frac{d}{dt}|\widehat{\theta}(l,t)| + \kappa|l|^{2\gamma}\,|\widehat{\theta}(l,t)| \leq \sum_{j+k=l} |k||\widehat{\theta}(j,t)|\,|\widehat{\theta}(k,t)|.$$

Sumando en l, obtenemos la desigualdad

$$\frac{d}{dt}\sum_{l\in\mathbb{Z}^2} |\widehat{\theta}(l,t)| + \kappa \sum_{l\in\mathbb{Z}^2} |l|^{2\gamma}\,|\widehat{\theta}(l,t)| \leq \left[\sum_{l\in\mathbb{Z}^2} |\widehat{\theta}(l,t)|\right]\left[\sum_{l\in\mathbb{Z}^2} |l||\widehat{\theta}(l,t)|\right],$$

de la que se deduce (18) cuando $\gamma \geq \frac{1}{2}$ y $\sum_{l\in\mathbb{Z}^2} |\widehat{\theta}(l,0)| \leq \kappa$.

En el trabajo en colaboración con Constantin y Wu [13], demostramos el siguiente resultado:

Teorema 3 *Existe una constante C_∞ tal que, para todo $\theta_0 \in H^2$ con*

$$\|\theta_0\|_{L^\infty} \leq C_\infty \kappa,$$

la solución θ del problema del valor inicial para QGV ($\gamma = \frac{1}{2}$) con dato inicial θ_0 satisface

$$\|\theta(\cdot,t)\|_{H^2} \leq \|\theta_0\|_{H^2} \quad \forall t \geq 0.$$

Bajo las hipótesis del teorema, probamos también que la solución es única y satisface

$$\|\theta(\cdot,t)\|_{H^2} \leq e^{-Ct}\|\theta_0\|_{H^2}.$$

La importancia de este resultado, que le distingue de otros de datos pequeños, radica en que en él vemos que la norma L^∞ decrece con el tiempo. En su Tesis Doctoral, Resnick [39] demostró de una forma muy ingeniosa que las soluciones de (17) satisfacen

$$\|\theta(\cdot,t)\|_{L^p} \leq \|\theta_0\|_{L^p} \quad \forall t \geq 0$$

para $1 < p \leq +\infty$.

En el caso de las ecuaciones de Navier-Stokes es posible probar resultados de regularidad bajo la hipótesis de que ciertas normas son pequeñas comparadas con la viscosidad. Pero no hay resultados de tipo principio del máximo y por tanto no se llega a la estimación (ni al decaimiento) de la norma L^∞.

Tratando de entender el decaimiento de la norma L^∞ de θ, en los trabajos [19] y [20] obtenemos la siguiente

Desiguladad puntual: Sean $0 \leq \gamma \leq 2$ y sea θ una función C_0^∞ (en $\mathbf{R}^2$ o Π^2). Entonces

$$2(\theta\Lambda^\gamma\theta)(x) \geq (\Lambda^\gamma\theta^2)(x)$$

(recuérdese que $\Lambda^\gamma = (-\Delta)^{\gamma/2}$).

Se trata de una estimación puntual, generalización de la regla de la cadena para derivadas fraccionarias, que implica diversos principios del máximo en modelos con origen en la Mecánica de medios continuos. En estos trabajos se demuestra una propiedad local que resulta sorprendente (dado el carácter no local de los operadores involucrados) y es muy útil y complementa la información que proporciona el Cálculo Diferencial.

Aplicando la desigualdad puntual y las desigualdades de energía en los espacios de Sobolev, a partir de la ecuación QGV obtenemos la siguiente estimación en L^p con $1 \leq p < +\infty$:

$$\|\theta(\cdot,t)\|_{L^p}^p \leq \frac{\|\theta_0\|_{L^p}^p}{(1+\epsilon Ct\|\theta_0\|_{L^p}^{p\epsilon})^{1/\epsilon}}\ , \tag{19}$$

donde $C = C(\kappa,\gamma,p,\|\theta_0\|_1)$ es una constante positiva y $\epsilon = \frac{\gamma}{2(p-1)}$.

Para estudiar el caso $p = +\infty$ no es suficiente tomar el límite $p \to +\infty$ en la desigualdad (19). Hay que estudiar la evolución de θ a lo largo de la trayectoria donde alcanza el máximo (o el mínimo) y usar las propiedades de diferenciabilidad de las funciones Lipschitz-continuas para justificar la existencia para casi todo tiempo de la derivada.

Teorema 4 *Sean θ y u funciones regulares en Q verificando* (17) *con $\kappa > 0$ y $0 < \gamma \leq 2$ y $\nabla \cdot u = 0$. Entonces*

$$\|\theta(\cdot,t)\|_{L^\infty} \leq \frac{\|\theta_0\|_{L^\infty}}{(1+\gamma Ct\|\theta_0\|_{L^\infty}^{\gamma})^{1/\gamma}} \quad \forall t \in [0,T),$$

donde $\theta_0 = \theta(\cdot,0)$ *y* $C = C(\kappa,\theta_0) > 0$. *Además, cuando* $\gamma = 0$, *tenemos un decaimiento exponencial de* $\|\theta(\cdot,t)\|_{L^\infty}$. *Más precisamente,*

$$\|\theta(\cdot,t)\|_{L^\infty} \le \|\theta_0\|_{L^\infty} e^{-\kappa t} \quad \forall t \in [0,T). \tag{20}$$

Los teoremas 3.1 y 3.2 nos permiten ahora estudiar la existencia de soluciones a partir de un tiempo T. Con ese propósito, nos interesamos por las soluciones débiles de

$$\theta_t + R(\theta)\cdot\nabla^\perp\theta = -\kappa\Lambda\theta. \tag{21}$$

Así, dado un dato inicial $\theta_0 \in H^s$ con $s > 1$, llamaremos *solución viscosa* a todo límite débil, cuando $\epsilon \to 0^+$, de una sucesíon de soluciones, cuando $\epsilon \to 0$, de la ecuación

$$\theta^\epsilon_t + R(\theta^\epsilon)\cdot\nabla^\perp\theta^\epsilon = -\kappa\Lambda\theta^\epsilon + \epsilon\Delta\theta^\epsilon$$

con $\theta^\epsilon(x,0) = \theta_0$. El resultado que se obtiene es el siguiente:

Teorema 5 *Sea* θ *una solución viscosa de* (21) *con dato inicial* $\theta_0 \in H^s$, *con* $s > 3/2$. *Entonces existen dos tiempos* T_1 *y* T_2 *con* $0 < T_1 \le T_2$ *que dependen sólo de* κ *y del dato inicial* θ_0, *tales que:*

1) $\theta|_{[0,T_1)} \in C^1([0,T_1);H^s)$ *es una solución fuerte de la ecuación que verifica*

$$\|\theta(\cdot,t)\|_{H^s} \le C\|\theta_0\|_{H^s} \quad \forall t \in [0,T_1).$$

2) $\theta|_{[T_2,+\infty)} \in C^1([T_2,+\infty);H^s)$ *también es solución fuerte y* $\|\theta(\cdot,t)\|_{H^s}$ *es monótona decreciente en t, está acotada por* $C\|\theta_0\|_{H^s}$ *y verifica*

$$\int_{T_2}^{+\infty} \|\theta\|^2_{H^s}\,dt < +\infty.$$

En particular, esto último implica que

$$\|\theta(\cdot,t)\|_{H^s} = O(t^{-1/2}) \quad \textit{cuando} \quad t \to +\infty.$$

La demostración del teorema está basada en el decaimiento de la norma L^∞ y un argumento de *bootstrap* asociado a la evolución de diferentes normas de Sobolev. Un ejemplo típico de este mecanismo es la siguiente cadena de desigualdades:

$$\begin{aligned}
\frac{d}{dt}\|\theta^\epsilon\|^2_{L^2} &= 2\int \theta^\epsilon R(\theta^\epsilon)\cdot\nabla^\perp\theta^\epsilon - 2\kappa\int\theta^\epsilon\Lambda\theta^\epsilon - 2\epsilon\int|\Lambda\theta^\epsilon|^2 \\
&= -2\kappa\|\Lambda^{\frac12}\theta^\epsilon\|^2_{L^2} - 2\epsilon\|\Lambda\theta^\epsilon\|^2_{L^2} \le -2\kappa\|\Lambda^{\frac12}\theta^\epsilon\|^2_{L^2},
\end{aligned}$$

$$\begin{aligned}
\frac{d}{dt}\|\Lambda^{\frac12}\theta^\epsilon\|^2_{L^2} &= 2\int \Lambda^{\frac12}\theta^\epsilon\Lambda^{\frac12}(R(\theta^\epsilon)\cdot\nabla^\perp\theta^\epsilon) - 2\kappa\|\Lambda\theta^\epsilon\|^2_{L^2} - 2\epsilon\|\Lambda^{\frac32}\theta^\epsilon\|^2_{L^2} \\
&\le (C\|\theta^\epsilon(\cdot,t)\|_{L^\infty} - 2\kappa)\|\Lambda\theta^\epsilon\|^2_{L^2}, \\
&\frac{d}{dt}\|\Lambda\theta^\epsilon\|^2_{L^2} \le (C\|\Lambda\theta^\epsilon\|_{L^2} - \kappa)\|\Lambda^{\frac32}\theta^\epsilon\|^2_{L^2}, \\
&\frac{d}{dt}\|\Lambda^{\frac32}\theta^\epsilon\|^2_{L^2} \le (C\|\theta^\epsilon\|_{L^\infty} - \kappa)\|\Delta\theta^\epsilon\|^2_{L^2},
\end{aligned}$$

donde C es una constante independiente de la viscosidad artificial ϵ.

4 Modelos unidimensionales

Siguiendo la línea de trabajo de [15], construimos modelos unidimensionales de la ecuación QG capturando la propiedad de que θ se mueve con un flujo no local, representado por una integral singular con respecto a θ, i.e. la convolución de θ con un núcleo de media cero en la esfera unidad y homogéneo de grado igual a menos la dimensión espacial. Si además conservamos la propiedad de que el escalar θ se mueve con el fluido, obtenemos el siguiente modelo:

$$\theta_t - H\theta\,\theta_x = 0, \tag{22}$$

donde la "velocidad" $H\theta$ es la transformada de Hilbert de θ, definida por

$$H\theta(x) = \frac{1}{\pi}\,\text{V.P.}\int_{-\infty}^{\infty}\frac{\theta(y)}{x-y}\,dy,$$

o bien

$$H\theta(x) = \frac{1}{2\pi}\,\text{V.P.}\int_{-\pi}^{\pi}\frac{\theta(x-y)}{\text{tg}\,\frac{y}{2}}dy,$$

según estemos considerando la ecuación (22) en $\mathbf{R}\times\mathbf{R}_+$ o $\Pi\times\mathbf{R}_+$.

Otra forma de escribir la ecuación QG es $\theta_t + \nabla\cdot(u\theta) = 0$. Por tanto, sustituyendo $u = (-R_2\theta, R_1\theta)$ por su equivalente unidimensional $H\theta$, se obtiene el modelo:

$$\theta_t + (\theta H\theta)_x = 0. \tag{23}$$

A. Morlet, motivado por una situación física diferente, estudió en [36] la ecuación

$$\theta_t + \delta(\theta H\theta)_x + (1-\delta)H\theta\,\theta_x = 0, \tag{24}$$

donde $0\le\delta\le 1$. Para esta ecuación, demostró la existencia de singularidades cuando $0<\delta<1/3$, $\delta = 1/2$ y $\delta = 1$. En [8] se demuestra el siguiente resultado:

Teorema 6 *Dado un dato inicial periódico $\theta_0\in C^1([-\pi,\pi])$, no constante y tal que*

$$\int_{-\pi}^{\pi}\theta_0\,dx = 0,$$

no existen soluciones $\theta\in C^1([-\pi,\pi]\times[0,\infty))$ de la ecuación (11) para $\delta>0$.

Idea de la demostración: Se observa que

$$\begin{aligned}\frac{d}{dt}\int_{-\pi}^{\pi}\theta(x,t)\,dx &= -\delta\int_{-\pi}^{\pi}(\theta H\theta)_x\,dx - (1-\delta)\int_{-\pi}^{\pi}\theta_x H\theta\,dx\\ &= (1-\delta)\int_{-\pi}^{\pi}\theta H\theta_x\,dx\\ &\ge 0.\end{aligned}$$

Por tanto, poniendo

$$M(t)\equiv\max_x\theta(x,t)\ge 0,\quad m(t)\equiv\min_x\theta(x,t),$$

tenemos en $t = 0$ las desigualdades $M(0) > 0$, $m(0) < 0$.

Las funciones M y m son Lipschitz-continuas y, por el teorema de H. Rademacher, diferenciables en casi todo t. Para cada t podemos elegir $x(t)$ y $\overline{x}(t)$ tales que

$$M(t) = \theta(x(t), t), \quad m(t) = \theta(\overline{x}(t), t).$$

Sea t_0 un punto de diferenciabilidad de $M(t)$. Por compacidad podemos escoger una sucesión $h_j \to 0$ tal que $x(t_0 + h_j)$ converge a x_0. Entonces por continuidad se obtiene que $M(t_0) = \theta(x_0, t_0)$ y además

$$\begin{aligned}
&\frac{M(t_0 + h_j) - M(t_0)}{h_j} = \frac{\theta(x(t_0 + h_j), t_0 + h_j) - \theta(x_0, t_0)}{h_j} \\
&= \frac{\theta(x(t_0 + h_j), t_0 + h_j) - \theta(x(t_0 + h_j), t_0)}{h_j} + \frac{\theta(x(t_0 + h_j), t_0) - \theta(x_0, t_0)}{h_j} \\
&\leq \frac{\theta_t(x(t_0 + h_j), t_0 + \overline{h}_j) \cdot h_j}{h_j} \\
&= -\theta_x(x(t_0 + h_j), t_0 + \overline{h}_j) \cdot H\theta(x(t_0 + h_j), t_0 + \overline{h}_j) \\
&-\theta(x(t_0 + h_j), t_0 + \overline{h}_j) \cdot \Lambda\theta(x(t_0 + h_j), t_0 + \overline{h}_j)
\end{aligned}$$

para ciertos $\overline{h}_j$, $0 \leq \overline{h}_j \leq h_j$.

Tomando el límite $h_j \to 0$ obtenemos la desigualdad

$$M'(t_0) \leq -\delta\theta(x_0, t_0)\Lambda\theta(x_0, t_0).$$

Cuando la sucesión h_j es negativa entonces se obtiene la desigualdad contraria que implica

$$M'(t_0) = -\delta\theta(x_0, t_0)\Lambda\theta(x_0, t_0).$$

Por un argumento análogo se demuestra que la función m decae y satisface:

$$m'(t) = -\frac{\delta}{2\pi} m(t) \int_{-\pi}^{\pi} \frac{\theta(\overline{x}, t) - \theta(y, t)}{\operatorname{sen}^2 \frac{\overline{x} - y}{2}} \, dy \leq 0$$

en casi todo t, donde $\overline{x}$ es un punto tal que $m(t) = \theta(\overline{x}, t)$. Además, $\int_{-\pi}^{\pi} \theta_0(x)\, dx \geq 0$, $M(t) \leq M(0)$ y $m(t) \leq m(0) < 0$. Luego el conjunto

$$\{\, y : \theta(y, t) \geq \frac{\theta(\overline{x}, t)}{2} \,\}$$

tiene medida esctrictamente positiva. En particular, existe una constante C tal que:

$$\frac{\delta}{2\pi} \int_{-\pi}^{\pi} \frac{\theta(y, t) - \theta(\overline{x}, t)}{\operatorname{sen}^2 \frac{\overline{x} - y}{2}} \, dy \geq C|\theta(\overline{x}, t)|.$$

Entonces

$$|m|'(t) \geq C|m(t)|^2$$

y la función m explota en tiempo finito, contradiciendo la hipótesis de existencia de solución regular θ para todo $t \geq 0$.

En el caso $\delta = 1$ se pueden construir soluciones exactas por medio de una *transformación hodógrafa*, con dato inicial $\theta_0 = \operatorname{sen} x$. Entonces las soluciones θ y $u = H\theta$ satisfacen

$$-t\theta = \log\sqrt{u^2+\theta^2}, \quad -(x-tu) = \operatorname{arctg}\frac{\theta}{u}.$$

En las Figuras 3 y 4 representamos los perfiles de θ y u en cinco instantes de tiempo diferentes: $t = 0, 0{,}09, 0{,}18, 0{,}27, e^{-1}$.

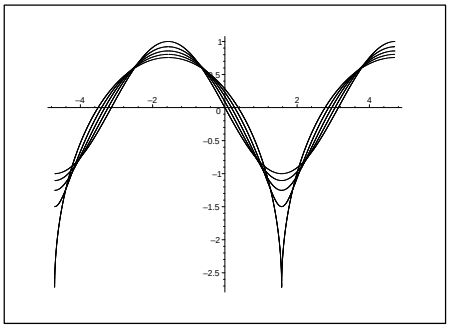

Figura 3: θ evaluado para $t = 0$, 0,09, 0,18, 0,27, e^{-1}.

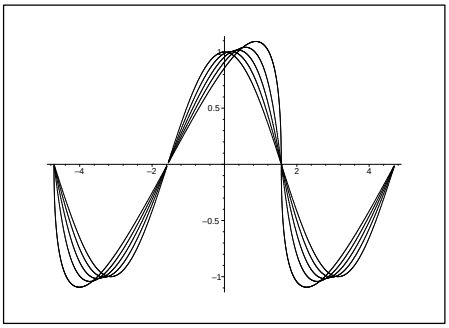

Figura 4: u evaluado para $t = 0$, 0,09, 0,18, 0,27, e^{-1}.

El caso $\delta = 0$ de (24), es decir, la ecuación (22), se estudia en [21]. Si se toma $-H\theta = v$, sin más que derivar respecto de x, vemos que $\theta_{xt} - H\theta\,\theta_{xx} = H\theta_x\,\theta_x$; se observa por tanto la similitud con (3) tomando $w = \theta_x$.

Para este modelo estudiamos la evolución de un dato inicial positivo simétrico, con $\max_x \theta_0 = \theta_0(0)$ y soporte compacto. Entonces el perfil de θ se transporta con el flujo $-H\theta$. Así, $\theta(\cdot,t)$ continúa siendo una función positiva simétrica, con soporte contenido en el soporte inicial y con $\|\theta(\cdot,t)\|_{L^2}$ acotada por $\|\theta_0\|_{L^2}$. Para datos de este este tipo, mediante uso de transformadas de Mellin, se obtiene en [21] que $\|\theta_x(\cdot,t)\|_{L^2}$ explota en tiempo finito. La idea de la demostración es escribir (22) en la forma

$$(1-\theta)_t = -H(1-\theta)(1-\theta)_x,$$

dividir por $x^{1+\delta}$ $(0 < \delta < 1)$ e integrar respecto de x en el intervalo $(0, L)$. Se obtiene que

$$\begin{aligned}\frac{d}{dt}\left(\int_0^L \frac{(1-\theta)}{x^{1+\delta}}\,dx\right) &= -\int_0^L \frac{(1-\theta)_x H(1-\theta)}{x^{1+\delta}}\,dx \\ &= -\int_0^\infty \frac{(1-\theta)_x H(1-\theta)}{x^{1+\delta}}\,dx. \qquad (25)\end{aligned}$$

Se usa el resultado siguiente:

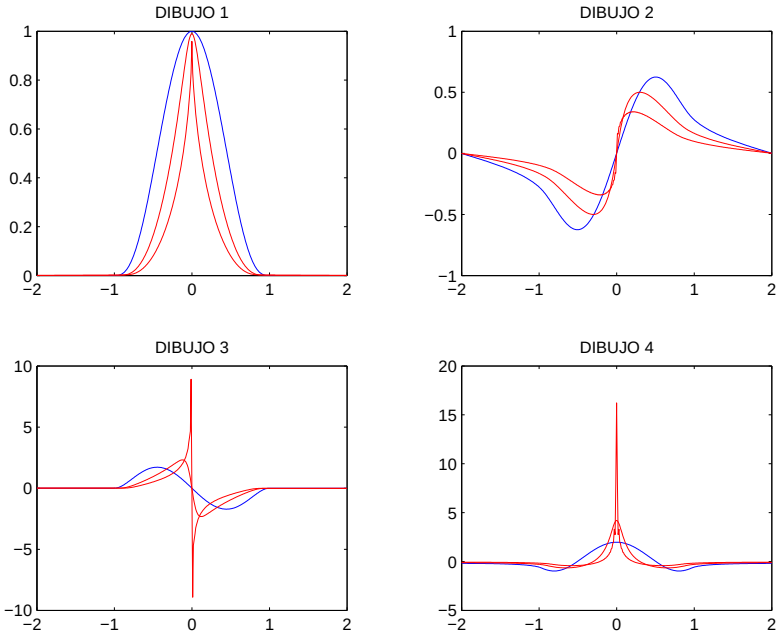

Figura 5: Se muestra la evolución para tiempos $t = 0$, $t = 0{,}35$ y $t = 0{,}7$ y viscosidad $\nu = 0{,}01$ de las siguientes cantidades: θ en Dibujo 1, $H\theta$ en Dibujo 2, θ_x en Dibujo 3 y $\Lambda\theta$ en Dibujo 4.

Lema 7 *Sea $f \in C_c^\infty(\mathbb{R}^+)$. Entonces, para cada $0 < \delta < 1$ existe una constante $C_\delta > 0$ tal que*

$$-\int_0^\infty \frac{f_x(x)(Hf)(x)}{x^{1+\delta}}\,dx \geq C_\delta \int_0^\infty \frac{1}{x^{2+\delta}} f^2(x)\,dx. \tag{26}$$

Teniendo en cuenta la desigualdad de Cauchy, se deduce que

$$\frac{d}{dt}\left(\int_0^L \frac{(1-\theta)}{x^{1+\delta}}\,dx\right) \geq C_{L,\delta}\left(\int_0^L \frac{(1-\theta)}{x^{1+\delta}}\,dx\right)^2,$$

con lo que se demuestra explosión en tiempo finito.

Si introducimos un término disipativo en la ecuación, es decir, poniendo

$$\theta_t - H\theta\,\theta_x = -\kappa\Lambda^\gamma\theta, \tag{27}$$

para datos iniciales positivos θ_0, obtenemos $0 \leq \theta(x,t) \leq \|\theta_0\|_{L^\infty}$ y $\|\theta(\cdot,t)\|_{L^2} \leq \|\theta_0\|_{L^2}$. Así, cuando $\gamma > 1$, se obtiene regularidad global. Aparece como caso crítico $\gamma = 1$, para el que tenemos existencia global cuando $\|\theta_0\|_{L^\infty}$ es pequeño, i.e. cuando $\|\theta_0\|_{L^\infty} < C\kappa$.

No se sabe qué ocurre en este caso crítico si el dato inicial inicial no es pequeño, ni cuál es el comportamiento de las soluciones cuando $0 < \gamma < 1$.

Mediante simulaciones numéricas obtenemos la evolución de θ, $H\theta$, θ_x y $\Lambda\theta$ según se muestra en la Figura 5, observándose la formación de singularidades.

5 "Patches"

El primero en abordar la formulación débil de (1) fue Resnick [39]. Este autor llamó solución débil a toda función θ que verifica

$$\int_{\Pi^2} \varphi(x)\theta(x,T)\,dx - \int_{\Pi^2} \varphi(x)\theta_0(x)\,dx = \int_0^T \int_{\Pi^2} \nabla\varphi\,\theta\,u\,dx\,dt$$

para toda función $\varphi \in C_c^\infty$, donde $u = (-R_2\theta, R_1\theta)$ para casi todo $t \in [0,T]$. Y demostró la existencia global por el método de Galerkin en Π^2. Esta solución cumple $\|\theta(\cdot,t)\|_{L^2} \le \|\theta_0\|_{L^2}$ y, por tanto, $\|u(\cdot,t)\|_{L^2} \le \|u_0\|_{L^2}$. El problema de la unicidad de solución débil está abierto.

La ecuación QG tiene la propiedad fundamental de que las curvas de nivel se mueven con el fluido, i.e. no se transfiere fluido a través de ellas. Entonces una solución natural, con energía finita, es una región cerrada (acotada y conexa) $\Omega(t)$ donde θ verifica

$$\theta(x,t) = \begin{cases} 1 & \text{si } x \in \Omega(t), \\ 0 & \text{si } x \in \mathbf{R}^2 \setminus \Omega(t), \end{cases}$$

que evoluciona con la velocidad del fluido, conservando el área inicial. Estas soluciones parten con un frente ya formado sobre la frontera de $\Omega(t)$ y se denominan "patches". Este tipo de soluciones fueron estudiadas en [2], [10] y [3] para la ecuación de la vorticidad para el sistema de Euler incompresible (donde la vorticidad se conserva a lo largo de trayectorias).

En [27] estudiamos la dinámica de α-"patches" para una familia de ecuaciones que "interpola" las ecuaciones QG y Euler 2D. Un α-patch ($0 < \alpha < 1$) consiste en una región $\Omega(t)$ de $\mathbf{R}^2$ (conexa y acotada) que se mueve con una velocidad dada por

$$u(x(s,t),t) = \frac{\theta_0}{2\pi} \int_{C(t)} |x(s,t) - x(s',t)|^{-\alpha} \frac{\partial x}{\partial s}(s',t)\,ds'.$$

Aquí, $x(s,t)$ determina la posición de la frontera del dominio $\Omega(t)$, parametrizada con s. La dinámica de la evolución del contorno $\partial\Omega(t)$ viene dada por

$$\frac{dx(s,t)}{dt} = u(x(s,t),t),$$

y los α-patches determinan soluciones débiles de la ecuación

$$\begin{cases} (\partial_t + u\cdot\nabla)\,\theta = 0, \\ u = \nabla^\perp\psi, \quad \theta = -(-\triangle)^{1-\gamma/2}\psi. \end{cases} \tag{28}$$

El caso límite en que $\gamma = 0$ (2D Euler) ha sido estudiado analíticamente con éxito por Chemin [10] y Bertozzi-Constantin [2], demostrándose la existencia

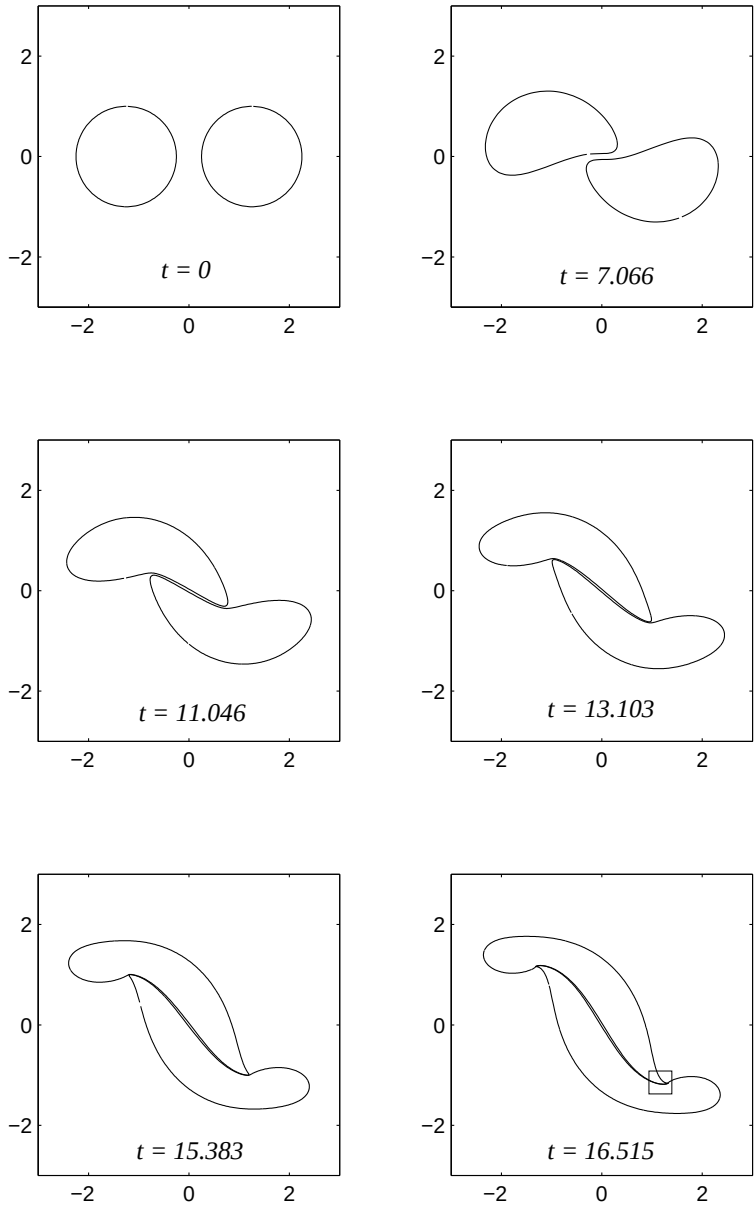

Figura 6: Evolución de dos patches con $\alpha = 0{,}5$. El recuadro que aparece en el tiempo t=16.515 está ampliada en la Figura 8 a)

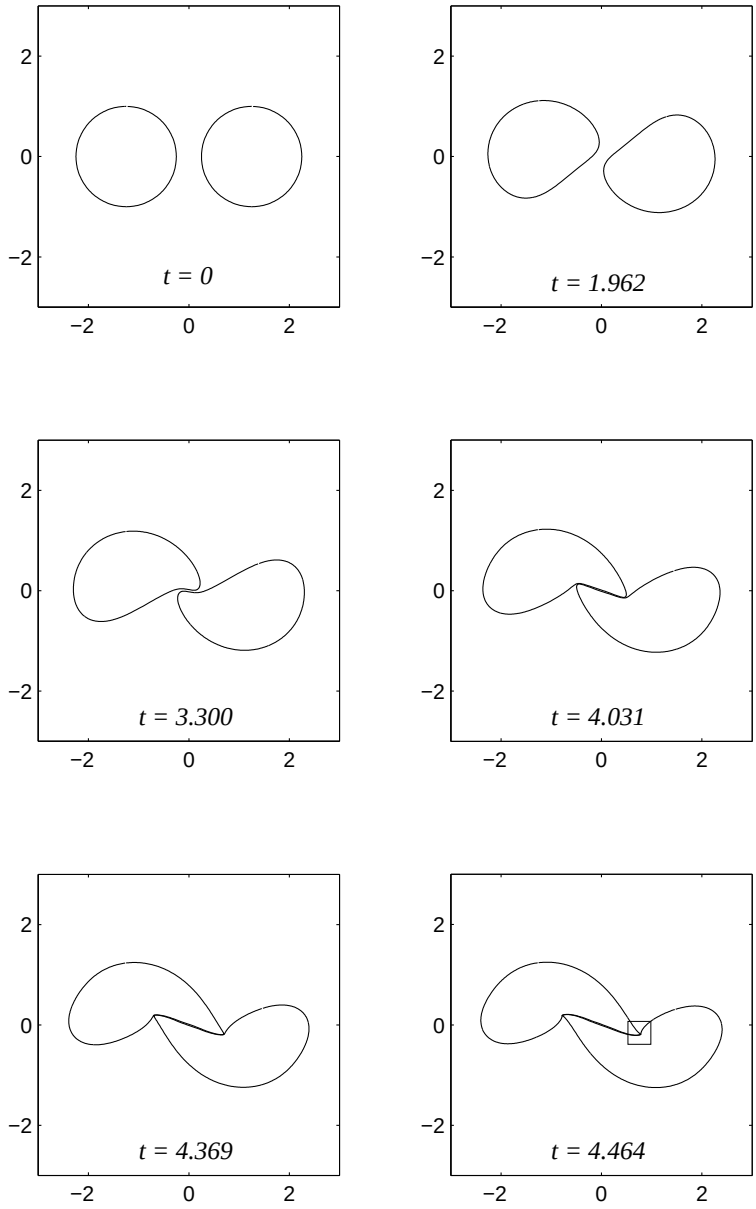

Figura 7: Evolución de dos patches con $\alpha = 1$. El recuadro que aparece en el tiempo t=4.464 está ampliada en la Figura 8 b)

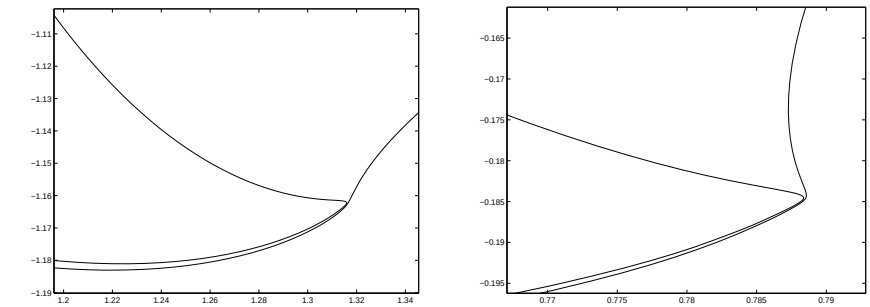

Figura 8: Colapso y explosión de la curvatura de los α-patches a) $\alpha = 0{,}5$ y b) $\alpha = 0{,}5$.

global de solución. En el caso $\gamma = 1$, Rodrigo [40] ha demostrado la existencia local de solución usando argumentos de tipo Nash-Moser.

En [27] hemos encontrado numéricamente posibles candidatos de singularidades para la familia de ecuaciones (28). En los casos particulares $\alpha = 0{,}8$ y $\alpha = 1$ (véase Figuras 6 y 7), observamos la formación de una "esquina" que desarrolla un alto crecimiento de la curvatura en el mismo punto donde se produce la mínima distancia entre los dos patches. En la Figura 7 aparece con más detalle el posible escenario para el colapso de patches.

Además, al re-escalar la variable espacial en la forma

$$x = (t_0 - t)^{\delta}, \quad \text{con} \quad \delta = 1/\alpha,$$

introduciendo la nueva variable $\tau = -\log(t_0 - t)$, la ecuación se transforma en

$$\frac{\partial y}{\partial \tau} - \delta y = \frac{\theta_0}{2\pi} \int_{C(t)} |y(s,t) - y(s',t)|^{-\alpha} \frac{\partial y}{\partial s}(s',t)\, ds'. \tag{29}$$

Las soluciones de (29) independientes de τ representan soluciones de (28) con la propiedad de que la curvatura máxima crece como

$$\kappa = \frac{1}{R} \sim \frac{C}{(t_0 - t)^{1/\gamma}} \quad \text{cuando} \quad t \to t_0$$

y la distancia mínima entre los dos patches satisface

$$d \sim C(t_0 - t)^{1/\gamma} \quad \text{cuando} \quad t \to t_0.$$

Estas singularidades tienen la característica de ser estables y auto-similares y aparecen en un punto del plano en el que la curvatura explota al mismo tiempo que colapsa dos curvas de nivel.

Referencias

[1] J. T. Beale, T. Kato, y A. Majda. Remarks on the breakdown of smooth solutions for the 3D Euler equations. *Comm. Math. Phys.*, 94:61–64, 1984.

[2] A. L. Bertozzi y P. Constantin. Global regularity for vortex patches. Commun. Math. Phys. **152** (1993), no.1, 19-28.

[3] A. L. Bertozzi y A. J. Majda. Vorticity and the Mathematical Theory of Incompresible Fluid Flow. *Cambridge Press*

[4] L. Caffarelli, A. Vasseur. Drift diffusion equations with fractional diffusion and the quasi-geostrophic equation. Arxiv preprint math.AP/0608447, 2006.

[5] J.A. Carrillo y L.C.F. Ferreira. Convergence towards a self-similar assymptotic behavior for the dissipative quasi-geostrophic equations.*Aparecera en Banach center of publications.*

[6] D. Chae. On the Euler equations in the critical Triebel-Lizorkin spaces. Arch. Ration. Mech. Anal. 170 (2003), no. 3, 185–210.

[7] D. Chae, The quasi-geostrophic equation in the Triebel-Lizorkin spaces. *Nonlinearity* **16** n^o 2 (2003), 479-495.

[8] D. Chae, A. Córdoba, D. Córdoba y M. Fontelos. Finite time singularities in a 1D model of the quasi-geostrophic equations., Advances in Math., 194 (2005).

[9] D. Chae and J. Lee, Global Well-Posedness in the super critical dissipative Quasi-geostrophic equations. *Commun. Math. Phys.* **233** (2003), 297-311.

[10] J.Y. Chemin. "Persistance de structures géométriques dans les fluides incompressibles bidimensionnels". Ann. Ec. Norm. Supér. **26** (1993), no.4, 1-16.

[11] P. Constantin. Geometric Statistics turbulence. *SIAM Rev.*, 36:73-98, 1994.

[12] P. Constantin, Energy Spectrum of Quasi-geostrophic Turbulence, *Phys. Rev. Lett.* **89** n^o 18 (2002), 1804501-4.

[13] P. Constantin, D. Córdoba y J. Wu. On the critical dissipative quasi-geostrophic equation. *Indiana Univ. Math. J.* 50: 97-107, 2001.

[14] P. Constantin, C. Fefferman, y A. J. Majda. Geometric constraints on potentially singular solutions for the 3-D Euler equations. *Commun. Part. Diff. Eq.*, 21:559–571, 1996.

[15] P. Constantin, P.D. Lax y A. J. Majda. A simple one-dimensional model for the three-dimensional vorticity equation *Comm. Pure Appl. Math* 38:715-724.

[16] P. Constantin, A. J. Majda, y E. Tabak. Formation of strong fronts in the 2-D quasigeostrophic thermal active scalar. *Nonlinearity*, 7:1495–1533, 1994.

[17] P. Constantin, P. Nie y N. Schorghofer. Nonsingular surface-quasi-geostrophic flow. *Phys. Lett. A* 241:168-172, 1998.

[18] P. Constantin y J. Wu. Behavior of solutions of 2D Quasi-geostrophic equations. *SIAM J. Math. Anal* 30:937-948, 1999.

[19] A. Córdoba y D. Córdoba, A pointwise estimate for fractionary derivatives with applications to P.D.E., *Proc. Natl. Acad. Sci.,* **100**, n^o 26, (2003), 15316-15317.

[20] A. Córdoba y D. Córdoba, A maximum principle applied to Quasi-geostrophic equations, Comm. Math. Phys. 249 (2004), no. 3, 511–528.

[21] A. Córdoba, D. Córdoba, y M. Fontelos. "Formation of singularities for a transport equation with nonlocal velocity", *Annals of Math.* 162 (3) (2005).

[22] D. Córdoba. Nonexistence of simple hyperbolic blow-up for the quasi-geostrophic equation. *Ann. of Math.*, 148(3), 1998.

[23] D. Córdoba y C. Fefferman. Scalars convected by a 2D incompressible flow. *Comm. Pure. Appl. Math.*, 55:255-260, 2002.

[24] D. Córdoba y C. Fefferman. Growth of solutions for QG and 2D Euler equations. *Journal Amer. Math. Soc.*, 15(3):665-670, 2002.

[25] D. Córdoba, C. Fefferman y R. de la LLave. On squirt singularities in hydrodynamics. SIAM J. Math. Anal. 36 (2004), no. 1, 204–213 .

[26] D. Córdoba, C. Fefferman y J.L. Rodrigo. Almost sharp fronts for the surface quasi-geostrophic equations, Proc. Natl. Acad. Sci., 101 (2004), no. 9, 2687–2691.

[27] D. Córdoba, M. Fontelos, A. Mancho y J.L. Rodrigo. "Evidence of singularities for a family of countor dynamics equations ", *Proc. Natl. Acad. Sci. USA* 102 (2005), no. 17, 5949–5952.

[28] E. Dinaburg, V. Posvyanskii y Ya. Sinai. On some approximations of the Quasi-geostrophic equation. Geometric methods in dynamics. II. Astérisque No. 287 (2003), xvii, 19–32.

[29] S. Friedlander y R. Shvydkoy. The unstable spectrum of the surface quasi-geostropic equation. J. Math. Fluid Mech. 7 (2005), suppl. 1, S81–S93.

[30] I. Held, R. Pierrehumbert y S. Garner. Surface quasi-geostrophic dynamics. *J. Fluid Mech.* 282:1-20, 1995.

[31] N. Ju. The maximum principle and the global attractor for the dissipative 2D quasi-geostrophic equations. Comm. Math. Phys. 255 (2005), no. 1, 161–181.

[32] N. Ju. On the two dimensional quasi-geostrophic equations. Indiana Univ. Math. J. 54 (2005), no. 3, 897–926. .

[33] A. Kiselev, F. Nazarov, A. Volberg. Global well-posedness for the critical 2D dissipative quasi-geostrophic equation. Arxiv preprint math.AP/0604185, 2006

[34] H. Kozono y Y. Taniuchi. "Limiting case of the Sobolev inequality in BMO, with application to the Euler equations." Comm. Math. Phys. **214** (2000), no. 1, 191–200.

[35] A. Majda y E. Tabak. A two-dimensional model for quasi-geostrophic flow: comparison with the two-dimensional Euler flow. *Physica D* , 98:515-522, 1996.

[36] A. Morlet. Further properties of a continuum of model equations with globally defined flux. *Journal of Mathematical Analysis and Applications* **221** (1998), 132-160.

[37] K. Ohkitani y M. Yamada. Inviscid and inviscid-limit behavior of a surface quasi-geostrophic flow. *Phys. Fluids* , 9: 876-882, 1997.

[38] J. Pedlosky. Geophysical fluid dynamics. *Springer-Verlag* New york, 345-368, 1987.

[39] S. Resnick. Dynamical problem in nonlinear advective partial differential equations. *PhD thesis University of Chicago*, 1995.

[40] J.L. Rodrigo. "On the evolution of sharp fronts for the Quasi-geostrophic equation". Comm. Pure Appl. Math. 58 (2005), 821-866.

[41] R. Salmon. Lectures on Geophysical Fluid Dynamics. *Oxford University Press*

[42] M.E. Schonbek y T.P. Schonbek, Asymptotic behavior to dissipative quasi-geostrophic flows, *SIAM J. Math. Anal.,* **35**, n^o 2, (2003), 357-375.

[43] E. Stein. Singular integrals and differentiability properties of functions. *Princeton University Press.* Princeton, NJ, 1970.

[44] E. Stein. Harmonic Analysis. *Princeton University Press.* Princeton, NJ, 1993.

[45] J. Wu. Dissipative quasi-geostrophic equations with L^p data, *Electronic Journal of Dfferential Equations* **56** (2001), 1-13.

[46] J. Wu. The quasi-geostrophic equations and its two regularizations. *Comm. Partial Differential Equations* **27** n^o 5-6 (2002), 1161-1181.

[47] J. Wu. Inviscid limits and regularity estimates for the solutions of the 2-D dissipative Quasi-geostrophic equations. *Indiana Univ. Math. J.* **46** n^o 4 (1997), 1113-1124.

Bol. Soc. Esp. Mat. Apl.
n°38(2007), 93–113

MULTIPHASE FLOW IN POROUS MEDIA

BENITO M. CHEN-CHARPENTIER

Department of Mathematics, University of Wyoming,
Laramie, WY 82071-3036, USA.

bchen@uwyo.edu

Abstract

In this short course we will derive the basic conservation laws for mass momentum and energy. We will extend the results to mixtures in general and then to multiphase flow in porous media. We will describe the black-oil models and the Buckley-Leverett problem.

Key words: *multiphase flow, porous media*
AMS subject classifications: *76S05 76T30*

1 Equations of Motion

We will start by deriving the equations of motion for a simple fluid consisting of only one phase and one component, such as water or oil. Assume the continuum hypothesis: we work at a scale large enough where we don't worry about individual molecules. When we talk about a particle of fluid we are refereing to a mass of fluid occupying a volume small from the macroscopic point of view but large enough to be considered a continuum.
Let $\underset{\sim}{x} = (x, y, z)$ be a point in space.
Let $\underset{\sim}{v}(\underset{\sim}{x}, t)$ be the velocity of a particle of fluid moving through $\underset{\sim}{x}$ at time t.
Let $\rho(\underset{\sim}{x}, t)$ be the mass density, so that the mass of a fluid region W is

$$m(W,t) = \int_W \rho(\underset{\sim}{x}, t) dV$$

The equations of motion are based on the following conservation principles:

1. Mass is neither created nor destroyed.
2. The rate of change of momentum equals the applied force.
3. Energy is conserved.

Fecha de recepción: 17/04/2006

1. Conservation of Mass
   Let W be a fixed region, the rate of change of mass in this region is

$$\frac{d}{dt}m(W,t) = \frac{d}{dt}\int_W \rho(\underset{\sim}{x},t)dV = \int_W \frac{\partial \rho}{\partial t}(\underset{\sim}{x},t)dV.$$

This rate of increase (decrease) of mass in W equals the rate of mass getting into (exiting) the volume:

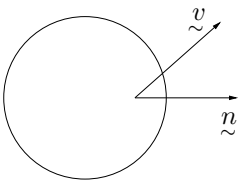

$$\frac{d}{dt}\int_W \rho dV = \oint_{\partial W} \rho \underset{\sim}{v} \cdot \underset{\sim}{n}\, dA,$$

where ∂W is the surface of W and $\underset{\sim}{n}$ is the outward unit normal vector. The divergence theorem states that:

$$\oint_{\partial W} \underset{\sim}{f} \cdot \underset{\sim}{n}\, dA = \int_W \mathrm{div}\underset{\sim}{f}\, dV.$$

Applying it, we then have

$$\int_W \left[\frac{\partial \rho}{\partial t} + \mathrm{div}\left(\rho \underset{\sim}{v}\right)\right] dV = 0.$$

This is the conservation law in integral form. Since this is valid for all W we have the differential conservation form:

$$\frac{\partial \rho}{\partial t} + \mathrm{div}\left(\rho \underset{\sim}{v}\right) = 0.$$

Of course, this requires that $\rho, \underset{\sim}{v}$ be differentiable.

2. Conservation of momentum:
   Let the velocity be

$$\underset{\sim}{v}(\underset{\sim}{x},t) = \frac{d\underset{\sim}{x}(t)}{dt}$$

and the acceleration be

$$\underset{\sim}{a}(t) = \frac{d^2\underset{\sim}{x}(t)}{dt^2}.$$

Then using the chain rule we have

$$\begin{aligned}\underset{\sim}{a}(t) &= \frac{\partial \underset{\sim}{v}}{\partial x}\dot{x} + \frac{\partial \underset{\sim}{v}}{\partial y}\dot{y} + \frac{\partial \underset{\sim}{v}}{\partial z}\dot{z} + \frac{\partial \underset{\sim}{v}}{\partial t} \\ &= \partial_t \underset{\sim}{v} + \underset{\sim}{v} \cdot \nabla \underset{\sim}{v},\end{aligned}$$

where $\partial_t \underset{\sim}{v} = \dfrac{\partial \underset{\sim}{v}}{\partial t}$ and $\underset{\sim}{v} \cdot \nabla = u\dfrac{\partial}{\partial x} + v\dfrac{\partial}{\partial y} + w\dfrac{\partial}{\partial z}$.

Let $\dfrac{D}{Dt} = \partial_t + \underset{\sim}{v} \cdot \nabla$ be the material derivative, that is, the derivative following a fluid particle.

First let's work with an ideal fluid: the only force is the pressure, there are no tangential stresses.

The force across the surface per unit area is $p(\underset{\sim}{x}, t)\underset{\sim}{n}$, where $p(\underset{\sim}{x}, t)$ is the pressure and $\underset{\sim}{n}$ is the outward unit normal. Then the total force exerted on the fluid through the boundary is

$$\underset{\sim}{S}_{\partial W} = -\oint_{\partial W} p\underset{\sim}{n}\, dA.$$

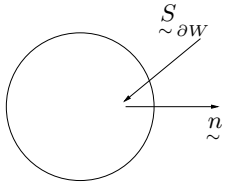

For any fixed vector $\underset{\sim}{e}$:

$$\underset{\sim}{e} \cdot \underset{\sim}{S}_{\partial W} = -\oint_{\partial W} p\underset{\sim}{e} \cdot \underset{\sim}{n}\, dA = -\int_W \operatorname{div}(p\underset{\sim}{e}) dV = -\int_W (\operatorname{grad} p) \cdot \underset{\sim}{e}\, dV.$$

The second equality is obtained using the divergence theorem and the third one by using the vector identity $\operatorname{div}(\phi \underset{\sim}{a}) = \phi \operatorname{div} \underset{\sim}{a} + \underset{\sim}{a} \cdot \operatorname{grad}\phi$ with $\underset{\sim}{a}$ fixed. Therefore we have that the surface force due to the pressure is $\underset{\sim}{S}_{\partial W} = -\displaystyle\int_W \operatorname{grad} p\, dV$.

If $\underset{\sim}{b}(\underset{\sim}{x}, t)$ is the body force per unit mass, usually only the force of gravity, then the total body force is $\underset{\sim}{B} = \displaystyle\int_W \rho \underset{\sim}{b}\, dV$.
Therefore, for any piece of material, the force per unit volume is $-\operatorname{grad} p + \rho\underset{\sim}{b}$. By Newton's second law, (which states that, for constant density, the force is equal to the mass times the acceleration), we have the balance of momentum law

$$\rho \frac{D\underset{\sim}{v}}{Dt} = -\operatorname{grad} p + \rho \underset{\sim}{b}.$$

3. Conservation of Energy

First we will deal only with mechanical energy, that is, kinetic energy. Over a volume W_t, that always has the same molecules, it is defined as

$$E_k = \frac{1}{2}\int_{W_t} \rho \left\| \underset{\sim}{v} \right\|^2 dV.$$

Its rate of change with time is

$$\begin{aligned}\frac{d}{dt}E_k &= \frac{d}{dt}\left[\frac{1}{2}\int_{W_t}\rho\left\|\underset{\sim}{v}\right\|^2 dV\right]\\ &= \frac{1}{2}\int_{W_t}\rho\frac{D\left\|\underset{\sim}{v}\right\|^2}{Dt}dV\\ &= \int_{W_t}\rho\left(\underset{\sim}{v}\cdot\left(\frac{\partial\underset{\sim}{v}}{\partial t}+\left(\underset{\sim}{v}\cdot\nabla\right)\underset{\sim}{v}\right)\right)dV.\end{aligned}$$

The last equality is since $\frac{1}{2}\frac{D}{D}\left\|\underset{\sim}{v}\right\|^2 = \underset{\sim}{v}\cdot\frac{\partial\underset{\sim}{v}}{\partial t}+\left(\underset{\sim}{v}\cdot\left(\underset{\sim}{v}\cdot\nabla\right)\underset{\sim}{v}\right)$ as can be proven working component-wise.

Incompressible Flow

The rate of change of the kinetic energy equals the rate at which the pressure and body forces do work:

$$\frac{d}{dt}E_k = -\int_{\partial W_t}p\underset{\sim}{v}\cdot\underset{\sim}{n}\,dA+\int_{W_t}\rho\underset{\sim}{v}\cdot\underset{\sim}{b}\,dV,$$

and using the divergence theorem we get:

$$\int_{W_t}\rho\left[\underset{\sim}{v}\cdot\left(\frac{\partial\underset{\sim}{v}}{\partial t}+\underset{\sim}{v}\cdot\nabla\underset{\sim}{v}\right)\right]dV = -\int_{W_t}\operatorname{div}(p\underset{\sim}{v})-(\rho\underset{\sim}{v}\cdot b)dV.$$

Since the fluid is incompressible the law of mass conservation, $\frac{D\rho}{Dt}+\rho\ \operatorname{div}\underset{\sim}{v} = 0$, implies that $\operatorname{div}\underset{\sim}{v} = 0$.

Therefore the last integral is

$$-\int_{W_t}\left(\underset{\sim}{v}\cdot\nabla p-\rho\underset{\sim}{v}\cdot\underset{\sim}{b}\right)dV.$$

And, since the volume is arbitrary:

$$\rho\left[\underset{\sim}{v}\cdot\left(\frac{\partial\underset{\sim}{v}}{\partial t}+\underset{\sim}{v}\cdot\nabla\underset{\sim}{v}\right)\right] = -\underset{\sim}{v}\cdot\nabla p+\rho\underset{\sim}{v}\cdot\underset{\sim}{b}$$

or $\rho\frac{D\underset{\sim}{v}}{Dt} = -\nabla p+\rho\underset{\sim}{b}$ which is the conservation of momentum law.

Navier-Stokes Equations

Now we will include the viscous forces, so the force acting on a surface S per unit area is $-p(\underset{\sim}{x},t)\underset{\sim}{n}+\underset{\sim}{\sigma}(x,t)\cdot\underset{\sim}{n}$, where $\underset{\sim}{\sigma}$ is the shear stress tensor, which is of rank 2.

We need more assumptions to be able to close the system. We assume that the fluid is newtonian, for which the shear tensor is given by

$$\underset{\sim}{\sigma}=2\mu\left[D-\frac{1}{3}\mathrm{div}\,\underset{\sim}{v}I\right]+\zeta(\mathrm{div}\,\underset{\sim}{v})I,$$

where μ is the first coefficient of viscosity,
$\zeta=\lambda+\dfrac{2}{3}\mu$ is the second coefficient of viscosity and
D is the deformation tensor, given by $D=\dfrac{1}{2}\left[\mathrm{grad}\,\underset{\sim}{v}+(\mathrm{grad}\,\underset{\sim}{v})^T\right]$.
Component-wise the deformation tensor is $D_{ij}=\dfrac{1}{2}\left(\dfrac{\partial u_i}{\partial x_j}+\dfrac{\partial u_j}{\partial x_i}\right)$.
And I is the identity matrix.

Using the divergence theorem as before, the moment balance law gives the Navier-Stokes equations:

$$\rho\frac{D\underset{\sim}{v}}{Dt}=-\nabla p+(\lambda+\mu)\nabla(\mathrm{div}\,\underset{\sim}{v})+\mu\Delta\underset{\sim}{v},$$

$$\text{where}\quad \Delta\underset{\sim}{v}=\left(\frac{\partial^2}{\partial x^2}+\frac{\partial^2}{\partial y^2}+\frac{\partial^2}{\partial z^2}\right)\underset{\sim}{v}.$$

2 Equations of Motion II

An alternative approach to deriving the equations of motion which is more powerful mathematically but less intuitive is presented next. Let ν be a material volume (one that contains the same material particles).

The general form of a global balance law for a given quantity ψ (per unit mass) is as follows:

$$\frac{d}{dt}\int_\nu\rho\psi dV-\oint_{\partial\nu}\underset{\sim}{\tau}\cdot\,\underset{\sim}{n}dA-\int_\nu\rho g dV=0.$$

$\underset{\sim}{\tau}$	is the flux of ψ across the surface
g	is the external supply of ψ inside the volume
$\partial\nu$	is the boundary of ν
$\underset{\sim}{n}$	is the outward normal to ν

The first term in the global balance law is the rate of change of ψ inside the volume, the second the amount of ψ transported through the boundary and the last term is the supply of ψ inside the volume.

Using the divergence theorem,

$$\int_\nu\mathrm{div}\,\underset{\sim}{f}dV=\oint_{\partial\nu}\underset{\sim}{f}\cdot\,\underset{\sim}{n}dA,$$

to convert the surface integral to a volume integral we get

$$\frac{d}{dt}\int_\nu \rho\psi dV - \int_\nu \underset{\sim}{\text{div}}\underset{\sim}{\tau} dV - \int_\nu \rho g dV = 0.$$

Reynolds transport theorem says that

$$\frac{d}{dt}\int_\nu f dV = \int_\nu \left(\frac{Df}{Dt} + f\underset{\sim}{\text{div}}\underset{\sim}{v}\right) dV.$$

Applying it:

$$\int_\nu \left[\frac{D\rho\psi}{Dt} + \rho\psi\underset{\sim}{\text{div}}\underset{\sim}{v} - \underset{\sim}{\text{div}}\underset{\sim}{\tau} - \rho g\right] dV = 0.$$

Since the above is valid for any arbitrary volume ν, we obtain the differential balance law:

$$\frac{D\rho\psi}{Dt} + \rho\psi\nabla\cdot\underset{\sim}{v} - \underset{\sim}{\text{div}}\underset{\sim}{\tau} - \rho g = 0.$$

Mass Balance

$$\psi = 1, \qquad \underset{\sim}{\tau} = \underset{\sim}{0}, \qquad g = 0$$

$$\frac{D\rho}{Dt} + \rho\underset{\sim}{\text{div}}\underset{\sim}{v} = 0 \quad \text{in Lagrangian coordinates}$$

$$\frac{\partial\rho}{\partial t} + v\cdot\nabla\rho + \rho\underset{\sim}{\text{div}}\underset{\sim}{v} = \frac{\partial\rho}{\partial t} + \text{div}\left(\rho\underset{\sim}{v}\right) = 0 \quad \text{in Eulerian}$$

Momentum balance

$$\psi = \underset{\sim}{v}, \qquad \underset{\sim}{\tau} = \underset{\approx}{t} \text{ stress tensor}, \quad g = \underset{\sim}{b} \text{ body forces (gravity)}$$

$$\frac{D}{Dt}(\rho\underset{\sim}{v}) + \rho\underset{\sim}{v}\underset{\sim}{\text{div}}\underset{\sim}{v} - \underset{\approx}{\text{div}}\underset{\approx}{t} - \rho\underset{\sim}{b} = 0$$

$$\rho\frac{D\underset{\sim}{v}}{Dt} + \underbrace{\underset{\sim}{v}\frac{D\rho}{Dt} + \rho\underset{\sim}{v}\underset{\sim}{\text{div}}\underset{\sim}{v}} - \underset{\approx}{\text{div}}\underset{\approx}{t} - \rho\underset{\sim}{b} = 0$$

$$\underset{\sim}{v}\left(\frac{D\rho}{Dt} + \rho\underset{\sim}{\text{div}}\underset{\sim}{v}\right) = 0 \quad \text{by mass balance.}$$

So the conservation of momentum gives

$$\rho\frac{D\underset{\sim}{v}}{Dt} - \underset{\approx}{\text{div}}\underset{\approx}{t} - \rho\underset{\sim}{b} = \underset{\sim}{0}.$$

Angular momentum balance

This implies that the stress tensor is symmetric:

$$\underset{\approx}{t} = \underset{\approx}{t}^T$$

Energy balance

$$\psi = \underbrace{E}_{\substack{\text{internal}\\ \text{energy}\\ \text{density}}} + \underbrace{\frac{1}{2}\underset{\sim}{v}\cdot\underset{\sim}{v}}_{\text{kinetic energy}}$$

$$\underset{\sim}{\tau} = \underbrace{\underset{\sim}{q}}_{\text{heat flux}} + \underbrace{\underset{\approx}{t}\cdot\underset{\sim}{v}}_{\text{work done by stress}} \qquad g = \underbrace{h}_{\text{heat supply}} + \underbrace{\underset{\sim}{b}\cdot\underset{\sim}{v}}_{\text{work of body forces}}$$

$$\frac{D}{Dt}\left[\rho\left(E+\frac{1}{2}\underset{\sim}{v}\cdot\underset{\sim}{v}\right)\right] + \rho\left(E+\frac{1}{2}\underset{\sim}{v}\cdot\underset{\sim}{v}\right)\operatorname{div}\underset{\sim}{v} - \operatorname{div}(\underset{\sim}{q} + \underset{\approx}{t}\cdot\underset{\sim}{v}) - \rho(h+\underset{\sim}{b}\cdot\underset{\sim}{v}) = 0$$

$$\rho\frac{DE}{Dt} + \rho\frac{D}{Dt}\left(\frac{1}{2}\underset{\sim}{v}\cdot\underset{\sim}{v}\right) + \left(E+\frac{1}{2}\underset{\sim}{v}\cdot\underset{\sim}{v}\right)\left(\frac{D\rho}{Dt} + \rho\operatorname{div}\underset{\sim}{v}\right) - \operatorname{div}\underset{\sim}{q}$$

$$-\underset{\sim}{v}\cdot(\operatorname{div}\underset{\approx}{t}) - \underbrace{\underset{\approx}{t} : \nabla\underset{\sim}{v}}_{\sum_i\sum_j t_{ij}\frac{\partial v_i}{\partial x_j}} - \rho h - \rho\underset{\sim}{b}\cdot\underset{\sim}{v} = 0$$

From the momentum equation:

$$\underbrace{\underset{\sim}{v}\cdot\left(\rho\frac{D\underset{\sim}{v}}{Dt} - \operatorname{div}\underset{\approx}{t} - \rho\underset{\sim}{b}\right)}_{\text{mechanical energy balance,}} = 0 \qquad \text{since} \qquad \underset{\sim}{v}\cdot\frac{D\underset{\sim}{v}}{Dt} = \frac{D}{Dt}\left(\frac{1}{2}\underset{\sim}{v}\cdot\underset{\sim}{v}\right)$$

we get the thermal energy balance:

$$\rho\frac{DE}{Dt} - \operatorname{div}\underset{\sim}{q} - \underset{\sim}{t} : \nabla\underset{\sim}{v} - \rho h = 0.$$

And finally, as before, we need to specify the material by giving the constitutive relations. For a Newtonian fluid

$$t_{ij} = p\delta_{ij} + \lambda\delta_{ij}\frac{\partial v_k}{\partial x_h} + \mu\left(\frac{\partial v_i}{\partial x_j} + \frac{\partial v_j}{\partial x_i}\right),$$

where we sum over repeated indices.

3 Mixtures

Many real life problems involve fluids that consist of more than one phase (liquid, gas) and more than one component or species (water, methane). So we have to determine how to study solutions, or fluids in permeable media, or mixtures with chemical reactions? To answer these questions we need to obtain the conservation laws for mixtures.
Definition: A mixture is a collection of N bodies called constituents, forming overlapping continua. At each point in space, $\underset{\sim}{x}$, we can have material from each constituent.

For example: Salt water has water and sodium, N_a^+, and chloride, Cl^- From a molecular point of view the species are separated but macroscopically they occupy the same space.

Another example is sandstone, which is a porous and permeable rock, filled with water. The segregation of the phases is observable at a microscopic scale much larger than the molecular scale. But macroscopically sandstone and water occupy the same space.

Suppose we have N constituents, $\alpha = 1, \ldots, N$ Each one has its own motion:

$$\underset{\sim}{x}^\alpha = \underset{\sim}{x}^\alpha(\underset{\sim}{X}^\alpha, t)$$

$$\underset{\sim}{X}^\alpha = \underset{\sim}{X}^\alpha(\underset{\sim}{x}^\alpha, t),$$

where $\underset{\sim}{X}^\alpha$ is the Lagrangian label of the particle initially at spatial (eulerian) position $\underset{\sim}{x}^\alpha$.

Also its own velocity:

$$\underset{\sim}{V}^\alpha\left(\underset{\sim}{X}^\alpha, t\right) = \frac{\partial \underset{\sim}{x}^\alpha}{\partial t}\left(\underset{\sim}{X}^\alpha, t\right); \quad \underset{\sim}{v}^\alpha\left(\underset{\sim}{x}^\alpha, t\right) = \underset{\sim}{V}^\alpha\left(\underset{\sim}{X}^\alpha(\underset{\sim}{x}^\alpha, t), t\right),$$

and its own density $\rho^\alpha(\underset{\sim}{x}^\alpha, t)$ (mass of α per unit volume of α).

The total mass of α in a part P of the mixture is

$$M^\alpha(P) = \int_{\underset{\sim}{x}^\alpha(P)} \rho^\alpha dV$$

For multiphase mixtures, we assign to each constituent α a volume fraction, $\phi^\alpha(\underset{\sim}{x}^\alpha, t)$, which is the fraction of the volume occupied by α. So that in any part P of the mixture the total volume within P occupied by α is

$$F^\alpha(P) = \int_{\underset{\sim}{x}^\alpha(P)} \phi^\alpha dV,$$

where $\phi^\alpha = \dfrac{\text{volume of } \alpha}{\text{volume of mixture}}$. Therefore, $0 \le \phi^\alpha \le 1$ and $\displaystyle\sum_{\alpha=1}^{N} \phi^\alpha = 1$.

We need some definitions.

Definition.- Overall mass density:

$$\rho = \begin{cases} \displaystyle\sum_{\alpha=1}^{N} \rho^{\alpha} & \text{multispecies mixtures} \\ \\ \displaystyle\sum_{\alpha=1}^{N} \phi^{\alpha}\rho^{\alpha} & \text{multiphase mixtures} \end{cases}$$

Definition.- Mass fraction:

$$w^{\alpha} = \begin{cases} \dfrac{\rho^{\alpha}}{\rho} & \text{multispecies mixtures} \\ \\ \phi^{\alpha}\dfrac{\rho^{\alpha}}{\rho} & \text{multiphase mixtures} \end{cases}$$

Note that

$$\sum_{\alpha=1}^{N} w^{\alpha} = 1.$$

Definition.- Baricentric velocity (mass weighted mean of velocities):

$$\underset{\sim}{v} = \begin{cases} \dfrac{1}{\rho}\displaystyle\sum_{\alpha=1}^{N} \rho^{\alpha}\underset{\sim}{v}^{\alpha} & \text{multispecies} \\ \\ \dfrac{1}{\rho}\displaystyle\sum_{\alpha=1}^{N} \phi^{\alpha}\rho^{\alpha}\underset{\sim}{v}^{\alpha} & \text{multiphase} \end{cases}$$

The diffusion velocity of a constituent α with respect to the mean mixture flow velocity is

$$\underset{\sim}{\nu}^{\alpha} = \underset{\sim}{v}^{\alpha} - \underset{\sim}{v}.$$

Note that for multispecies mixtures

$$\sum_{\alpha} w^{\alpha}\underset{\sim}{\nu}^{\alpha} = \frac{1}{\rho}\sum_{\alpha} \rho^{\alpha}(\underset{\sim}{v}^{\alpha} - \underset{\sim}{v}) = \frac{1}{\rho}\left[\sum_{\alpha} \rho^{\alpha}\underset{\sim}{v}^{\alpha} - \underset{\sim}{v}\sum_{\alpha} \rho^{\alpha}\right]$$

$$= \underset{\sim}{v} - \frac{1}{\rho}\underset{\sim}{v}\rho = \underset{\sim}{0}.$$

And similarity for multiphase mixtures.

For mixtures the general global balance laws are:

Multispecies

$$\sum_{\alpha=1}^{N}\left(\frac{d}{dt}\int_{\nu_\alpha}\rho^\alpha\psi^\alpha dV-\oint_{\partial\nu_\alpha}\underset{\sim}{\tau}^\alpha\cdot\underset{\sim}{n}dA-\int_{\nu_\alpha}\rho^\alpha g^\alpha dV\right)=0.$$

Multiphase

$$\sum_{\alpha=1}^{N}\left(\frac{d}{dt}\int_{\nu_\alpha}\phi^\alpha\rho^\alpha\psi^\alpha dV-\oint_{\partial\nu_\alpha}\underset{\sim}{\tau}^\alpha\cdot\underset{\sim}{n}dA-\int_{\nu_\alpha}\phi^\alpha\rho^\alpha g^\alpha dV\right)=0.$$

Local or differential mixture balance laws are obtained in a similar way to the one constituent case.
Multispecies:

$$\sum_{\alpha=1}^{N}\left[\frac{D^\alpha}{Dt}(\rho^\alpha\psi^\alpha)+\rho^\alpha\psi^\alpha\mathrm{div}\underset{\sim}{v}^\alpha-\mathrm{div}\underset{\sim}{\tau}^\alpha-\rho^\alpha g^\alpha\right]=0.$$

Multiphase:

$$\sum_{\alpha=1}^{N}\left[\frac{D^\alpha}{Dt}(\phi^\alpha\rho^\alpha\psi^\alpha)+\phi^\alpha\rho^\alpha\psi^\alpha\mathrm{div}\underset{\sim}{v}^\alpha-\mathrm{div}\underset{\sim}{\tau}^\alpha-\phi^\alpha\rho^\alpha g^\alpha\right]=0.$$

Here

$$\frac{D^\alpha}{Dt}=\begin{cases}\dfrac{\partial}{\partial t} & \text{for functions of Lagrange coordinates}\left(\underset{\sim}{X}^\alpha,t\right)\\[2ex] \dfrac{\partial}{\partial t}+\underset{\sim}{v}^\alpha\cdot\nabla & \text{for functions of spatial coordinates }(\underset{\sim}{x}^\alpha,t).\end{cases}$$

To write the conservation law for each constituent we need to take into account the interactions among constituents. Let e^α be a measurement of the exchange of ψ into constituent α from other constituents. Therefore we have:
Multispecies

$$\frac{D^\alpha}{Dt}(\rho^\alpha\psi^\alpha)+\rho^\alpha\psi^\alpha\mathrm{div}\underset{\sim}{v}^\alpha-\mathrm{div}\underset{\sim}{\tau}^\alpha-\rho^\alpha g^\alpha=e^\alpha,\qquad\alpha=1,\ldots,N.$$

Multiphase

$$\frac{D^\alpha}{Dt}(\phi^\alpha\rho^\alpha\psi^\alpha)+\phi^\alpha\rho^\alpha\psi^\alpha\mathrm{div}\underset{\sim}{v}^\alpha-\mathrm{div}\underset{\sim}{\tau}^\alpha-\phi^\alpha\rho^\alpha g^\alpha=e^\alpha,\qquad\alpha=1,\ldots,N.$$

From the laws for the whole mixture we can see that

$$\sum_{\alpha=1}^{N}e^\alpha=0.$$

As a first example, consider the transport of a dissolved contaminant by a fluid.
The constituents are: S=solute(contaminant) F=fluid.
So we have a multispecies mixture with no chemical reactions.
Looking at the mass balance: $\psi^\alpha = 1 \qquad \tau^\alpha = 0, \qquad g^\alpha = 0, \qquad e^\alpha = 0.$
(e^α is the production of constituent α by chemical reaction but in this case there is none).

$$\frac{D^\alpha \rho^\alpha}{Dt} + \rho^\alpha \mathrm{div} \underset{\sim}{v}^\alpha = \frac{\partial \rho^\alpha}{\partial t} + \mathrm{div}(\rho^\alpha \underset{\sim}{v}^\alpha) = 0 \qquad \alpha = S, F$$
$$\frac{\partial \rho^\alpha}{\partial t} + \mathrm{div}(\rho^\alpha \underset{\sim}{v}) + \mathrm{div} \underset{\sim}{j}^\alpha = 0,$$

where: $\underset{\sim}{j}^\alpha = \rho^\alpha \underset{\sim}{\nu}^\alpha$ is the diffusive flux.

Consider the solute, we need a constitutive law for $\underset{\sim}{j}^S$. Use Fick's Law:

$$\underset{\sim}{j}^S = -K^S \nabla \rho^S \text{ with } K^S > 0, \text{ the diffusion coefficient.}$$

This implies $\dfrac{\partial \rho^S}{\partial t} + \mathrm{div}\left(\rho^S \underset{\sim}{v}\right) - \mathrm{div}\left(K^S \nabla \rho^S\right) = 0$ Advection-diffusion transport equation.

Example: Fluid Flow in porous rock. Even for one fluid this is multiphase. We have two constituents: F fluid, R, rock. Assume that the flow is chemically inert (no mass exchanges) and that the rock is immobile ($\underset{\sim}{v}^R = 0$). Lets look at the conservation of momentum law:

$$\begin{aligned}
&\psi^\alpha = \underset{\sim}{v}^\alpha, && \text{velocity}\\
&\underset{\sim}{\tau}^\alpha = \mathbf{t}^\alpha, && \text{stress tensor}\\
&g^\alpha = \underset{\sim}{b}^\alpha, && \text{body forces}\\
&e^\alpha = \underset{\sim}{m}^\alpha, && \text{rate of momentum exchange.}
\end{aligned}$$

The differential conservation law is then:

$$\frac{D^\alpha}{Dt}\left(\phi^\alpha \rho^\alpha \underset{\sim}{v}^\alpha\right) + \phi^\alpha \rho^\alpha \underset{\sim}{v}^\alpha \mathrm{div} \underset{\sim}{v}^\alpha - \mathrm{div}\mathbf{t}^\alpha - \phi^\alpha \rho^\alpha \underset{\sim}{b}^\alpha = \underset{\sim}{m}^\alpha$$
$$\rho^\alpha \phi^\alpha \frac{D^\alpha \underset{\sim}{v}^\alpha}{Dt} + v^\alpha \underbrace{\left[\frac{D}{Dt}\left(\phi^\alpha \rho^\alpha\right) + \phi^\alpha \rho^\alpha \mathrm{div} \underset{\sim}{v}^\alpha\right]}_{\text{mass balance}} - \mathrm{div}\mathbf{t}^\alpha - \phi^\alpha \rho^\alpha \underset{\sim}{b}^\alpha = \underset{\sim}{m}^\alpha$$

Suppose the fluid is inviscid:

$$t^F = -pI.$$

and that the only body force is gravity:

$$\phi^F \underset{\sim}{b}^F = g \nabla z, \qquad z \text{ is the depth below a reference level.}$$

Suppose the momentum transfer is given by Stokes drag which says that $\underset{\sim}{m}^F$ is proportional to the fluid velocity:

$$\underset{\sim}{m}^F = \frac{\phi^F}{\Lambda}\left(-\underset{\sim}{v}^F\right) = -\frac{\phi^F}{\Lambda}\underset{\sim}{v}^F, \quad \text{where} \Lambda \text{ is the fluid mobility.}$$

The conservation law is now:

$$\phi^F \rho^F \frac{D^F \underset{\sim}{v}^F}{Dt} + \nabla p^F - \rho^F g \nabla z = -\frac{\phi^F}{\Lambda}\underset{\sim}{v}^F.$$

A common assumption is that the fluid inertia is negligible compared with the pressure, gravity and momentum exchanges:

$$\frac{D^F \underset{\sim}{v}^F}{Dt} = 0.$$

So the conservation law simplifies to:

$$\underset{\sim}{v}^F = \frac{\Lambda}{\phi^F}\left(\nabla p^F - \rho^F g \nabla z\right).$$

The fluid mobility, Λ, depends on both the fluid and the rock:

$$\Lambda = \frac{k}{\mu^F},$$

where μ^F is the fluid dynamic viscosity and k is the permeability of the rock. So finally, we obtain the well known Darcy's law:

$$\underset{\sim}{v}^F = -\frac{k}{\mu^F \phi^F}\left(\nabla p^F - \rho^F g \nabla z\right).$$

To a macroscopic observer $\underset{\sim}{v}^F$ is the mean fluid velocity through the pores of the rock. An observer at the pore scale would need to use the Navier-Stokes equations on the irregular geometry given by the pores. Darcy derived the law that has his name from experimental observations.

For many sedimentary porous media, the flow is anisotropic. To take this into account let k be a tensor

$$\underset{\sim}{v}^k = -\frac{\mathbf{k}}{\phi \mu_F} \cdot \left(\nabla p^F = \rho^I g \nabla z\right)$$

Although k is supposed to depend only on the rock it is different for gases than for liquids. For liquids there is friction between the liquid and the rock, there is a no-slip boundary condition between the two. For gases the friction is negligible.

4 Multiphase Flows in Porous Media

Lets look at the simplest of what is commonly called multiphase flow. That is, a flow with two fluid phases. So we have three phases: rock R, aqueous fluid W, and nonaqueous fluid N. Assume Darcy's Law holds for both W and N:

$$\underset{\sim}{v}^W = -\frac{\Lambda^W}{\phi^W}\left(\nabla p_W - \rho^W g \nabla z\right)$$

$$\underset{\sim}{v}^N = -\frac{\Lambda^N}{\phi^N}\left(\nabla p_N - \rho^N g \nabla z\right).$$

A lot of work has been done into simplifying the problem. One possibility is to work with different variables. Let $\phi = 1 - \phi^R = \phi^W + \phi^N$ be the porosity of the rock. Define the saturations as $S_W = \dfrac{\phi^W}{\phi}$, $S_N = \dfrac{\phi^N}{\phi}$, fraction of pore spore occupied by the respective fluids. So we have

$$S_W + S_N = 1.$$

Decompose the fluid mobilities, Λ^W and Λ^N, into

$$\Lambda^W = \frac{k_W}{\mu^W}, \qquad \Lambda^N = \frac{k_N}{\mu_N}.$$

k_W and k_N are no longer rock properties alone, since one fluid blocks the flow of the other. Suppose that the effective permeability depends on the fluid saturation of the phase increasing with its saturation. This is because the more we have of fluid α the less the other fluid interferes with its flow.

$$k_W = k k_{rW}(S_W),$$
$$k_N = k k_{rN}(S_W), \qquad S_N = 1 - S_W.$$

For two fluids with a fixed interfacial tension, the interfacial geometry varies with saturation so we can expect $p_N - p_W$ to be a function of the saturation S_W :

$$p_N - p_W = p_{CNW}(S_W).$$

The capillary pressure may be a multivalued function due to hysteresis.

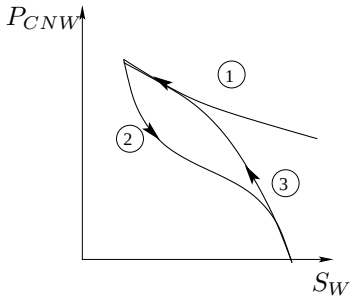

Mass Balance

The differential mass balance is given by:

$$\frac{\partial}{\partial t}\left(\phi^\alpha \rho^\alpha\right) + \operatorname{div}\left(\phi^\alpha \rho^\alpha \underset{\sim}{v}^\alpha\right) = r^\alpha$$

If we assume there is no interphase mass transfer, $r^\alpha = 0$.

Eliminating the mass fractions in favor of the saturations, $\phi^\alpha = \phi S_\alpha$ we have

$$\frac{\partial}{\partial t}\left(\phi S_\alpha \rho^\alpha\right) + \operatorname{div}\left(\phi S_\alpha \rho^\alpha \underset{\sim}{v}^\alpha\right) = 0.$$

Substitute $\underset{\sim}{v}^\alpha$ from Darcy's law (which is the conservation of momentum) into the conservation of W and N:

$$\frac{\partial}{\partial t}\left(\phi S_W \rho^W\right) - \operatorname{div}\left[\rho^W \frac{k k_{rW}}{\mu_W}\left(\nabla p_W - \rho^W g \nabla z\right)\right] = 0$$

$$\frac{\partial}{\partial t}\left(\phi(1-S_W)\rho^N\right) - \operatorname{div}\left[\rho^N \frac{k k_{rN}}{\mu_N}\left(\nabla p_W + \nabla p_{CNW} - \rho^N g \nabla z\right)\right] = 0.$$

Here, p_W and S_W are considered the primary unknowns. Empirical measurements are necessary to establish the relationships

$$\begin{aligned}
&k_{r\alpha} = k_{r\alpha}(S_W) \qquad \alpha = W, N\\
&p_{CNW} = p_{CNW}(S_W)\\
&\rho^W = \rho^W(p_W)\\
&\rho^N = \rho^N(p_N) = \rho^N\left(p_W, p_{CNW}(S_W)\right)
\end{aligned}$$

We also need initial conditions $p_W(\underset{\sim}{x}, 0), S_W(\underset{\sim}{x}, 0)$. These are known from measurements and interpolated to get the desired functions.

The final thing that we need are boundary conditions. Specify p_W at the boundaries of the flow region. Also, specify the normal flux of aqueous fluid across the boundaries. That is, give

$$\underset{\sim}{v}^W \cdot \underset{\sim}{n} = -\frac{\Lambda^W}{\phi^W}\left(\nabla p_W - \rho^W g \nabla z\right) \cdot \underset{\sim}{n}$$

Many times, such as in oil reservoirs, there is no flux at the boundary: $\underset{\sim}{v}^W \cdot \underset{\sim}{n} = 0$.

Buckley-Leverett (1942)

Almost all multiphase flow problems require numerical approximations. However, there is a simple case that can be done analytically. Consider the

conservation of mass equations for the aqueous phase W and the nonaqueous phase N:

$$\frac{\partial}{\partial t}\left(\phi S_W \rho^W\right) - \operatorname{div}\left[\rho^W \Lambda_W \left(\nabla p_W - \rho^W g \nabla z\right)\right] = 0$$

$$\frac{\partial}{\partial t}\left[\phi(1 - S_W)\rho^W\right] - \operatorname{div}\left[\rho^N \Lambda_N \left(\nabla p_W + \nabla p_{CNW} - \rho^N g \nabla z\right)\right] = 0.$$

Assume the effect of gravity is negligible, that the flow is only in x direction and that the reservoir geometry is uniform in the y and z directions with cross sectional area A.

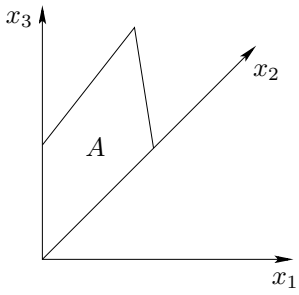

Integrate with respect to y and z:

$$A\frac{\partial}{\partial t}\left(\phi S_W \rho^W\right) - A\frac{\partial}{\partial x}\left(\Lambda_W \rho^W \frac{\partial p_W}{\partial x}\right) = 0$$

$$A\frac{\partial}{\partial t}\left(\phi S_N \rho^N\right) - A\frac{\partial}{\partial x}\left[\Lambda_N \rho^N \left(\frac{\partial p_W}{\partial x} + \frac{\partial p_{CNW}}{\partial x}\right)\right] = 0.$$

Also, since wicking force is not an important driving force, capillary effects are not important:

$$\frac{\partial p_{CNW}}{\partial x} \simeq 0.$$

The fluids, usually water and oil, and the rock can be considered incompressible. That is, ϕ, ρ^N, ρ^W are constant in time and uniform in space. The equations then simplify to:

$$\phi\frac{\partial S_W}{\partial t} - \frac{\partial}{\partial x}\left(\Lambda_W \frac{\partial p_W}{\partial x}\right) = 0$$

$$\phi\frac{\partial}{\partial t}(1 - S_W) - \frac{\partial}{\partial x}\left(\Lambda_N \frac{\partial p_W}{\partial x}\right) = 0.$$

$-\Lambda_\alpha \dfrac{\partial p_W}{\partial x} - q_\alpha$ represents the volumetric flow rate of the fluid α. If the total flow rate $q = q_N + q_W$ is constant, the two equations are the same and we are down to solving only one equation.

Also, the flow rate of the aqueous phase can be written as

$$q_W = \frac{\Lambda_W q}{\Lambda_N + \Lambda_W} \equiv f_W q,$$

where f_W is the fractional flow of aqueous fluid, that is, the fraction of the flow that belongs to the aqueous phase. If we work with a uniform rock from the macroscopic point of view, f_W depends only on the saturation of the aqueous phase S_W:

$$f_W = f_W(S_W)$$

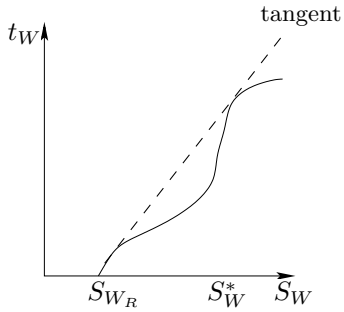

So finally we have what is known as the Buckley-Leverett saturation equation:

$$\frac{\partial S_W}{\partial t} + \frac{q}{\phi}\frac{\partial f_W}{\partial x} = 0.$$

The system is closed by giving initial conditions, $S_W(x,0)$ and boundary conditions, $S_W(0,t)$.

The equation can be solved using the method of characteristics. Write it as

$$\frac{\partial S_W}{\partial t} + \frac{q}{\phi} f'_W(S_W)\frac{\partial S_W}{\partial x} = 0,$$

valid where f_W and S_W are differentiable.

By the chain rule we have: $\dfrac{dS_W}{dt} = \dfrac{\partial S_W}{\partial t} + \dfrac{\partial x}{\partial t}\dfrac{\partial S_W}{\partial x}$

so that the equation is equivalent to $\dfrac{dS_W}{dt} = 0$ along $\dfrac{dx}{dt} = \dfrac{q}{\phi} f'_W(S_W)$. This second condition defines the characteristics.

There is a problem when the characteristics collide.

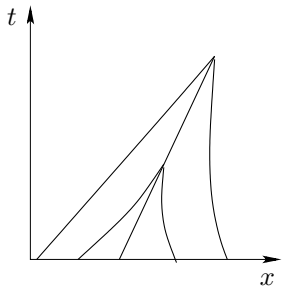

The solution is to admit jump discontinuities, which are known as shocks, in the solution. This avoids multivalued functions. But we cannot use the differential conservation laws. To get an equation valid at isolated jump discontinuities we must go back to an integral form of the flow equation. Consider the interval (x_L, x_R) that contains exactly one jump discontinuity at $\sum(t)$. Integrating the Buckley Leverett equation

$$\frac{d}{dt}\int_{x_L}^{\sum(t)} S_W(x,t)dx + \frac{d}{dt}\int_{\sum(t)}^{x_R} S_W(x,t)dx$$

$$= \frac{q}{\phi} f_W\left(S_W(x_L,t)\right) - \frac{q}{\phi} f_W\left(S_W(x_R,t)\right).$$

Differentiating using Leibnitz formula

$$\int_{x_L}^{\sum(t)} \frac{\partial S_W}{\partial t}dx + \int_{\sum(t)}^{x_K} \frac{\partial S_W}{\partial t}dx - [S_W]\frac{d\sum}{dt}$$

$$= \frac{q}{\phi}\left[f_W\left(S_W(x_L,t)\right) - f_W\left(S_W(x_R,t)\right)\right].$$

where $[S_W] \equiv \lim_{x\to\sum_+} S_W - \lim_{x\to\sum_-} S_W(x,t)$. is the jump at the discontinuity.

Since S_W is continuous on $(x_L, \sum)$ and $(\sum, x_R)$ taking one-sided limits as $x_L \to \sum$ and $x_K \to \sum_t$ we get the jump condition

$$\frac{d\sum}{dt} = \frac{q}{\phi}\frac{[f_W]}{[S_W]}.$$

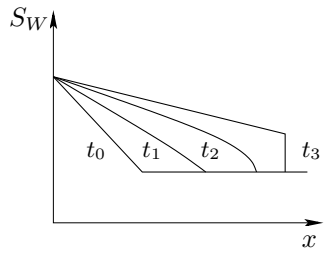

5 Multiphase-multispecies flows

Many mixtures of interest, such as oil reservoirs, consist of several phases and several species. They consist of several phases including rock, oil, water and gas. They also consist of many molecular species such as methane, propane, water and salt.

Let the species be $i = 1, \ldots N+1$ and consider three fluid phases, aqueous(W), oil(O) and gas(G) and one rock phase(R). One of the species is the rock material, for example, sandstone. In contamination problems, the

phase may be rock, water and DNAPL (dense nonaqueous phase liquids) or maybe even bacteria. We will concentrate on modelling an oil reservoir.

In this mixture each pair (i, α) with i chosen from the species indices and α from the phases is a constituent. Example: methane in gas is one constituent and methane in oil is another.

ρ_i^α, intrinsic mass density of species i in phase α (mass of i/unit volume of α)
ϕ_α, volume fraction of phase α
S_α, saturation of phase $\alpha = \phi_\alpha/\phi$, $\quad \phi = 1 - \phi_R$, porosity
$\rho^\alpha = \sum_{i=1}^{N} \rho_i^\alpha$, intrinsic mass density of phase α
$W_i^\alpha = \dfrac{\rho_i^\alpha}{\rho^\alpha}$, mass fraction of species i in phase α [mass i/mass α]
$\rho = \phi \sum_{\alpha \neq R} S_\alpha \rho^\alpha$, bulk density of fluids [mass of fluids/volume]
$W_i = \left(\dfrac{\phi}{\rho}\right) \sum_{\alpha \neq R} S_\alpha \rho^\alpha W_i^\alpha$, total mass fraction of species i in the fluids [mass of i/mass of fluids]
The baricentric velocity of phase α is

$$\underset{\sim}{v}^\alpha = \frac{1}{\rho^\alpha} \sum_{i=1}^{n} \rho_i^\alpha \underset{\sim}{v}_i^\alpha.$$

The diffusion velocity of species i in phase α is

$$\underset{\sim}{u}_i^\alpha = \underset{\sim}{v}_i^\alpha - \underset{\sim}{v}^\alpha.$$

Constraints

$$\sum_{i=1}^{N} W_i = \sum_{i=1}^{N} W_i^\alpha = 1, \qquad \text{for every } \alpha$$

$$\sum_{\alpha} \phi_\alpha = \sum_{\alpha \neq R} S_\alpha = 1$$

$$\sum_{i=1}^{N} \rho_i^\alpha \underset{\sim}{u}_i^\alpha = \underset{\sim}{0}.$$

The mass balance law for constituent (i, α) is:

$$\frac{\partial}{\partial t}\left(\phi_\alpha \rho_i^\alpha\right) + \operatorname{div}\left(\phi_\alpha \rho_i^\alpha \underset{\sim}{v}_i^\alpha\right) = \underset{\text{exchange terms}}{r_i^\alpha}. \qquad (*)$$

Rewrite $(*)$ as

$$\frac{\partial}{\partial t}\left(\underbrace{\phi S_\alpha}_{\phi_\alpha}\underbrace{\rho^\alpha W_i^\alpha}_{\rho_i^\alpha}\right) + \operatorname{div}\left(\phi S_\alpha \rho^\alpha W_i^\alpha \underbrace{\overset{\alpha}{\underset{\sim}{v}}}_{\text{velocity of phase}}\right) + \operatorname{div}\underset{\sim}{j}_i^\alpha = r_i^\alpha, \qquad (**)$$

where $\underset{\sim}{j}_i^\alpha = \phi S_\alpha \rho^\alpha W_i^\alpha \underset{\sim}{u}_i^\alpha$ is the diffusive flux.

Assume no intraphase chemical reactions and $\sum_{\alpha \neq R} r_i^\alpha = 0$ for each species.

Sum $(**)$ over all fluid phases to get the total balance law for each species.

$$\frac{\partial}{\partial t}(\rho W_i) + \operatorname{div}\left[\phi\left(S_W \rho^W W_i^W \underset{\sim}{v}^W + S_O \rho^O W_i^O \underset{\sim}{v}^O + S_G \rho^G W_i^G \underset{\sim}{v}^G\right)\right]$$
$$+\operatorname{div}\left(\underset{\sim}{j}_i^W + \underset{\sim}{j}_i^O + \underset{\sim}{j}_i^G\right) = 0 \qquad i = 1, \ldots W.$$

Assume Darcy's law for each phase

$$\underset{\sim}{v}^\alpha = -\frac{k k_{r\alpha}}{\mu^\alpha \phi S_\alpha}\left(\nabla p^\alpha - \rho^\alpha g \nabla z\right) \qquad \alpha = W, O, G.$$

Assume the hydrodynamic dispersion is small

$$\underset{\sim}{j}_i^W + \underset{\sim}{j}_i^O + \underset{\sim}{j}_i^G \simeq \underset{\sim}{0}$$

$$\frac{\partial}{\partial t}\left[\phi\left(S_W \rho^W W_i^W + S_O \rho^O W_i^O + S_G \rho^G W_i^G\right)\right] q$$
$$- \operatorname{div}\left[\frac{k k_{rW} \rho^W W_i^W}{\mu^W}\left(\nabla p_W - \rho_g^W \nabla z\right) + \frac{k k_{rO} \rho^O W_i^O}{\mu^O}\left(\nabla p_O - \rho^O g \nabla z\right) q\right.$$
$$\left. - \frac{-k k_{rG} \rho^G w_i^G}{\mu_G}\left(\nabla p_G - \rho^G g \nabla z\right)\right] = 0 \qquad i = 1, \ldots N.$$

To close the system, we need some supplementary constraints. Some are the equations of state:

$$\begin{aligned} \rho^\alpha &= \rho^\alpha(W_1^\alpha, \cdots, W_N^\alpha, p_\alpha) && \alpha = W, O, G \\ W_i^\alpha &= W_i^\alpha(W_1, \cdots, W_N, p_\alpha) && \alpha = W, O, G \\ S_\alpha &= S_\alpha(W_1, \cdots, W_N, p_\alpha) && \alpha = W, O, G, \end{aligned}$$

which may be given explicitly, implicitly or in tabular form.

The other constraints are the constitutive relations:

$$\begin{aligned} &p_O - p_W = p_{COW} = p_{COW}(S_O, S_G) \\ &p_G - p_O = p_{CGO}(S_0, S_G) \\ &k_{r\alpha} = k_{r\alpha}(S_0, S_G \quad \alpha = W, O, G. \end{aligned}$$

The following bibliography includes not only the works referenced in this paper, but also some additional references that complement and extend the present work.

References

[1] M.B. Allen, *Basic mechanics of oil reservoir flows*, in Multiphase Flow in Porous Media, M.B. Allen III, G.A. Behie, and J.A. Trangenstein, Lecture Notes in Engineering, vol. 34, C.A. Brebia and S.A. Orszag, Eds., Springer-Verlag, New York, 1988, pp. 1–81.

[2] J. Bear, *Dynamics of Fluids in Porous Media*,Dover, New Yor, NY, 1988.

[3] Z.X. Chen, G.R. Huan and H.M. Wang, *Simulation of a compositional model for multiphase flow in porous media*, Num. Meth. Part. Diff. Equat. 21, 2002, 726–741.

[4] Z.X. Chen, G.R. Huan, and Y.L. Ma, *Computational Methods for Multiphase Flows in Porous Media*, SIAM, Philadelphia, 2006.

[5] S. Crone, C. Berginsand K. Strauss, *Multiphase flow in homogeneous porous media with phase change. Part I: Numerical modeling*, Trans. Porous Media 49, 2002, 291–312.

[6] I. Garrido, G.E. Fladmark and M. Espedal, *An improved numerical simulator for multiphase flow in porous media*, Int. J. Num. Meth. in Fluids 44, 2004, 447+.

[7] M.G. Gerritsenand L.J. Durlofsky, *Modeling fluid flow in oil reservoirs*, Annual Rev. Fluid Mech. 37, 2005, 211–238.

[8] W.G. Gray and C.T. Miller, *Thermodynamically constrained averaging theory approach for modeling flow and transport phenomena in porous medium systems: 1. Motivation and overview*, Adv. Water Res. 28, 2005, 161–180.

[9] P. Jenny, S.H. Lee and H.A. Tchelepi, *Adaptive multiscale finite-volume method for multiphase flow and transport in porous media*, Mult. Mod. and Sim. 3, 2004, 50–64.

[10] R. Juanes, *A variational multiscale finite element method for multiphase flow in porous media*, Fin. Elem. Anal. and Des. 41, 2005, 763–777.

[11] R. Juanes and T.W. Patzek, *Multiscale-stabilized finite element methods for miscible and immiscible flow in porous media*, J. Hydr. Res. 42, 2004, 131–140.

[12] S. Liu, *A continuum approach to multiphase flows in porous media*, J. Porous Media 2, 1999, 295–308.

[13] J.G. Kimand H.W. Park HW, *Advanced simulation technique for modeling multiphase fluid flow in porous media*, Lecture Notes in Comp. Science 3044, 2004, 1–9.

[14] C. M. Marle, *Multiphase Flow in Porous Media*, Gulf Publishing Company, Houston, 1981.

[15] A.Michel, *A finite volume scheme for two-phase immiscible flow in porous media*, SIAM J. Num. Anal. 41, 2003, 1301–1317.

[16] C.T. Miller and W.G. Gray, *Thermodynamically constrained averaging theory approach for modeling flow and transport phenomena in porous medium systems: 2. Foundation*, Adv. Water Res. 28, 2005, 181–202.

[17] H. J. Morel-Seytoux, *Introduction to Flow of Immiscible Liquids in Porous Media*,in Flow through Porous Media, Ed. R. J. M. De Wiest, Academic Press, New York, NY, 1969.

[18] M. Peszynska, M.F. Wheeler and I. Yotov, *Mortar upscaling for multiphase flow in porous media*, Comp. Geos. 6, 2002, 73–100.

[19] S.L., *Multiphase fluid dynamics*, Gower Technical, Brookfield, USA, 1990.

[20] S.Y.Sun and M.F. Wheeler, *Discontinuous Galerkin methods for coupled flow and reactive transport problems*, Appl. Num. Math. 52, 2005, 273–298.

[21] M. F. Wheeler and M. Peszynska, *Computational engineering and science methodologies for modeling and simulation of subsurface applications*, Adv. in Water Res. 25, 2002, 1147–1173.

[22] Y.S. Wu and P.A. Forsyth, *On the selection of primary variables in numerical formulation for modeling multiphase flow in porous media*, J. of Contam. Hydro. 48, 2001, 277–304.

Título:	Propiedades Cualitativas De Esquemas Numéricos De Aproximación De Ecuaciones De Difusión y de Dispersión.
Doctorando:	Ioan Liviu Ignat.
Director/es:	Enrique Zuazua Iriondo.
Defensa:	15 de septiembre de 2006, Madrid.
Calificación:	Sobresaliente cum Laude.

Resumen:

Esta memoria tiene como objeto el estudio de diversos esquemas numéricos para ecuaciones del calor, de Schrödinger y de ondas. Nuestro principal objetivo es describir el comportamiento de las soluciones de discretizaciones numéricas clásicas por diferencias finitas prestando especial atención a sus propiedades cualitativas como decaimiento, dispersión, propagación, etc.

Para la ecuación del calor demostramos que las soluciones del método semi-discreto de diferencias finitas estándar reproducen exactamente el decaimiento de las soluciones continuas. Para probar este hecho se demuestran estimaciones del núcleo de convolución discreto en variable Fourier. Este resultado es útil posteriormente en el estudio de las aproximaciones viscosas de la ecuación de Schrödinger. También obtenemos una expansión completa de las soluciones discretas, usando los momentos del dato inicial, semejante a la bien conocida en el caso continuo.

En referencia a la semi-discretización clásica conservativa por diferencias finitas de la ecuación de Schrödinger probamos en primer lugar que no se tienen propiedades dispersivas independientes del parámetro de la discretización. Lo hacemos construyendo paquetes de ondas concentrados en los puntos del espectro donde el símbolo del laplaciano discreto anula todas sus derivadas de segundo orden. Se trata por tanto de un fenómeno debido a la presencia de altas frecuencias espurias.

Para remediar este hecho introducimos tres métodos numéricos: filtrado de los datos iniciales en variable Fourier; viscosidad numérica; precondicionamiento bimalla. Para cada uno de estos tres esquemas probamos estimaciones dispersivas y de ganancia de regularidad espacial local, uniformes en los parámetros de discretización. Los métodos empleados se basan en las estimaciones previas obtenidas para la ecuación del calor y estimaciones clásicas para integrales oscilatorias. Gracias a estos resultados obtenemos desigualdades de tipo Strichartz para los modelos numéricos. Esto nos permite abordar problemas no lineales para datos iniciales en el espacio L^2, sin hipótesis adicionales de regularidad. Probamos la convergencia para no linealidades que no se pueden abordar por métodos de energía y que, incluso en el caso continuo, exigen estimaciones de tipo Strichartz.

Analizamos también esquemas totalmente discretos para la ecuación de Schrödinger unidimensional. Obtenemos condiciones necesarias y suficientes para garantizar que las mismas propiedades analizadas en el caso semi-direcreto se cumplen con independencia de los parámetros de las discretización. Usando una aproximación de Euler implícito para el semigrupo lineal introducimos un esquema numérico convergente para la ecuación no lineal bajo las mismas propiedades de regularidad del caso anterior.

En el caso del problema de Cauchy para la ecuación de ondas multidimensional introducimos un esquema semi-discreto en diferencias finitas. Probamos que para datos iniciales en el espacio de Besov discreto $\dot{B}^{d-1/2}_{1,1}(h\mathbf{Z}^d)$, las soluciones decaen en norma $l^\infty(hh\mathbf{Z}^d)$ como $t^{-1/2}$ uniformemente con respecto al paso del mallado, a diferencia de las soluciones continuas que para datos iniciales en $\dot{B}^{(d+1)/2}_{1,1}(\mathbf{R}^d)$ decaen como $t^{-(d-1)/2}$. Sobre la base de este resultado de decaimiento, a pesar de la falta de homogeneidad del símbolo de la ecuación semi-discreta, utilizando una descomposición de tipo Paley-Littlewood, conseguimos probar desigualdades de tipo Strichartz en una clase de espacios que no cubre por completo la del modelo continuo, dado que la tasa de decaimiento en norma L^∞ es distinta. Sin embargo, en tres dimensiones espaciales, las estimaciones obtenidas son suficientes para probar que el esquema numérico en diferencias finitas, para la ecuación de ondas semi-lineal con exponente subcrítico, tiene soluciones uniformemente acotadas en uno de los espacios donde la ecuación continua está también bien puesta.

Los resultados obtenidos son analizados no sólo en el contexto de la aproximación numérica de ondas continuas, sino también en el contexto de la ecuación de ondas en retículos, donde la cuestión de la uniformidad con respecto al tamaño del retículo se obvia.

Finalmente, consideramos el esquema conservativo semi-discreto clásico en diferencias finitas para la ecuación de ondas en un cuadrado, y estudiamos la observabilidad frontera desde dos lados consecutivos del mismo, motivado en el control de vibraciones. Consideramos una clase de datos iniciales obtenidos por un método de filtrado bimalla. A partir de resultados conocidos de observabilidad uniforme para datos filtrados en Fourier, obtenemos el mismo resultado en esta clase bimalla. La demostración utiliza una descomposición espectral diádica introducida en el contexto del control de la ecuaciones de Schrödinger y de ondas. Este resultado es novedoso puesto que extiende a varias dimensiones resultados que solo se conocían en una dimensión espacial. Este método que desarrollamos permite abordar el mismo tipo de problemas para una clase más amplia de ecuaciones.

Wave Propagation, Observation and Control in 1–d Flexible Multi–structures
René Dáger, Enrique Zuazua
Mathématiques & Applications, Springer
ISBN: 3–540–27239–9 (221 páginas) – 2005

Por C. Castro

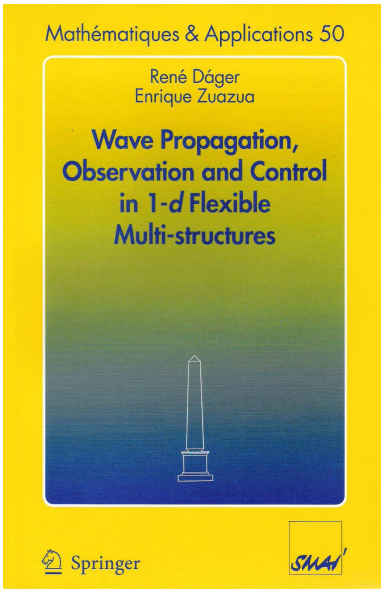

Este libro se encuentra publicado en la colección *Mathematics and Applications* editada por la SMAI, en colaboración con Springer, y dedicada a la difusión de cursos avanzados en temas específicos que sirvan de referencia o iniciación a no expertos en la materia. Se puede decir que encaja perfectamente dentro de esta filosofía ofreciendo un texto autocontenido y bastante exhaustivo tanto en resultados como en las técnicas más eficaces en el área del control, y muy particularmente en el campo de las multiestructuras.

Está escrito por dos especialistas en este campo y, de hecho, es destacable que una buena parte de los resultados contenidos sean fruto de su trabajo conjunto.

Los primeros tres capítulos son introductorios y describen por un lado nociones elementales sobre redes de cuerdas, y su representación en forma de grafo, y por otro se hace una descripción general de los problemas de control, con especial atención al caso del control de una cuerda desde un punto interior o de la frontera. En particular se describen con detalle las técnicas más conocidas como son el llamado *método de momentos*, desarrollado principalmente en los trabajos de H.O. Fattorini y D. Russell en los años 60, y el más versátil *Hilbert Uniqueness Method*, introducido por J.-L. Lions en los años 80. Ambos métodos reducen el problema de control a unas ciertas desigualdades conocidas como desigualdades de observabilidad cuyo estudio, aplicado a redes de cuerdas, es el principal objetivo del resto del libro. Las técnicas utilizadas para obtener estas desigualdades están basadas en el uso de la fórmula de D'Alambert, las series de Fourier no armónicas y teoría de números.

El capítulo 4 está dedicado al estudio del modelo de multiestructura más simple compuesto por tres cuerdas vibrantes unidas por un punto común. Se estudian separadamente los casos en los que se colocan controles en dos de los extremos libres y un único control en uno de los extremos libres. Resulta curioso observar cómo muchos resultados dependen muy sensiblemente del grado de irracionalidad del cociente de las longitudes de las cuerdas.

El análisis hecho para la red de tres cuerdas se generaliza a redes más complejas en forma de árbol (capítulo 5) y redes generales (capítulo 6). También se estudian problemas relacionados como el control simultáneo de cuerdas o el control de redes coloreadas.

En el capítulo 7 se aborda el problema del control simultáneo de cuerdas cuando el control actúa sobre un abierto. A diferencia de los casos anteriores, en los que el control se situaba en los extremos libres, las propiedades de controlabilidad son más robustas y ya no dependen del grado de irracionalidad de los cocientes de las longitudes de las cuerdas. Al final del capítulo también se aborda el caso multidimensional cuando el control actúa en todo el dominio.

En el capítulo 8 se analiza la extensión de los resultados anteriores a redes gobernadas por otro tipo de ecuaciones como la ecuación del calor, Schrödinger o vigas. Para ello se plantean los problemas de momentos asociados y ciertas transformaciones conocidas que permiten reducir estos problemas de momentos al caso de las redes de cuerdas.

Por último hay un interesante capítulo que plantea una serie de dificultades y problemas abiertos recogidos de la propia experiencia del trabajo realizado por los autores en este campo.

VIII PREMIO S$\vec{e}$MA A LA "DIVULGACIÓN DE LA MATEMÁTICA APLICADA"

SOCIEDAD ESPAÑOLA DE MATEMÁTICA APLICADA

(PATROCINADO POR IBERDROLA)

PREÁMBULO

La Sociedad Española de Matemática Aplicada (S$\vec{e}$MA), en cumplimiento de su objetivo de contribuir al desarrollo en nuestro país de las Matemáticas y sus aplicaciones, consciente del notable desarrollo que las Matemáticas están experimentando, del incremento de su influencia sobre todos los aspectos de la vida en las sociedades desarrolladas, de la conveniencia de promover el interés de los investigadores por este punto de vista sin por ello ocultar sus peligros o dilemas, de la necesidad no menos acuciante de estimular el interés del público por la cultura científica y, finalmente continuando con una tradición honrosa y habitual tanto en las Artes como en las Ciencias, convoca el "VIII Premio S$\vec{e}$MA de Divulgación de la Matemática aplicada", según las bases que se adjuntan.

S$\vec{e}$MA busca ante todo promover la divulgación de las Matemáticas, su relevancia y su eficacia. Dada la enorme variedad de intereses aplicados de las Matemáticas, las Bases del concurso pretenden dar preferencia a los temas que tradicionalmente han estado ligados a S$\vec{e}$MA de una u otra manera. Muy en especial, deben ser mencionados el análisis teórico y numérico, el control y los aspectos computacionales de sistemas que permiten modelizar fenómenos con origen en otras Ciencias.

BASES DE LA CONVOCATORIA

1. La Sociedad Española de Matemática aplicada (S$\vec{e}$MA) convoca el "Premio S$\vec{e}$MA a la Divulgación de la Matemática aplicada", que se concederá anualmente.

2. Son posibles candidatos todos los ciudadanos del mundo que sometan un texto de acuerdo con los puntos 4 y 9 de estas Bases.

3. El Premio está destinado a promover los valores de la belleza, relevancia y eficacia de las Matemáticas como instrumento indispensable del funcionamiento de la sociedad y cultura modernas. El Premio tomará en especial consideración los temas que incidan en la realidad de la Matemática aplicada en la sociedad española.

4. Los candidatos habrán de presentar dentro del plazo fijado en el punto 10 un texto original de una longitud mínima de 20 páginas mecanografiadas a un espacio y con el formato que juzguen conveniente. Los requisitos básicos son que el texto contribuya a la divulgación de algún aspecto relevante de la Matemática Aplicada y que su contenido esté pensado para un público no exclusivamente formado por profesionales de las Matemáticas. El trabajo será presentados bajo un seudónimo, incluyendo con el mismo un sobre cerrado en el que figuren el nombre y dirección del autor. El autor no podrá formar parte del Comité Científico que habrá de juzgar los trabajos por lo que en caso de ser propuesto para el mismo, deberá indicar al Presidente su incompatibilidad.

5. Los méritos serán juzgados por un Comité Científico de cinco miembros nombrados por el Comité Ejecutivo de la Sociedad, personalidades de probado prestigio en la Ciencia Matemática y la cultura científica. Este Comité tendrá su propio reglamento de funcionamiento, pudiendo quedar desierto el Premio. En todo caso, el Comité será presidido por el Presidente de la Sociedad u otro miembro del Comité Ejecutivo en quien delegue, no pudiendo ser miembros del Comité Científico más de dos miembros del Comité Ejecutivo.

6. El galardonado con el Premio recibirá de la Sociedad un Diploma acreditativo y una cuantía de 1500 euros. Además quedará eximido del pago de las cuotas como socio de S$\vec{e}$MA correspondientes a los años 2008 y 2009. En caso de no ser miembro de S$\vec{e}$MA, pasaría automáticamente a serlo.

7. El fallo del concurso es irrevocable. El Comité acompañará la concesión del Premio de una exposición de los méritos hallados en el candidato galardonado.

8. La Sociedad publicará la obra premiada en su Boletín.

9. Si el texto original no estuviera escrito en castellano, el jurado podrá solicitar al autor su traducción si así lo estimase necesario.

10. La fecha limite de presentación de originales es el 15 de mayo de 2007.

11. La documentación, compuesta del texto por quintuplicado, su traducción si ha lugar, así como los datos identificativos, debe ser dirigida a

    Prof. Carlos Vázquez Cendón
    VIII Premio S$\vec{e}$MA a la Divulgación de la Matemática Aplicada
    Departamento de Matemáticas
    Facultad de Informática
    Campus de Elviña s/n
    Universidad de La Coruña
    15071 – A Coruña

12. El Premio será fallado antes del 31 de agosto del año 2007 y será entregado con ocasión de la Asamblea anual de la Sociedad, en el marco del XX CEDYA / X CMA que tendrá lugar en Sevilla del 24 al 28 de Septiembre de 2007.

X PREMIO S$\vec{e}$MA AL JOVEN INVESTIGADOR

SOCIEDAD ESPAÑOLA DE MATEMÁTICA APLICADA

(PATROCINADO POR ADDLINK)

PREÁMBULO

La Sociedad Española de Matemática Aplicada (S$\vec{e}$MA), en cumplimiento de su objetivo de contribuir al desarrollo en nuestro país de las Matemáticas y sus aplicaciones y, más en concreto, de promover y estimular la investigación y procurar medios para efectuarla, consciente del notable desarrollo que las Matemáticas están experimentando y de la necesidad de promover el interés de las jóvenes generaciones por la tarea de la creación científica, convencida del papel positivo que el aprecio de la comunidad juega en la vida científica de los investigadores y siguiendo con una tradición honrosa y habitual tanto en las Artes como en las Ciencias, convoca el "X Premio S$\vec{e}$MA al Joven Investigador", según las bases que se adjuntan.

BASES GENERALES

1. La Sociedad Española de Matemática aplicada (S$\vec{e}$MA) convoca el "Premio S$\vec{e}$MA al Joven Investigador", que se concederá anualmente.

2. Son posibles candidatos todos los investigadores españoles que, a la fecha del límite de presentación de candidaturas, no rebasen la edad de 33 años. También pueden serlo aquellos investigadores de otras nacionalidades que tengan un puesto de trabajo permanente en una Universidad o Centro de investigación español y cumplan la condición de edad. No pueden concurrir al Premio candidatos galardonados en convocatorias precedentes.

3. El Premio está destinado a promover la excelencia en el trabajo matemático original en todas las ramas de las Matemáticas que tienen una componente aplicada. Su objetivo es premiar la contribución personal del candidato. El limite de edad fijado pretende señalar candidatos que hayan tenido tiempo de desarrollar su creatividad matemática independiente tras la etapa formativa correspondiente a la Tesis Doctoral. El Premio tiene así por objetivo abrirles el camino de su periodo de madurez y reconocer al mismo tiempo sus capacidades demostradas.

4. Los méritos serán juzgados por un Comité Científico de cinco miembros, nombrado por el Consejo Ejecutivo de la Sociedad entre investigadores de probado prestigio. Este Comité tendrá su propio reglamento de funcionamiento. En todo caso, será presidido por el Presidente de la Sociedad u otro miembro del Consejo Ejecutivo en quien delegue, no pudiendo ser miembros del Comité Científico más de dos miembros del Consejo Ejecutivo.

5. Los candidatos habrán de presentar, dentro del plazo que se cite, una Memoria exponiendo la trayectoria vital y los méritos que concurren, un currículum normalizado, así como otros documentos que puedan ser pertinentes para acreditar sus contribuciones originales a las Matemáticas y sus aplicaciones. Las candidaturas pueden ser presentadas también por otros investigadores. El Comité se reserva el derecho de recabar la información complementaria necesaria del candidato o de quien le haya presentado.

6. El galardonado con el Premio recibirá de la Sociedad un Diploma acreditativo y una cuantía que será establecida en cada convocatoria por la Sociedad.

7. La Sociedad requerirá al candidato galardonado un resumen de su trabajo de investigación escrito en estilo divulgativo, con una extensión a convenir entre las 6 y las 20 páginas, para su publicación en el Boletín de la Sociedad. Este resumen puede formar parte de la Memoria mencionada en el punto 5.

8. El fallo del concurso es irrevocable. El Comité acompañará la concesión del Premio de una exposición de los méritos hallados en el candidato galardonado. Por lo demás, las deliberaciones y resoluciones del Comité serán regidas por su reglamento.

BASES PARTICULARES DE LA CONVOCATORIA DE 2007

9. La fecha límite de presentación de candidaturas es el 30 de abril de 2007. Podrán concursar por tanto las personas que hayan nacido después del 30 de abril de 1973.

10. La documentación presentada constará de la Memoria y el currículo citados, así como copia de las cinco contribuciones más importantes del investigador a las Matemáticas y sus aplicaciones, todo ello por quintuplicado.

11. Se recomienda a los candidatos que presenten su propia candidatura y que la Memoria se adecúe, o en su caso contenga el resumen del trabajo de investigación referido en el apartado 7.

12. La documentación debe ser dirigida a:

    Prof. Carlos Vázquez Cendón
    X Premio S$\vec{e}$MA al Joven Investigador
    Departamento de Matemáticas
    Facultad de Informática
    Campus de Elviña s/n
    Universidad de La Coruña
    15071 – A Coruña

13. La cuantía del Premio es de 1500 euros. El Premio es indivisible. Además, el candidato galardonado quedará eximido del pago de las cuotas como socio de S$\vec{e}$MA correspondientes a los años 2008 y 2009. En caso de no ser miembro de S$\vec{e}$MA, pasaría automáticamente a serlo.

14. El Premio será fallado antes del 31 de agosto de 2007 y será entregado con ocasión de la Asamblea Anual de la Sociedad, en el marco del XX CEDYA - X CMA, que tendrá lugar en Sevilla, del 24 al 28 de septiembre de 2007.

    A Coruña, a 26 de enero de 2006

Tipo de evento:	Curso y encuentro
Nombre:	ZARAGOZA NUMÉRICA. Curso y Encuentro de Análisis Numérico
Lugar:	Zaragoza
Fecha:	del 18 al 22 de junio de 2007
Organiza:	Grupo PDIE, Dep. Matemática Aplicada, Universidad de Zaragoza
Información:	F.J. Sayas, S. Meddahi
E-mail:	jsayas@unizar.es salim@uniovi.es
WWW:	www.unizar.es/pdie/zn07.html

Tipo de evento:	Congreso
Nombre:	Nonlinear Evolution Equations and Dynamical Systems (NEEDS 2007)
Lugar:	L'Ametlla de Mar (Barcelona)
Fecha:	del 18 al 23 de junio de 2007
E-mail:	needs2007@needs-conferences.net
WWW:	www.needs-conferences.net/2007

Tipo de evento:	Congreso
Nombre:	1ST International Summer School On Geometry, Mechanics And Control
Lugar:	Castro Urdiales (Cantabria)
Fecha:	del 25 al 29 de junio de 2007
E-mail:	gmcnet@ull.es
WWW:	http://webpages.ull.es/users/gmcnet/Summer_School/index.htm

Tipo de evento:	Congreso
Nombre:	Non-linear diffusion: Mathematics and Applications. An International Conference to celebrate the 60th birthday of Juan Luis Vázquez
Lugar:	El Escorial (Madrid)
Fecha:	del 26 al 29 de junio de 2007
E-mail:	fernando.quiros@uam.es (Prof. Fernando Quirós)
WWW:	www.uam.es/cristina.brandle/jlv60

Tipo de evento:	Congreso
Nombre:	Des équations aux dérivés partielles au calcul scientifique Congrès en l'honneur de Luc Tartar à l'occasion de son soixantième anniversaire
Lugar:	París
Fecha:	del 2 al 6 de julio de 2007
E-mail:	edp-cs@ann.jussieu.fr
WWW:	www.cmap.polytechnique.fr/edp-cs

Tipo de evento:	Congreso
Nombre:	2007 International Conference on Engineering and Mathematics (ENMA 2007)
Lugar:	Bilbao
Fecha:	del 9 al 11 de julio de 2007
E-mail:	javier.bilbao@ehu.es
WWW:	http://enma.org.es

Tipo de evento:	Congreso
Nombre:	Primer Congreso Hispano-Francés de Matemáticas
Lugar:	Zaragoza
Fecha:	del 9 al 13 de julio de 2007
Organiza:	Real Sociedad Matemática Española (RSME) y Sociedad Española de Matemática Aplicada (SeMA)
WWW:	www.unizar.es/ICHFM07

Tipo de evento:	Congreso
Nombre:	Dynamical Methods and Mathematical Modelling
Lugar:	Valladolid
Fecha:	del 18 al 22 de septiembre de 2007
E-mail:	dm07@wmatem.eis.uva.es
WWW:	http://wmatem.eis.uva.es/∼dm07

Tipo de evento:	Congreso
Nombre:	The Eighth Hellenic European Research On Computer Mathematics And Its Applications Conference
Lugar:	Atenas
Fecha:	del 20 al 22 de septiembre de 2007
Organiza:	Dept. of Informatics and Research Group for Advanced Computational Mathematics and Parallel Processing (Athens University of Economics & Business, 76 Patission St., Athens GR-104 34, Greece)
E-mail:	eal@aueb.gr (Prof. Elias A. Lipitakis)
WWW:	www.aueb.gr/conferences/hercma2007/

Tipo de evento:	Congreso
Nombre:	XX Congreso de Ecuaciones Diferenciales y Aplicaciones (CEDYA)/X Congreso de Matemática Aplicada (CMA)
Lugar:	Sevilla
Fecha:	del 24 al 28 de septiembre de 2007
WWW:	www.congreso.us.es/cedya2007

Borges Rutz, Ricardo
Estudiante. – Univ. Autónoma de Barcelona – Fac. de Ciencias – Dpto. de Matemáticas – Campus de la UAB, Edifici C. 08193 Bellaterra (Cerdanyola del Vallès).
Tlf.: 935811137. *Fax:* 935812790.
e-mail: Ricardo.Borges@campus.uab.es.

Donoso Bellón, Alberto
Prof. Ayudante de Universidad. – Univ. de Castilla La Mancha – E.T.S. de Ingenieros Industriales – Dpto. de Matemáticas – Avda. Camilo José Cela, s/n. 13071 Ciudad Real.
Tlf.: 926295300 Ext. 3859. *Fax:* 926295361.
e-mail: Alberto.Donoso@uclm.es.

Gómez–Ullate Oteiza, David
Investigador. – Univ. Complutense de Madrid – Fac. de Ciencias Físicas – Dpto. de Física Teórica II – Avda. Complutense, s/n. 28040 Madrid.
Tlf.: 913945198. *Fax:* 913944557.
e-mail: david.gomez-ullate@fis.ucm.es.

González Taboada, María
Prof. Titular de Universidad. – Univ. de La Coruña – Fac. de Informática – Dpto. de Matemáticas – Campus de Elviña, s/n. 15071 La Coruña.
Tlf.: 981167000 Ext. 1326. *Fax:* 981167160.
e-mail: mgtaboad@udc.es.

Juan Huguet, Jordi
Becario Predoctoral. – Univ. Politécnica de Valencia – Instituto de Matemática Pura y Aplicada – Camino de Vera, s/n. 46022 Valencia.
Tlf.: 963877000 Ext. 88398. *Fax:*
e-mail: jorjuahu@doctor.upv.es.

Martínez Aroza, José
Prof. Titular de Universidad. – Univ. de Granada – Fac. de Ciencias – Dpto. de Matemática Aplicada – Avda. Fuentenueva, s/n. 18071 Granada.
Tlf.: 958242940. *Fax:* 958248596.
e-mail: jmaroza@ugr.es.

Núñez Jiménez, Carmen
Prof. Titular de Universidad. – Univ. de Valladolid – E.T.S. de Ingenieros Industriales – Dpto. de Matemática Aplicada – Paseo del Cauce, s/n. 47011 Valladolid.
Tlf.: 983423792. *Fax:* 983423406.
e-mail: carnun@wmatem.eis.uva.es.

Díaz de Santos, S. A.

Departamento 0002637-00958/03
Albasanz, 2. 28037 Madrid. *Tlf.:* 917434890. *Fax:* 917434023.
e-mail: suscr06@diazdesantos.es.
http://www.diazdesantos.es/

Direcciones útiles

Consejo Ejecutivo de SëMA

Presidente:

Carlos Vázquez Cendón. (carlosv@udc.es).
Dpto. de Matemáticas. Facultad de Informática. Univ. de A Coruña. Campus de Elviña, s/n. 15071 A Coruña. *Tel:* 981 16 7000-1335.

Secretario:

Carlos Castro Barbero. (ccastro@caminos.upm.es).
Dpto. de Matemática e Informática. E.T.S.I. Caminos, Canales y Puertos. Univ. Politécnica de Madrid. Av. Aranguren s/n. 28040 Madrid. *Tel:* 91 336 6664.

Vocales:

Rafael Bru García. (rbru@mat.upv.es)
Dpto. de Matemática Aplicada. E.T.S.I. Agrónomos. Univ. Politécnica de Valencia. Camí de Vera, s/n. 46022 Valencia. *Tel:* 963 879 669.

José Antonio Carrillo de la Plata. (carrillo@mat.uab.es)
Dpto. de Matemáticas. Univ. Autónoma de Barcelona. Edifici C. 08193 Bellaterra (Barcelona). *Tel:* 935 812 413.

Rosa María Donat Beneito. (Rosa.M.Donat@uv.es) Dpto. de Matemática Aplicada. Fac. de Matemàtiques. Univ. de Valencia. Dr. Moliner, 50. 46100 Burjassot (Valencia) *Tel:* 963 544 727.

Inmaculada Higueras Sanz. (higueras@unavarra.es).
Dpto de Matemática e Informática Univ. Pública de Navarra. Campus de Arrosadía, s/n. *Tel:* 948 169 526. 31006 Pamplona.

Carlos Parés Madroñal. (carlos_pares@uma.es).
Dpto. de Análisis Matemático. Fac. de Ciencias. Univ. de Málaga. Campus de Teatinos, s/n. 29080 Málaga. *Tel:* 952 132 017.

Pablo Pedregal Tercero. (Pablo.Pedregal@uclm.es).
Dpto. de Matemáticas. E.T.S.I. Industriales Univ. de Castilla-La Mancha. Avda. de Camilo José Cela, s/n. 13071 Ciudad Real. *Tel:* 926 295 436

Enrique Zuazua Iriondo. (enrique.zuazua@uam.es).
Dpto. de Matemáticas. Fac. de Ciencias. Univ. Aut. de Madrid. Cantoblanco, Ctra. de Colmenar, km. 14. 28049 Madrid. *Tel:* 914 974 368.

Tesorero

Íñigo Arregui Álvarez. (arregui@udc.es).
Dpto. de Matemáticas. Fac. de Informática. Univ. de A Coruña. Campus de Elviña, s/n. 15071 A Coruña. *Tel:* 981 16 7000-1327.

Comité Científico del Boletín de SëMA

Enrique Fernández Cara. (cara@us.es).
Dpto. de Ecuaciones Diferenciales y An.Ñumérico. Fac. de Matemáticas. Univ. de Sevilla. Tarfia, s/n. 41012 Sevilla. *Tel:* 954 557 992.

Alfredo Bermúdez de Castro. (mabermud@usc.es).
Dpto. de Matemática Aplicada. Fac. de Matemáticas. Univ. de Santiago de Compostela. Campus Univ.. 15706 Santiago (A Coruña) *Tel:* 981 563 100.

Eduardo Casas Rentería. (eduardo.casas@unican.es).
Dpto. de Matemática Aplicada y C.C.. E.T.S.I. Ind. y Telec. Univ. de Cantabria. Avda. de Los Castros s/n. 39005 Santander. *Tel:* 942 201 427.

José Luis Cruz Soto. (jlcruz@uco.es).
Dpto. de Informática y An.Ñumérico. Univ. de Córdoba. Campus de Rabanales. Edificio C-2. 14071 Córdoba. *Tel:* 957 218 629.

José Manuel Mazón Ruiz. (Jose.M.Mazon@uv.es).
Dpto. de Análisis Matemático. Fac. de Matemáticas. Univ. de Valencia. Dr. Moliner, 50. 46100 Burjassot (Valencia) *Tel:* 963 664 721.

Ireneo Peral Alonso. (ireneo.peral@uam.es).
Dpto. de Matemáticas, C-XV. Fac. de Ciencias. Univ. Aut. de Madrid. Cantoblanco, Ctra. de Colmenar, km. 14. 28049 Madrid. *Tel:* 913 974 204.

Pablo Pedregal Tercero. (Pablo.Pedregal@uclm.es).
Dpto. de Matemáticas. E.T.S.I. Industriales Univ. de Castilla-La Mancha. Avda. Camilo José Cela s/n. 13071 Ciudad Real. *Tel:* 926 295 436 .

Juan Luis Vázquez Suárez. (juanluis.vazquez@uam.es).
Dpto. de Matemáticas, C-XV. Fac. de Ciencias. Univ. Aut. de Madrid. Cantoblanco, Crta. de Colmenar, km. 14. 28049 Madrid. *Tel:* 913 974 935.

Luis Vega González. (mtpvegol@lg.ehu.es).
Dpto. de Matemáticas. Fac. de Ciencias. Univ. del País Vasco. Aptdo. 644. 48080 Bilbao (Vizcaya). *Tel:* 944 647 700.

Enrique Zuazua Iriondo. (enrique.zuazua@uam.es).
Dpto. de Matemáticas. Fac. de Ciencias. Univ. Aut. de Madrid. Cantoblanco, Ctra. de Colmenar, km. 14. 28049 Madrid. *Tel:* 913 974 368.

Grupo Editor del Boletín de SëMA

Pablo Pedregal Tercero. (Pablo.Pedregal@uclm.es).
Dpto. de Matemáticas. E.T.S.I. Industriales Univ. de Castilla-La Mancha. Avda. Camilo José Cela, s/n. 13071 Ciudad Real. *Tel:* 926 295 300 ext. 3809

Enrique Fernández Cara. (cara@us.es).
Dpto. de Ecuaciones Diferenciales y An. Numérico. Fac. de Matemáticas. Univ. de Sevilla. Tarfia, s/n. 41012 Sevilla. *Tel:* 954 557 992.

Ernesto Aranda Ortega. (Ernesto.Aranda@uclm.es).
Dpto. de Matemáticas. E.T.S.I. Industriales Univ. de Castilla-La Mancha. Avda. Camilo José Cela, s/n. 13071 Ciudad Real. *Tel:* 926 295 300 ext. 3813

José Carlos Bellido Guerrero. (JoseCarlos.Bellido@uclm.es).
Dpto. de Matemáticas. E.T.S.I. Industriales Univ. de Castilla-La Mancha. Avda. Camilo José Cela, s/n. 13071 Ciudad Real. *Tel:* 926 295 300 ext. 3859

Alfonso Bueno Orovio. (Alfonso.Bueno@uclm.es).
Dpto. de Matemáticas. Fac. de Químicas Univ. de Castilla-La Mancha. Avda. Camilo José Cela, s/n. 13071 Ciudad Real. *Tel:* 926 295 300

Alberto Donoso Bellón. (Alberto.Donoso@uclm.es).
Dpto. de Matemáticas. E.T.S.I. Industriales Univ. de Castilla-La Mancha. Avda. Camilo José Cela, s/n. 13071 Ciudad Real. *Tel:* 926 295 300 ext. 3859

Responsables de secciones del Boletín de SëMA

Artículos:

Enrique Fernández Cara. (cara@us.es).
Dpto. de Ecuaciones Diferenciales y An. Numérico. Fac. de Matemáticas. Univ. de Sevilla. Tarfia, s/n. 41012 Sevilla. *Tel:* 954 557 992.

Matemáticas e Industria:

Mikel Lezaun Iturralde. (mepleitm@lg.ehu.es).
Dpto. de Matemática Aplicada, Estadística e I. O. Fac. de Ciencias. Univ. del País Vasco. Aptdo. 644. 48080 Bilbao (Vizcaya). *Tel:* 944 647 700.

Educación Matemática:

Roberto Rodríguez del Río. (rr_delrio@mat.ucm.es).
Dpto. de Matemática Aplicada. Fac. de Químicas. Univ. Compl. de Madrid. Ciudad Universitaria. 28040 Madrid. *Tel:* 913 944 102.

Resúmenes de libros:

Fco. Javier Sayas González. (jsayas@posta.unizar.es).
Dpto. de Matemática Aplicada. Centro Politécnico Superior . Universidad de Zaragoza. C/María de Luna, 3. 50015 Zaragoza. *Tel:* 976 762 148.

Noticias de SëMA:

Carlos Castro Barbero. (ccastro@caminos.upm.es).
Dpto. de Matemática e Informática. E.T.S.I. Caminos, Canales y Puertos. Univ. Politécnica de Madrid. Av. Aranguren s/n. 28040 Madrid. *Tel:* 91 336 6664.

Anuncios:

Óscar López Pouso. (oscarlp@usc.es).
Dpto. de Matemática Aplicada. Fac. de Matemáticas. Univ. de Santiago de Compostela. Campus sur, s/n. 15782 Santiago de Compostela *Tel:* 981 563 100, ext. 13228.

Responsables de otras secciones de SëMA

Gestión de Socios:

Íñigo Arregui Álvarez. (arregui@udc.es).
Dpto. de Matemáticas. Fac. de Informática. Univ. de A Coruña. Campus de Elviña, s/n. 15071 A Coruña. *Tel:* 981 16 7000-1327.

Página web: www.sema.org.es/**:**

Carlos Castro Barbero. (ccastro@caminos.upm.es).
Dpto. de Matemática e Informática. E.T.S.I. Caminos, Canales y Puertos. Univ. Politécnica de Madrid. Av. Aranguren s/n. 28040 Madrid. *Tel:* 91 336 6664.

1. Los artículos publicados en este Boletín podrán ser escritos en español o inglés y deberán ser enviados por correo certificado a

   Prof. E. FERNÁNDEZ CARA
   Presidente del Comité Científico, Boletín SëMA
   Dpto. E.D.A.N., Facultad de Matemáticas
   Aptdo. 1160, 41080 SEVILLA

   También podrán ser enviados por correo electrónico a la dirección

   `boletin_sema@usal.es`

   En ambos casos, el/los autor/es deberán enviar por correo certificado una carta a la dirección precedente mencionando explícitamente que el artículo es sometido a publicación e indicando el nombre y dirección del autor corresponsal. En esta carta, podrán sugerirse nombres de miembros del Comité Científico que, a juicio de los autores, sean especialmente adecuados para juzgar el trabajo.

   La decisión final sobre aceptación del trabajo será precedida de un procedimiento de revisión anónima.

2. Las contribuciones serán preferiblemente de una longitud inferior a 24 páginas y se deberán ajustar al formato indicado en los ficheros a tal efecto disponibles en la página web de la Sociedad (`http://www.sema.org.es/`).

3. El contenido de los artículos publicados corresponderá a un área de trabajo preferiblemente conectada a los objetivos propios de la Matemática Aplicada. En los trabajos podrá incluirse información sobre resultados conocidos y/o previamente publicados. Se anima especialmente a los autores a presentar sus propios resultados (y en su caso los de otros investigadores) con estilo y objetivos divulgativos.

Ficha de Inscripción Individual

Sociedad Española de Matemática Aplicada SëMA

Remitir a: SEMA, Despacho 520, Facultad de Matemáticas,
Universidad Complutense. 28040 Madrid.
Fax: 913 944 607. CIF: G-80581911

Datos Personales

- Apellidos: .....
- Nombre: .....
- Domicilio: .....
- C.P.: ..... Población: .....
- Teléfono: ..... DNI/CIF: .....
- Fecha de inscripción: .....

Datos Profesionales

- Departamento: .....
- Facultad o Escuela: .....
- Universidad o Institución: .....
- Domicilio: .....
- C.P.: ..... Población: .....
- Teléfono: ..... Fax: .....
- Correo electrónico: .....
- Página web: `http://` .....
- Categoría Profesional: .....
- Líneas de Investigación: .....

.....

Dirección para la correspondencia: ☐ Profesional ☐ Personal

Cuota anual para el año 2005

☐ Socio ordinario: 30 EUR. ☐ Socio de reciprocidad con la RSME: 12 EUR.
☐ Socio estudiante: 15 EUR. ☐ Socio extranjero: 25 EUR.

Datos bancarios

... de ..... de 200..

Muy Sres. Míos:

Ruego a Uds. que los recibos que emitan a mi cargo en concepto de cuotas de inscripción y posteriores cuotas anuales de SëMA (Sociedad Española de Matemática Aplicada) sean pasados al cobro en la cuenta cuyos datos figuran a continuación

Entidad (4 dígitos)	Oficina (4 dígitos)	D.C. (2 dígitos)	Número de cuenta (10 dígitos)

- Entidad bancaria: .....
- Domicilio: .....
- C.P.: ..... Población: .....

Con esta fecha, doy instrucciones a dicha entidad bancaria para que obren en consecuencia.

Atentamente,

Fdo. .....

Para remitir a la entidad bancaria

... de ..... de 200..

Muy Sres. Míos:

Ruego a Uds. que los recibos que emitan a mi cargo en concepto de cuotas de inscripción y posteriores cuotas anuales de SëMA (Sociedad Española de Matemática Aplicada) sean cargados a mi cuenta corriente/libreta ..... en esa Agencia Urbana y transferidas a

SEMA: 0128 - 0380 - 03 - 0100034244
Bankinter
C/ Hernán Cortés, 63
39003 Santander

Atentamente,

Fdo. .....

Ficha de Inscripción Institucional

Sociedad Española de Matemática Aplicada SëMA

Remitir a: SEMA, Despacho 520, Facultad de Matemáticas,
Universidad Complutense. 28040 Madrid.
Fax: 913 944 607. CIF: G-80581911

Datos de la Institución

- Departamento: .....
- Facultad o Escuela: .....
- Universidad o Institución: .....
- Domicilio: .....
- C.P.: ..... Población: .....
- Teléfono: ..... DNI/CIF: .....
- Correo electrónico: .....
- Página web: `http://` .....
- Fecha de inscripción: .....

Forma de pago

La cuota anual para el año 2005 como Socio Institucional es de 150 EUR.
El pago se realiza mediante transferencia bancaria a

SEMA: 0128 - 0380 - 03 - 0100034244
Bankinter
C/ Hernán Cortés, 63
39003 Santander